MIGRATION BY THE DIFFRACTION STACK METHOD

PRIYA RANJAN MOHANTY

NOTICE

AVIS

The quality of this microform is heavily dependent upon the quality of the original thesis submitted for microfilming. Every effort has been made to ensure the highest quality of reproduction possible.

If pages are missing, contact the university which granted the degree.

Some pages may have indistinct print especially if the original pages were typed with a poor typewriter ribbon or if the university sent us an inferior photocopy.

Reproduction in full or in part of this microform is governed by the Canadian Copyright Act, R.S.C. 1970, c. C-30, and subsequent amendments.

La qualité de cette microforme dépend grandement de la qualité de la thèse soumise au microfilmage. Nous avons tout fait pour assurer une qualité supérieure de reproduction.

S'il manque des pages, veuillez communiquer avec l'université qui a conféré le grade.

La qualité d'impression de certaines pages peut laisser à désirer, surtout si les pages originales ont été dactylogra phiées à l'aide d'un ruban usé ou si l'université nous a fait parvenir une photocopie de qualité inférieure.

La reproduction, même partielle, de cette microforme est soumise à la Loi canadienne sur la droit d'auteur, SRC 1970, c. C-30, et ses amendements subséquents.

Canada

MIGRATION BY THE DIFFRACTION STACK METHOD

by

Priya Ranjan Mohanty, M. Phil.

A thesis submitted in partial fulfilment

of the requirements for the degree of

Master of Science

Department of Earth Sciences (Geophysics)

Memorial University of Newfoundland

April 1984

St. John's   Newfoundland

The author has granted an irrevocable non-exclusive licence allowing the National Library of Canada to reproduce, loan, distribute or sell copies of his/her thesis by any means and in any form or format, making this thesis available to interested persons.

The author retains ownership of the copyright in his/her thesis. Neither the thesis nor substantial extracts from it may be printed or otherwise reproduced without his/her permission.

L'auteur a accordé une licence irrévocable et non exclusive permettant à la Bibliothèque nationale du Canada de reproduire, prêter, distribuer ou vendre des copies de sa thèse de quelque manière et sous quelque forme que ce soit pour mettre des exemplaires de cette thèse à la disposition des personnes intéressées.

L'auteur conserve la propriété du droit d'auteur qui protège sa thèse. Ni la thèse ni des extraits substantiels de celle-ci ne doivent être imprimés ou autrement reproduits sans son autorisation.

Canadä

ABSTRACT

Computer programmes were developed to implement the diffraction stack migration scheme. In order to test the above technique, zero offset synthetic seismograms were generated for two simple models; a dipping layer and an anticline. Later the diffraction stack algorithm was applied to the field seismic data for the Adolphus structure.

The general structure of the subsurface reflectors were better clarified in the migrated sections than the unmigrated sections for both synthetic and field seismic data. The anticline breadth was reduced in both synthetic and field migrated sections after collapsing the diffraction patterns generated at the sharp boundaries. The salt flank in Adolphus structure was delineated better than the original stacked section. It is also observed from migrated sections on the two synthetic models that the diffraction stack method works efficiently for steep dip reflectors up to dip angle 40 degrees.

(i)

TABLE OF CONTENTS

TABLE OF CONTENTS (cont'd)

(iii)

LIST OF FIGURES

LIST OF FIGURES (cont'd)

LIST OF FIGURES (cont'd)

(vi)

LIST OF TABLES

CHAPTER 1

1.0 INTRODUCTION

The present study was undertaken to investigate the diffracton stack
migration technique and apply it to the stacked seismic data for the
Adolphus structure on the Grand Banks. The Grand Banks basins are located
approximately 315 km southeast of St. John's, Newfoundland and cover an
offshore area of 17000 square kilometers (Fig. 1.1). Economic interest in
the basins of the area arises from hydrocarbon occurrences of the
Heron (H-73) well drilled on a flank of a salt diapir in the South Whale
Subbasin (Procter et al., 1983), from the tested flow at the Adolphus
2K-41 well, from the major discoveries on the Hibernia structure, and
other discoveries in the same area of the Jeanne d'Arc Subbasin.

1.1 Objective

The aim of the present study was to apply the diffraction stack migration
technique to aid in the interpretation of seismic time sections. Computer
programmes were developed to implement the migration technique. The
application of the diffraction stack migration method was investigated for
zero offset (stacked) synthetic seismic data generated by considering
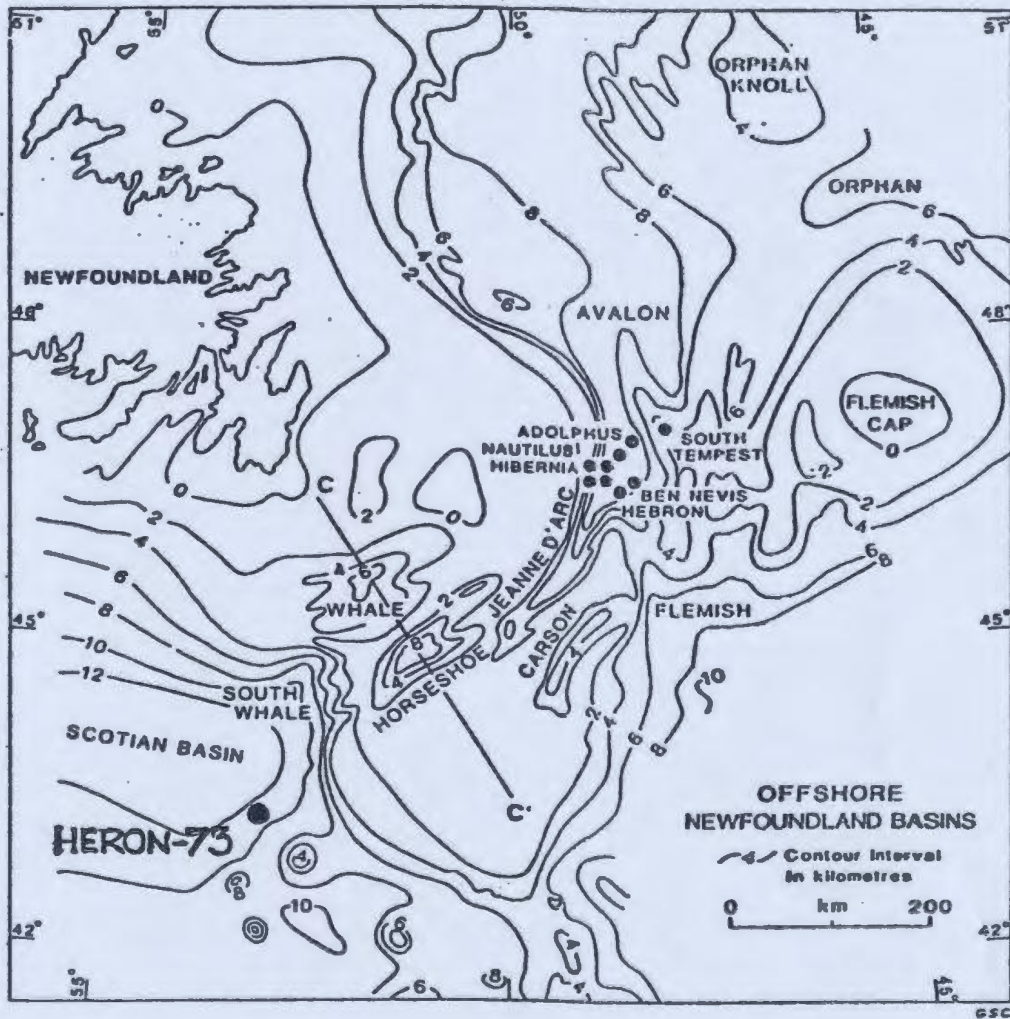
Figure 1.1   Index map for basins in Grand Banks (south),
East Newfoundland Shelf and East Newfoundland
Basin.   Contours indicate depth from seafloor.
(After McMillan, 1982).

two different simple models. The effects of migration velocity and dip
angle on the application of the above technique were studied. After
testing the method on synthetic data the programmes were applied to the
existing seismic data for the Adolphus structure. The results from model
and real data were analysed in terms of subsurface reflectors.

1.2 Regional Geology

The Grand Banks (Figure 1.1) are located east of Newfoundland. Extensive
geophysical and drilling operations within the area of the Grand Banks
have established the presence of a thick sedimentary section suitable for
petroleum accumulations (Amoco and Imperial, 1973). The major sedimentary
section in the area under study comprises Tertiary, Mesozoic and Paleozoic
strata. There are two distinct geological units separated by an angular
unconformity of early Cretaceous age. The "upper wedge" is mainly
composed of Tertiary and Cretaceous strata. The other unit
"Subunconformity basins" contains Jurassic and older rocks. The "upper
wedge" is relatively simple with gentle dip, disturbed locally by
salt-dome and rollover fault controlled structures. The "Subunconformity
basins" contain different structural traps, including salt domes, salt
ridges, faults, drape folds over basement rocks and major sedimentary
truncations at the unconformity. The general stratigraphic sequence of
the Grand Banks is shown in Figure 1.2.

Upper Cretaceous and Tertiary shales overlying the unconformity have potential as source rocks but are thermally immature (Procter et al., 1983). The lower and middle Jurassic are considered as poor, gas prone source rocks. The major potential reservoir rocks constitute basal transgressive porous sand and upper Cretaceous limestone units. The Verrill Canyon shale constitutes the major source rock found in the west flank of the Avalon Uplift.

1.3 Previous Geophysical Work

The first refraction seismic measurements were taken in the Grand Banks area by a group from Woods Hole Oceanographic Institution in 1951. Subsequently Press and Beckmann (1954) reported the sedimentary layers thickness range from 700m to 3300m on the basis of previous refraction data. Additional data collected by Bently and Worzel (1956) indicated low-velocity sedimentary layers beneath the western Grand Banks and Laurentian Fan deep-water area. Ewing and Ewing (1959) reported the results of a refraction study indicating the sedimentary layers thickness of Grand Banks as 4900m.

In the same year the Geological Survey of Canada and the Canadian Hydrographic Service conducted sea-magnetometer surveys covering a part of the Grand Banks (Bower, 1962). The results show the depths to magnetic basement varied from 76m below the seafloor in the Virgin Rocks-Eastern Shoals area to 2300m on the northern Grand Banks. Hood and Godby (1965) reported the sedimentary thicknesses in Grand Banks to be 2400m from their
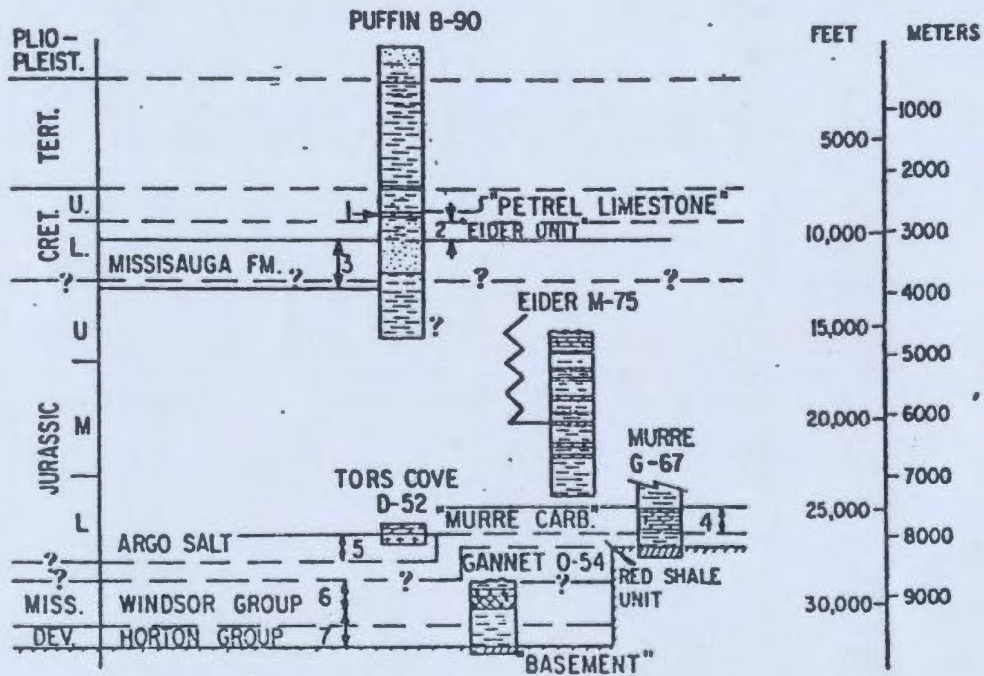
Figure 1.2   Composite stratigraphic section, Grand
Banks (After Amoco and Imperial Oil, 1973).

long aeromagnetic profile running from Prince Edward Island, through the
Cabot Strait to the trail of the Grand Banks of Newfoundland and
subsequently over the Flemish Cap.

Direct geological information about the sedimentary rocks beneath the
Grand Banks came from Lilly (1965). Lilly also reported the outcropping
Precambrian basement-rock on the Eastern Shoals and Ballard Banks.
Pelletier (1971) reported on the basement rock confirming the earlier
result from a core of granodiorite in Flemish Cap area of the eastern
Canadian continental margin located 500 km east of St. John's,
Newfoundland (Figure 1.1).

In 1964, Amoco conducted both aeromagnetic and shallow seismic reflection
surveys in the Grand Banks area (Figure 1.3). The basin shape (southern
Grand Banks) was first delineated from the aeromagnetic interpretation
whereas shallow seismic indicated the major structures associated with
salt domes. Between 1964 to 1965, 15,300 km of gas-exploder seismic
surveys were conducted. These surveys indicated two major structural
features of the area - namely, a mid-Cretaceous angular unconformity, and
salt piercement structures. In 1965, multifold seismic data were
collected for the first time with dynamite as energy source. This led to
the locations of two exploratory wells Tors Cove and Grand Falls in the
Grand Banks area (Figure 1.3). Since 1967, approximately 32,000 km of 12
and 24 fold seismic data have been acquired, with dynamite, Flexotir, and
airgun as energy sources. By the end of 1974 40 dry wells had been
drilled on the Grand Banks. Between 1974 and 1976 three wells were
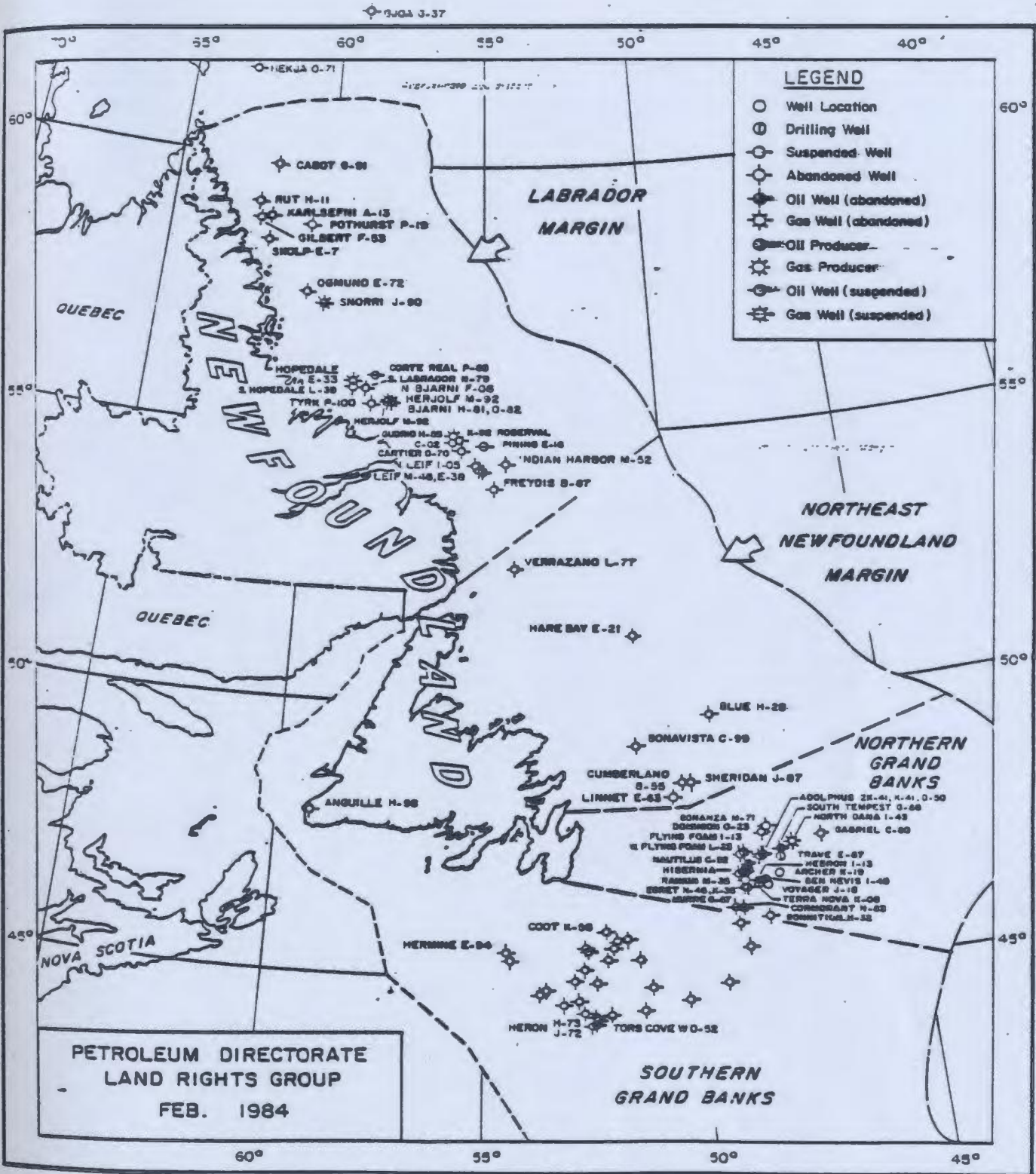
Figure 1.3   Well location map.

drilled on the northeast Newfoundland shelf area: Bonavista C-99,
Cumberland B-55 and Verrazano L-77.

Geophysical investigations from Mobil's survey indicated the presence of
various structures - salt diapirs, basement highs and tilted fault blocks
in the northern Grand Banks area.   Up to the end of 1974, no commercial
hydrocarbon reserves were found in the above area.   However, minor flows
of oil and gas from the upper Cretaceous sandstones were noticed from the
Adolphus 2K-41 well (Figure 1.3) on a salt piercement structure drilled by
Mobil Oil Limited.   Drilling again resumed in 1979 on the Grand Banks area
and Gabriel C-60 well was spudded.   This well indicated the presence of
noncommercial amounts of oil in a lower Cretaceous core (Petroleum
Directorate Information Kit, 1984).   In September 1979, Chevron tested the
Hibernia P-15 well and made a significant discovery of hydrocarbon
accumulations in the Hibernia structure.   The total flow rate was 20,000
barrels of oil per day which is thought to be viable for commercial
production.   Later it was established as a commercial oilfield on the
basis of further exploratory drilling on the Hibernia structure (Petroleum
Directorate Information Kit, 1984).

1.4   Present Survey

The present seismic survey was conducted during December 1975 by
Geophysical Services Incorporated (GSI), Calgary with Mobil Oil Canada
Limited as operator.   Forty eight fold seismic data were collected on
seismic line G-583B on the Adolphus structure in the Grand Banks,

Newfoundland (Fig. 1.3) with 9 track DFS III recording system. The
direction of seismic line was south-east. Tuned airgun arrays were used
as energy source with air pressure of 1600 psi. Hydrophone groups with
group interval of 50m and 30 hydrophones per group were arranged in the
streamer cable with a hydrophone spacing of 1.1m. A spread length of
2350m was used for the entire data acquisition process. Shots were fired
at every 25m to acquire the seismic data. All data were recorded
digitally for 5 seconds using a 2ms sampling rate. Satellite navigation
for position location in the offshore area was provided by GEONAV system.

The data were processed by GSI headquarters in Calgary. The data
processing sequence applied to this data is presented in Fig. 1.4. The
present analysis was carried out using the stacked seismic data (for line
G-583B). The stacked data for the above seismic line was provided by
Mobil Oil Canada Limited at Calgary in form of consul staked reels. In
this thesis, migration (Chapter 2), and the application of diffraction
stack method to synthetic models (Chapter 3) are discussed. Application
of the above migration method to field data is described in the Chapter 4.
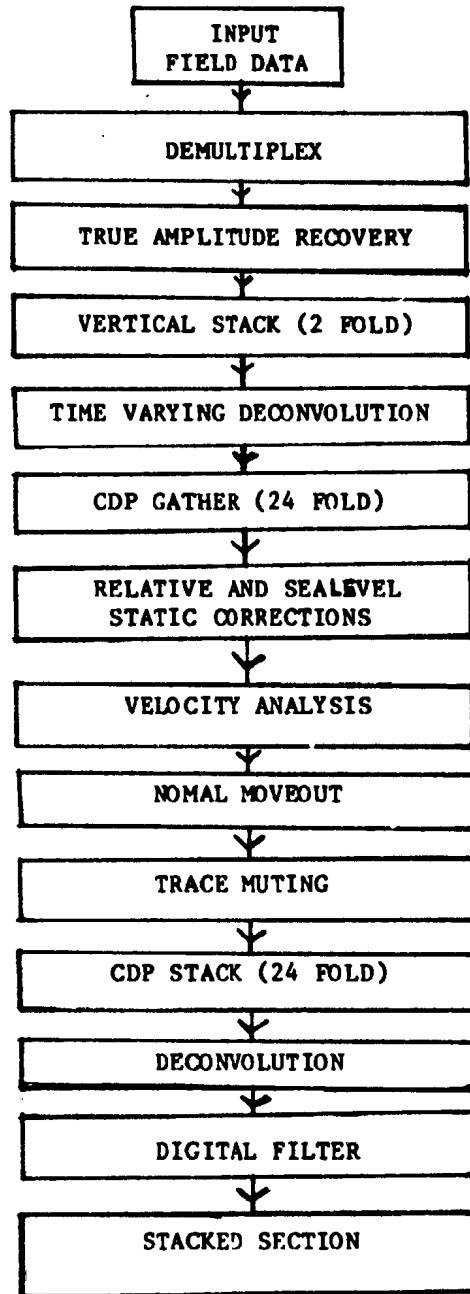
Figure 1.4 Seismic data processing sequence

CHAPTER 2

2.0 MIGRATION

Conventional time sections are often interpreted directly in terms of
subsurface geometry. However, the interpretations can be misleading and
are often hard to interpret geologically in areas of complex structure and
high angles of dip. Unmigrated sections give an apparent subsurface
picture which becomes increasingly distorted with increasing dip angle of
the reflector. To overcome this problem migration of seismic traces is an
essential aid in interpretation. The basic purpose of this technique is to
plot the dipping reflections (apparent reflections) in the true spatial
positions rather than plotting directly beneath the point midway between
the shot point and centre of the geophone spread or vertically below the
point (common reflection point) of coincident source and receiver
position. Figure 2.1 shows the effect of migration in determining the
position.

2.1 Methods of Migration

Up to the late 1960s migration was performed on a single stacked trace by
graphical and mechani l methods using Hagedoorn's (1954) method. Rapid
processing of multifold seismic data became possible with the rapid growth
of digital computers in the 1960s. Automatic migration techniques were
introduced around 1970 based on Hagedoorn's concept of the surface of
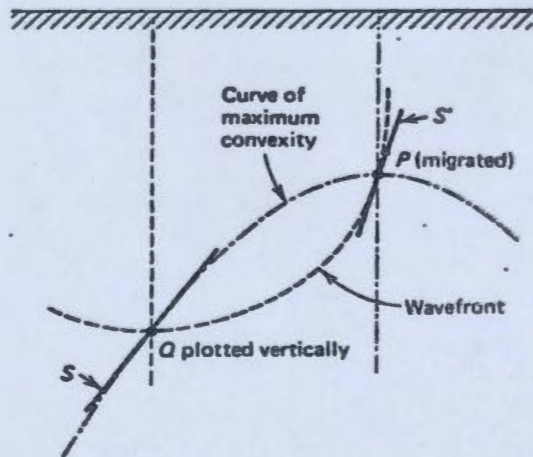
Figure 2.1   Use of curve of maximum convexity and
wavefront for migrating reflection from
apparent position at Q to actual position
at P (After Hagedoorn, 1954).

maximum convexity. Later Rockwell (1971) introduced the diffraction stack
migration method for steep-dip reflection data.

Several major developments have taken place in the late 1970s. For the
first time, Hagedoorn's ray theory concept was replaced by wave theory in
migration by Claerbout (1970) who developed the finite-difference method
based on the scalar wave equation. Another development has taken place in
implementing the diffraction stack method through Kirchhoff integral
theory (French, 1975). Stolt (1978) suggested a new technique called
frequency - wavenumber method based on wave theory concept. Each of these
methods is summarised below.

2.1.1   Maximum Convexity Curves

Hagedoorn (1954) introduced migration using surfaces of maximum convexity
(Figure 2.1.1) which he defined for a two-dimensional case. These
surfaces represent the time along a slant path that would be due to a
reflection or diffraction event from a given point in the subsurface to
travel to a receiver as its horizontal distance from that point changes
(Dobrin, 1976). This is also referred to as a diffraction curve. This is
a ray tracing method which obeys Snell's Law. If the constant velocity
assumption is used the wavefronts are arcs of circles with centre being at
the shot point. Wavefronts will still be circles for velocity increasing
linearly with depth. Maximum convexity charts are prepared by combining
individual curves of maximum convexity for successive source depth over
the required migration range.
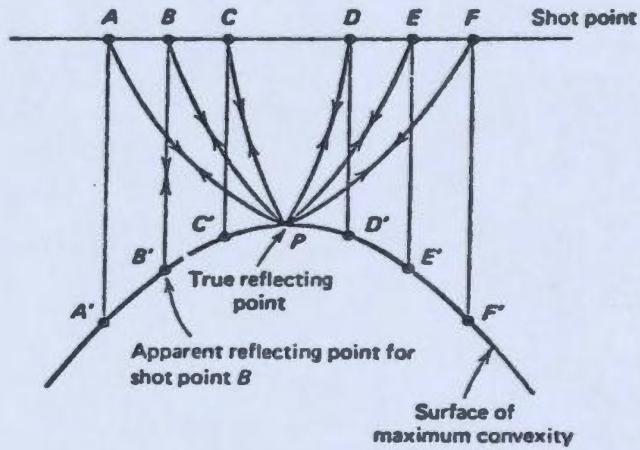
Figure 2.1.1   Surface of maximum convexity for
                reflecting point at P. Positions
                along curve are shown for six shot points
                with concident geophones (After Dobrin, 1976).

To use Hagedoorn's technique, one requires two charts, a wavefront chart (chart of equal reflection times) and a chart containing curves of maximum convexity for closely spaced vertical two-way times. Initially the two curves are placed on each other with the zero depth positions coincident. The reflecting point is found along the curve on the wavefront chart corresponding to the time of the reflection along the central (vertical) axis of the chart. Then the maximum convexity curves are slid laterally until a line is found that is tangent to the apparent (unmigrated) dip at the depth of the reflecting point. The migrated position of the point is found at the vertex of this curve, and the dip of the migrated segment is found by drawing a line tangent to the wavefront circle corresponding to the reflection time where it intersects this vertex. Usually wavefront charts are prepared for a constant velocity function. For inhomogenous media the charts are also constructed taking known velocity as a function of depth.

2.1.2 Diffraction Stack Method

This method is based on the assumption that a reflector consists of packed series of diffraction points or scatterers (Al-Sadi, 1980). This method can easily be implemented by doing addition along hyperbolic diffraction curves in the space-time domain. The basic object of this technique is to collapse diffracting events and reposition the reflections correctly. This technique is applied to the images caused by diffraction. A diffraction hyperbola is constructed for each point in the subsurface for different source and receiver positions along the horizontal axis considering a

constant velocity medium. During the diffraction stack process the diffraction curves of the true reflections will lie on the apex of the hyperbola forming a clear a reflection line whereas the diffracting events are eliminated statistically. This process is shown in Figure 2.1.2. This method can be applied both to common mid-point (CMP) or zero offset stacked seismic time sections.

2.1.3 Finite-Difference Method

Finite-difference or wave equation migration was introduced by Claerbout (1970). This technique uses the downward continuation process by solving the scalar wave equation using a differential form of solution. Wave-equation migration is based on the concept of separating the seismic wave into upgoing and downgoing waves by a mathematical procedure involving the use of a coordinate frame which moves downward at the speed of backward wave propagation. Basically the seismic section is reduced as if the time runs backward until it reaches the situation where the source-receiver common position is placed on the actual reflector. This method can be applied to stacked and unstacked data. It employs a grid of seismic data and works quite well up to true dip angles of 45°. It has the advantage over diffraction stack method while considering the factors such as computational cost, low noise from gently dipping events and lateral velocity variations. Diffraction stack migration can only handle lateral velocity variations if a raytracing technique is used.
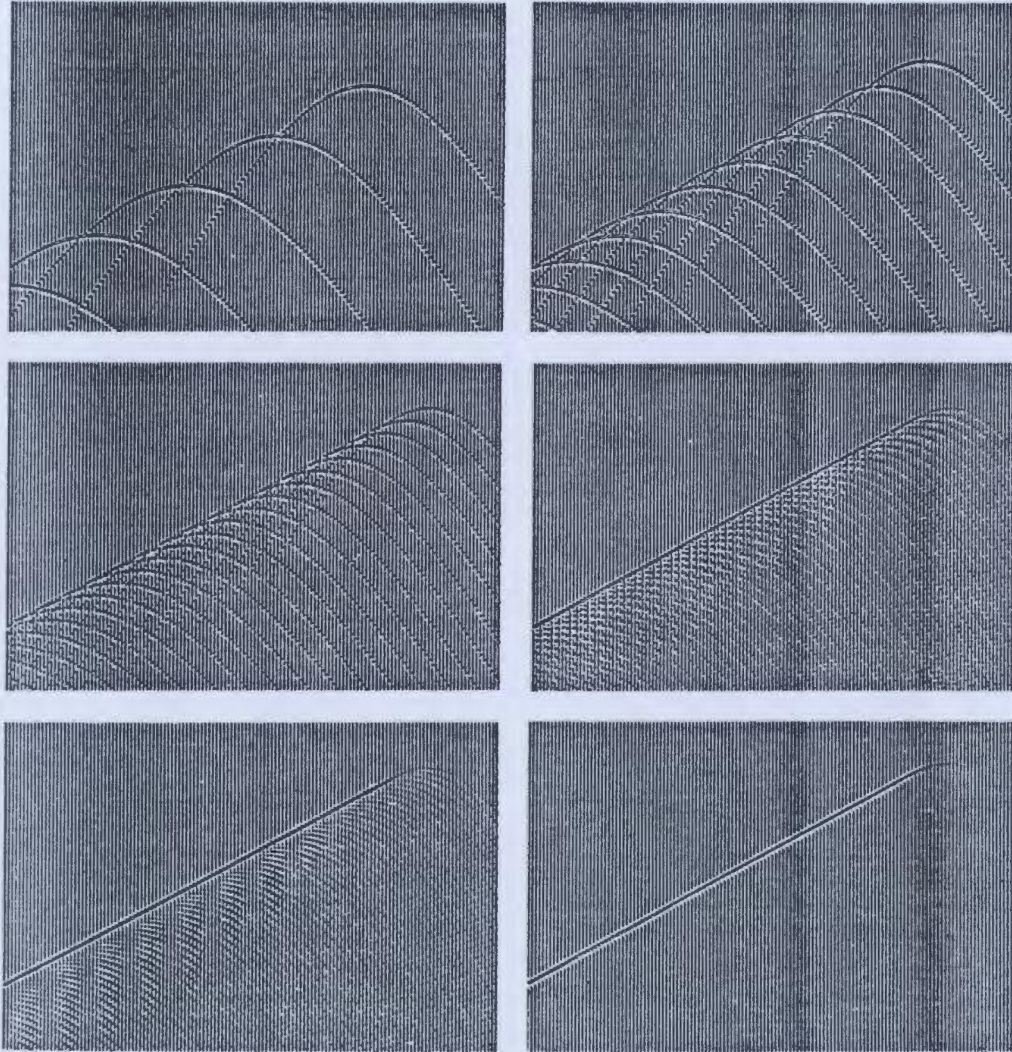
Figure 2.1.2   Diffraction stacking illustrating the
                principle of migration (After Dohr, 1981).

2.1.4 Frequency - Wavenumber Method

The last method called frequency-wavenumber method was developed by Stolt
(1978). This method is computationally fast because it uses the fast
Fourier transform algorithm. This technique is also based on the concept
of downward continuation of seismic waves and works moderately well for
steep dip reflectors. Stolt developed a frequency-wavenumber technique
replacing the horizontal co-ordinate by their Fourier conjugates. This
technique extends the Claerbout finite-difference concept, greatly
reducing dispersion problems that are associated with higher dips and
frequencies. Moreover, Stolt's method can be applied to three-dimensional
migration and migration before stack. Generally this method considers a
constant velocity medium but it can be extended to lateral variation in
velocity under certain assumptions.

For our present analysis, the diffracton stack migration method in
space-time domain was used to migrate the stacked seismic data over
Adolphus structure on the Grand Banks area. The mathematical theory and
summation technique are described in the next sections of this chapter.

2.2 Mathematical Formulation of Diffraction Stack Method

Consider the diffraction front due to point reflector at (x,z) as given in
Figure 2.2. Assume coincident source-receiver placed at $(x_o,0)$. The
distance from $(x_o,0)$ to the point reflector is $ct/2$, where c is the wave
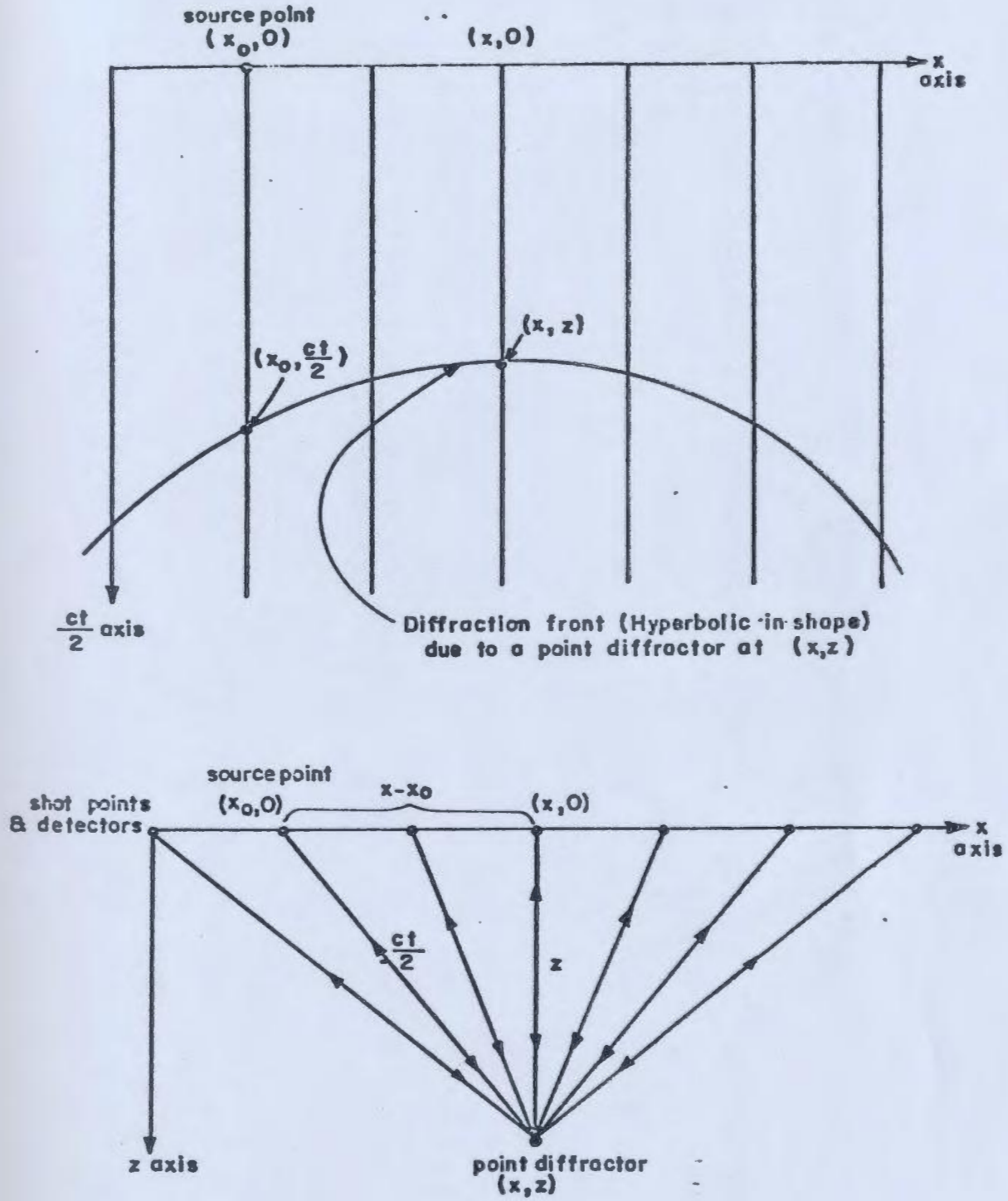
Figure 2.2   The diffraction front and its construction
(After Robinson et al, 1977).

velocity and t is the two-way time.

Then,

$$\frac{ct}{2} = [(x-x_o)^2 + z^2]^{1/2} \qquad\qquad 2.2.1$$

The event is plotted at time 't' i.e., two-way time directly under the source-receiver point at $(x_o,0)$ that is, the event corresponding to the point reflector (x,z) is

$$(x_o,\frac{ct}{2})=(x_o,[(x-x_o)^2+z^2]^{1/2}) \qquad\qquad 2.2.2$$

Now the diffraction front is defined as the event given by reflections from the point reflector for all source-receiver points $(x_o, 0)$. Hence, the diffraction front is the locus given by

$$\frac{ct}{2} = [(x-x_o)^2 + z^2]^{1/2} \qquad\qquad 2.2.3$$

which is the semi-hyperbola in x, ct/2 space given by

$$(ct/2)^2 - (x-x_o)^2 = z^2 \qquad\qquad 2.2.4$$

for a fixed depth.

2.3 Diffraction Summation

To reconstruct the energy due to a given true reflection point, the summation operation has to be carried out. Migration velocity depends on the shape of hyperbola along which the summation is to be carried out.

Migration velocity was considered the same as the material velocity in the synthetic stacked sections constructed for two simple models. In the field seismic stacked data, the migration velocity was determined through a trial and error method by examining the coherency energy at the apex of the diffraction hyperbola as follows:

First take the diffraction curve determined from the equation (2.2.4) using an assumed velocity and see where it intersects each trace. Then the amplitude value of each trace at the point of intersection is taken and all the values are summed together. The energy due to the given true reflection point adds inphase and is preserved. The extraneous energy adds out of phase and is cancelled. As a result of this summation the energy due to the true point reflector is positioned correctly and is plotted at the apex of the diffraction curve.

Three different constant migration velocities 2500 m/s, 3500 m/s and 4500 m/s were chosen to construct the diffraction hyperbola in order to get the maximum energy at the apex of the diffraction hyperbola. The migration velocity 3500 m/s was found best because it gave the maximum energy at the diffraction curve. The process is carried out for subsequent traces that are falling on the diffraction curve and the result is plotted at its apex. The process of doing such summations for all possible apexes is the migrated or true seismic section. This method of migration is called diffraction stack migration. Figure 2.3 shows the process of diffraction summation. A Fortran progiamme (Appendix 1) was developed using equation 2.2.4 to implement the diffraction stack migration technique.
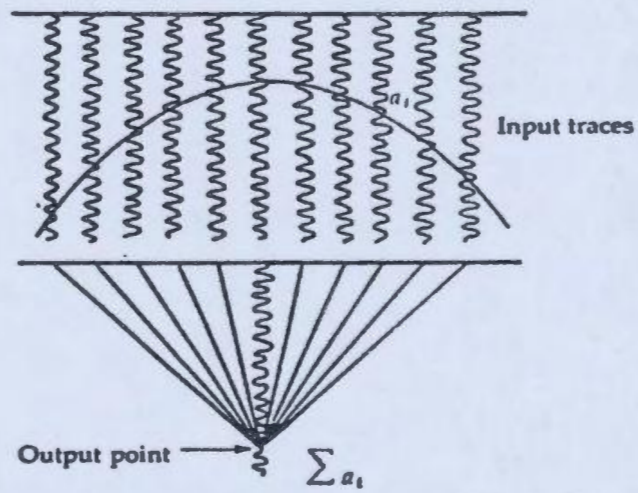
Figure 2.3   Diffraction summation migration as seen
by the output trace (From Robinson, 1983).

CHAPTER 3

3.0 APPLICATION OF DIFFRACTION STACK METHOD TO SYNTHETIC MODELS

In practice, migration schemes are applied to zero offset seismic data to improve the lateral resolution and true amplitudes of the reflected events. The diffraction stack migration technique is very sensitive to velocity variation. One way to overcome this problem is to do conventional velocity analysis and take the correct stacking velocity for migrating the time section. The other alternative is to model the configuration of the subsurface by which a discrete velocity can be assigned. For our present analysis ideal synthetic seismograms using a fixed velocity were constructed for two geological models to test the above migration technique.

3.1 Generation of Zero Offset Synthetic Seismic Data

Conventional methods of migration make use of the zero offset (stacked) seismic record section which is based on coincident source-receiver geometry (Fig. 3.1). The coincident source-receiver geometry accomplishes the objective of the diffraction stack method considering only the diffraction effects while rejecting those refraction effects caused by lateral changes in velocity. The refraction effects are avoided as the rays travel to the reflector and back along the same path, with the rays normal to their final reflecting interface. Two synthetic models were
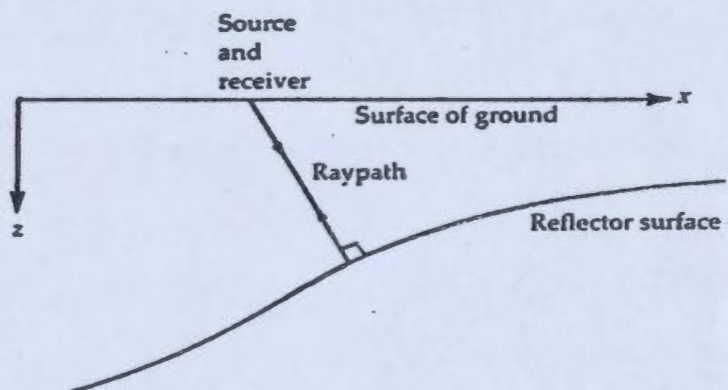
Figure 3.1   Ray paths for coincident source-receiver locations (After Robinson, 1983).

- 25 -

used to generate zero offset seismic data to implement the diffraction stack migration.

3.1.1 An Inclined Reflector

We consider straight ray paths constructed along perpendiculars to the beds from coincident source-receiver position (zero offset section) on the surface and the final seismic section is presented in vertical orientation. In areas of steep dip (more than ten degrees), the reflections from dipping beds emanate from depth points which are up dip from the surface source-receiver positions. In general plotted seismic time sections display these depths points directly beneath the surface source-receiver location depicting apparent subsurface structure. This introduces an error in interpreting the subsurface location of the reflector and in its geometry. Simple ray-path modelling at normal incidence is adequate to show the expected apparent interface caused due to an inclined reflector.

Synthetic seismograms can be constructed through manual, analog and digital methods. For our present analysis digital techniques are implemented to generate zero offset synthetic seismograms. Synthetic time data were generated for a zero offset section assuming a simple geologic model having depths, velocities and densities shown in (Fig. 3.1.1). To produce this zero offset synthetic section means to generate synthetic seismograms (Peterson et al, 1955) which are artificial reflection records
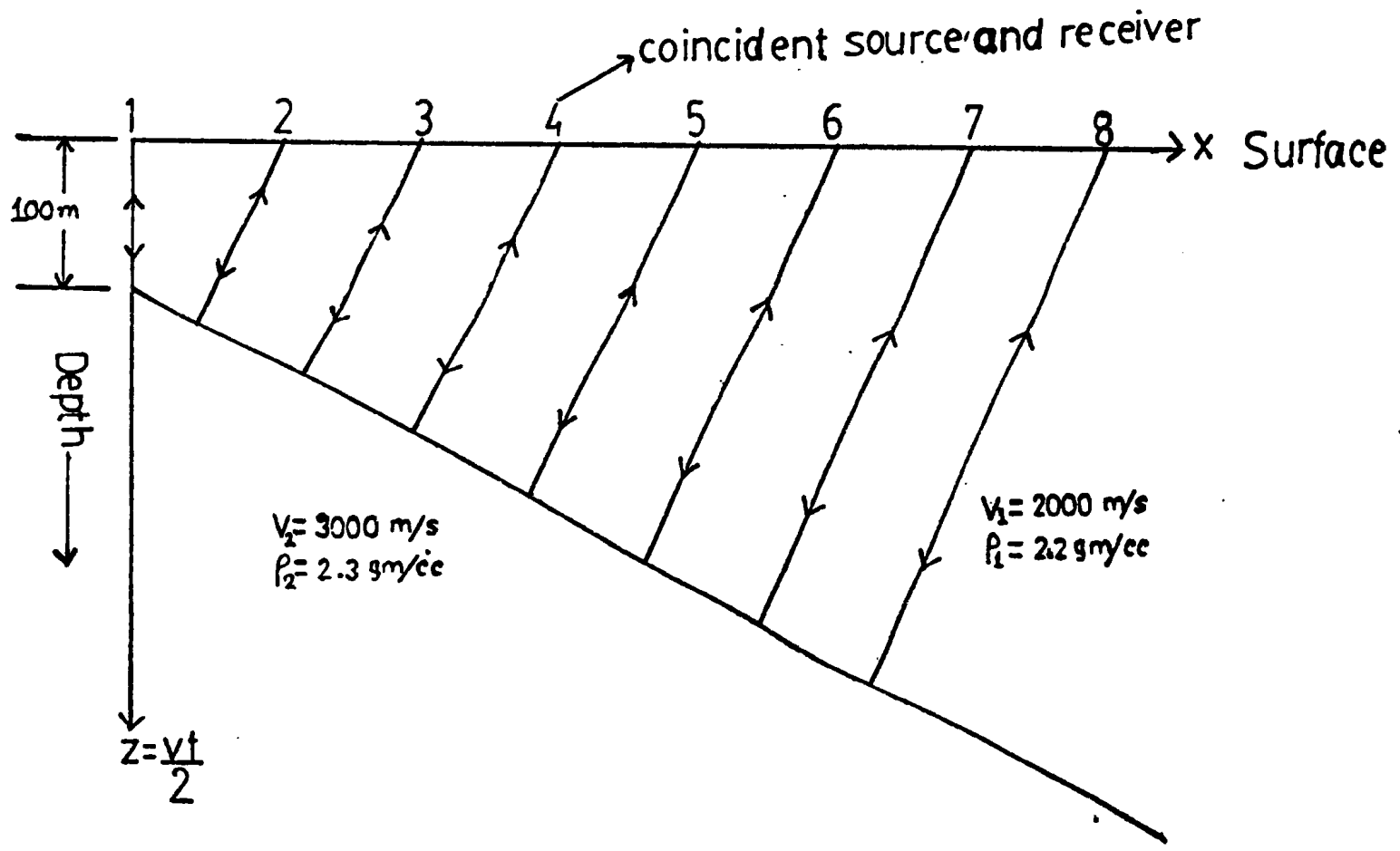
FIG. 3.1.1 An inclined reflector model.

constructed by convolution of the reflectivity function with a source pulse.

First the two-way travel times from coincident source-receiver position to the inclined reflector were calculated for each offset distance. Then the seismic trace was digitised at 1 ms interval which is same as the sampling interval used for the migration process. Multiples were not included in generating the zero offset synthetic section to minimise migration noise in the implementation of the diffraction stack technique. The reflectivity was calculated (Appendix-2) assuming the above geological model (Figure 3.1.1). A 25HZ Ricker wavelet was chosen as the source pulse because good Ricker wavelets were observed in the unmigrated field data (Fig. 4.1.1). The chosen 25HZ frequency is within the seismic range.

3.1.2 An Anticline

In normal seismic sections, an anticline structure can easily be mapped by reflection if the data are of good quality. Normally we expect oil-bearing anticlinal structures associated with rising salt domes or other diapiric features. The time sections over such anticlines do not display a clear picture of the subsurface structure. Migration is applied to such cases to collapse the diffraction patterns generated at the sharp boundaries and to reduce the breadth of anticlines to their correct values. One can model the anticlinal structure and see its response before and after migration.

For our analysis an anticline model is chosen to generate zero offset the synthetic data implementing the concept described in earlier section 3.1.1. Figure 3.1.2 shows the anticline model to generate the zero offset synthetic data. The velocity and density parameters were kept constant with the earlier model discussed. Two computer programmes were developed to generate vertical travel time and zero offset synthetic seismogram respectively (Appendix-1).

3.2 Migration of Synthetic Sections

The migration is carried out in two stages:

1) The migration where the reflection segment is moved to its new position horizontally. The reflection time is kept as vertical axis.

2) Depth conversion, in which the vertical scale is changed to depth.

In time migration diffraction events only are considered but not those refraction events caused by lateral changes in velocity. The first stage of migration is preferred here for our present work because it accomplishes all the objectives concerned with the collapse of diffraction and general clarification of structure (Anstey, 1977). Depth conversion is not attempted in our analysis because of the nonavailability of velocity information for the field seismic data over the Grand Banks area.
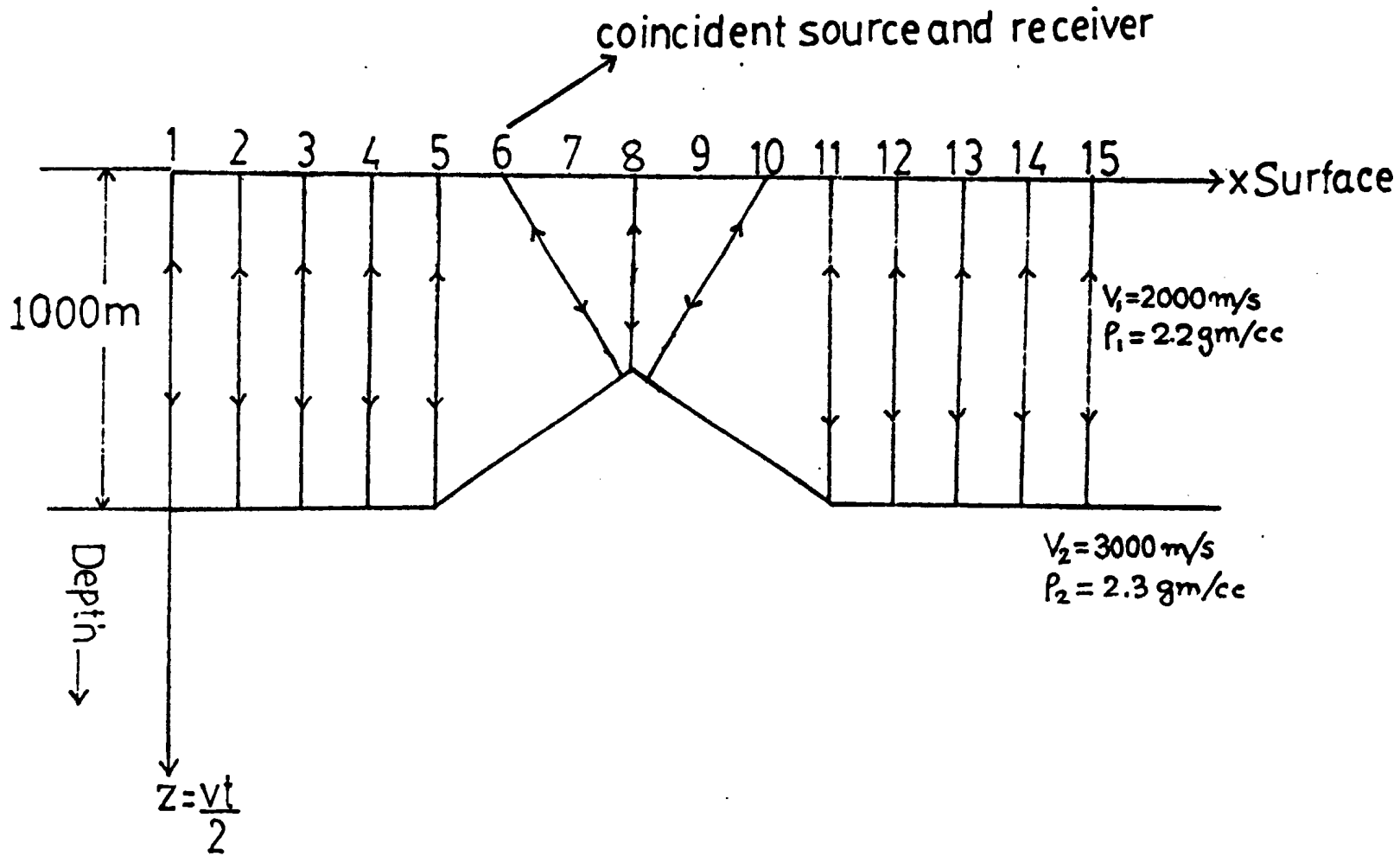
FIG. 3.1.2 An anticline model.

3.2.1 Parameters for Migration of Synthetic Data

The three basic parameters sampling interval, aperture and velocity should be fixed before applying the migration scheme. The first requirement, the input trace time sampling interval Δt must be chosen such that the highest frequency in the analog data f_h satisfies the sampling theorem given as

$$\Delta t \leq 1/2f_h \qquad\qquad 3.2.1.1$$

where f_h is the highest frequency in the input trace, Δt is the sampling interval.

In our synthetic data, the sampling interval was taken as 1 ms while the f_h was 25 HZ. The output sampling interval is also taken as 1 ms to minimize the aliasing conditions during the migration process. The second requirement is to find the appropriate aperture for the migration method. Before implementing the migration programme, it is necessary to estimate the "aperture" (window) within which the input traces must be enclosed. The number of traces must be such as to include the horizontal zones which provide the final migrated reflection (Fig. 3.2.1). If too small an aperture is chosen, the migrated section will be distorted. Usually computer time increases proportionately with the increase of aperture size.

It is necessary to preselect the aperture from the unmigrated data by some calculative process. The aperture is related to the horizontal
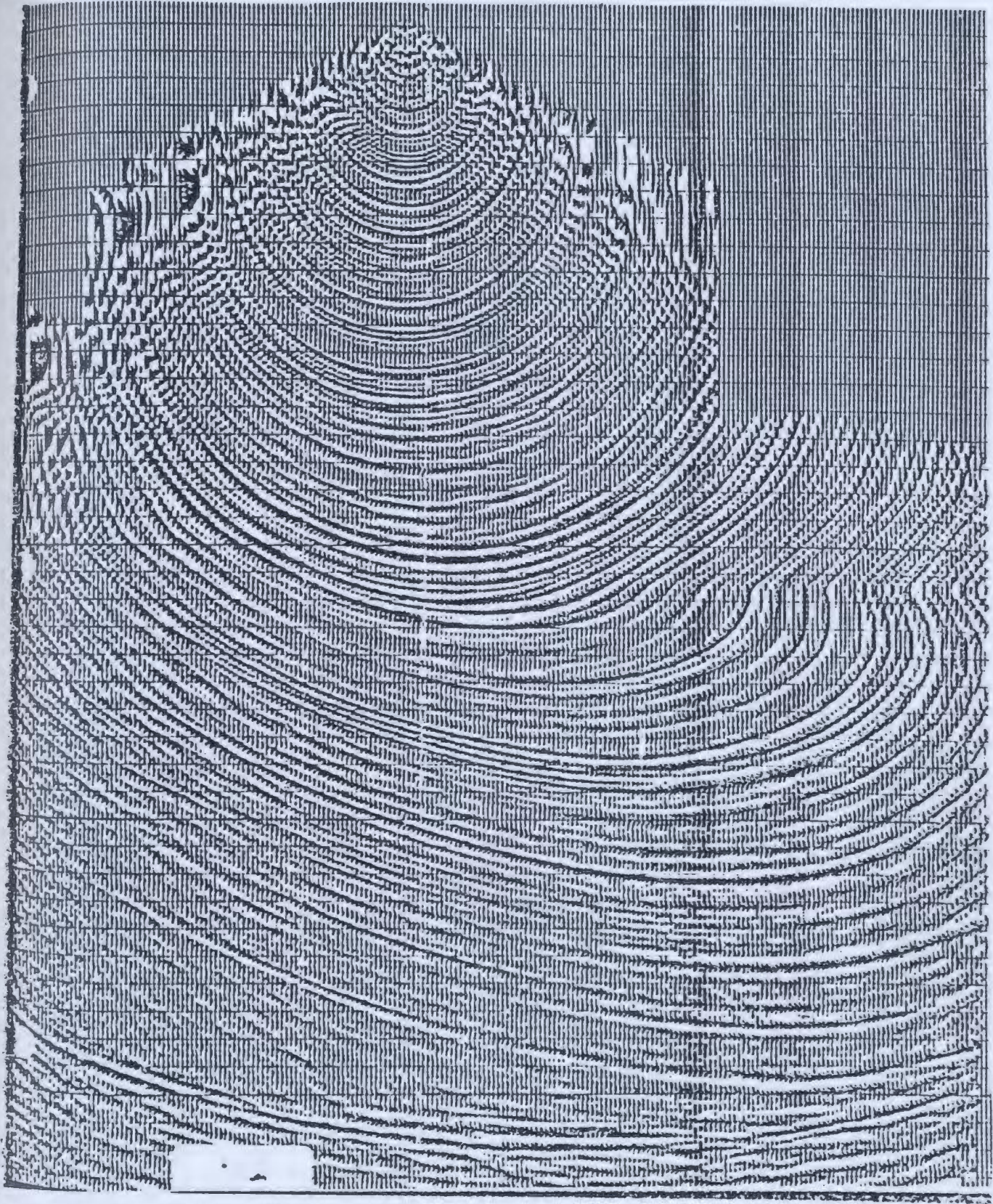
Figure 3.2.1   The reflection patterns due to different apertures
                (After Anstey, 1977).

displacement of the reflection point and can be calculated from the time gradient on the unmigrated section and the velocity distribution (Anstey, 1977). For our present analysis the apertures were calculated using the relation (Owusu et al., 1981).

$$r = (vz/2f)^{1/2}$$
3.2.1.2

where r is the migration aperture

v is the medium velocity

z is the depth of the reflector

and f is the frequency of the pulse

Table 3.2.1 gives the apertures used for different sets of synthetic data.

Reflector's Dip of the model 'degree'	Velocity of the medium 'm/s'	Frequency of the pulse 'HZ'	Maximum depth considered 'm'	Aperture value equivalent to no. of traces
10	2000	25	376	5
20	2000	25	564	6
30	2000	25	777	7
40	2000	25	1039	8
50	2000	25	1392	9
60	2000	25	1932	11

Table 3.2.1   Different apertures values for different sets of synthetic model data.

The third requirement is to assign a velocity for the migration scheme.
The correct migration velocity can be obtained by generating migrated
traces with a number of constant velocities. The velocity that gives the
best migration stack will be taken as the correct migration velocity.
This correct velocity used in migration defines the effective Huygens
hyperbola on the assumption that all the Huygen's sources are in the plane
of the section (Anstey, 1977). For our present analysis a constant
velocity of 2000 m/s was used to migrate the synthetic data. The above
velocity choice was suitable because the synthetic time sections were
generated assuming a constant velocity which was the same as the migration
velocity.

3.2.2   Implementation of Migration by Computer

A computer programme was developed (Appendix-1) to implement the
diffraction stack migration on the VAX/VMS 11/780 computer system. The
entire procedure is presented here in considering the aperture (5 traces)
for the synthetic data generated with reflector dip equal to five
degrees. First the input traces 1 through 11 were composited to obtain
data for plotting on a single output trace (trace 6),which was printed out
on the final record section (Fig. 3.2.2). This output trace (trace 6)
gives the time at the vertex position for a particular curve of maximum
convexity that crosses the input traces 1 to 11. The sampling time was
used to determine trace amplitudes on each of the 11 input traces at the
position where the trace was crossed by the curve of maximum convexity
having its vertex at a time equals to T_o (two-way vertical time) on the

OUTPUT TRACES

Vertex for $T_0 = 1.200s$

Curve of maximum convexity-window for addition of signals

INPUT TRACES 1 to 11

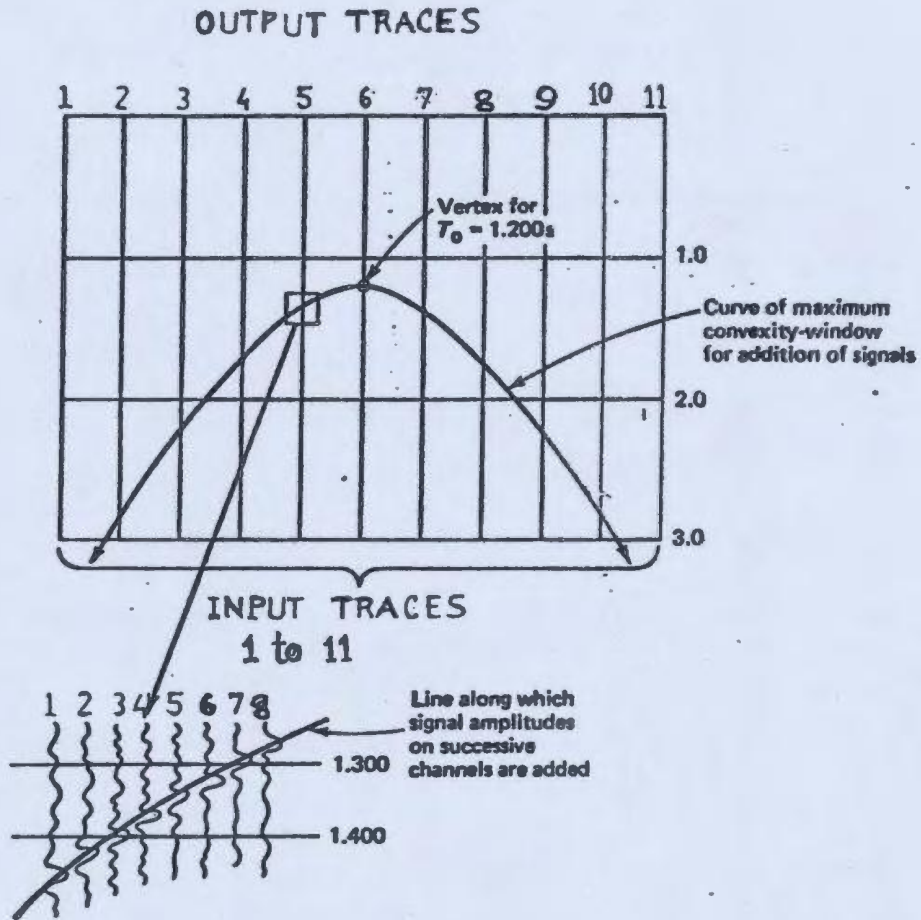Line along which signal amplitudes on successive channels are added

Figure 3.2.2   Principle of computer migration using curve of maximum convexity with an aperture of 5 input traces.

trace number 6. The amplitudes at these time were summed to obtain an output value which was plotted on the centre trace (6) at a time equal two-way vertical time T . Strong reflection or diffraction peaks were enhanced at the vertex position resulting in a large amplitude value in the output trace. The vertex position represents the true position of the event in space.

The vertex times for which amplitudes stored were separated by the next sampling interval for the subsequent summation process on trace number 6. Now this will generate a different curve of maximum convexity. A total of 1800 curves of maximum convexity were generated for summation of points for a 1.8 second synthetic section considering the sampling interval as 1 ms.

After completing all output values for the trace number 6, the computation was carried out in the similar fashion for the next trace number 7. Now the input window (aperture) was extended from traces 2 to 12. The whole process was continued up to the end of required migrated traces. Finally the migrated record sections were plotted using the computer programme developed (Appendix-1) for plotting the migrated sections. For our analysis each migration job took exactly one hour CPU time on the VAX/VMS 11/780 computer system.

3.3   Results of Migrated Sections

Two synthetic models were used - an inclined reflector and an anticline to
implement the diffraction stack algorithm (Appendix-1). Both models
consist of a single reflecting surface overlain by a material of constant
velocity 2000 m/s (Fig. 3.1.1 and Fig. 3.1.2). Zero offset (stacked)
single fold synthetic reflection data were generated over an area above
the reflecting surface and are used as an input to the migration scheme.
Both models were investigated for various dip angles of the subsurface
reflector with dip values 10°, 20°, 30°, 40°, 50° and 60°.
Finally, the models were tested with different migration velocities to
implement the diffraction stack method. A record length of 1.8 sec
equivalent to 1800 data samples were used for diffraction stack migration.
A trace interval of 25m was used for all the migrated sections. The
horizontal and vertical scales were kept constant for both migrated and
unmigrated sections for plotting. The amplitude scale was also kept
constant in both migrated and unmigrated sections.

3.3.1   An Inclined Reflector

Figures 3.3.1.1 to 3.3.1.6 represent the stacked (unmigrated) synthetic
time sections generated for dip angles 10°, 20°, 30°, 40° 50°
and 60° respectively. The corresponding migrated sections are presented
in Figures 3.3.1.7 to 3.3.1.12. These migrated sections were produced
with a migration velocity 2000 m/s which was same as the material velocity
considered for the synthetic model.

DIP OF REFLECTOR=10DEGREES

FIG.3.11   UNMIGRATED SECTION

DIP OF REFLECTOR=20DEGREES
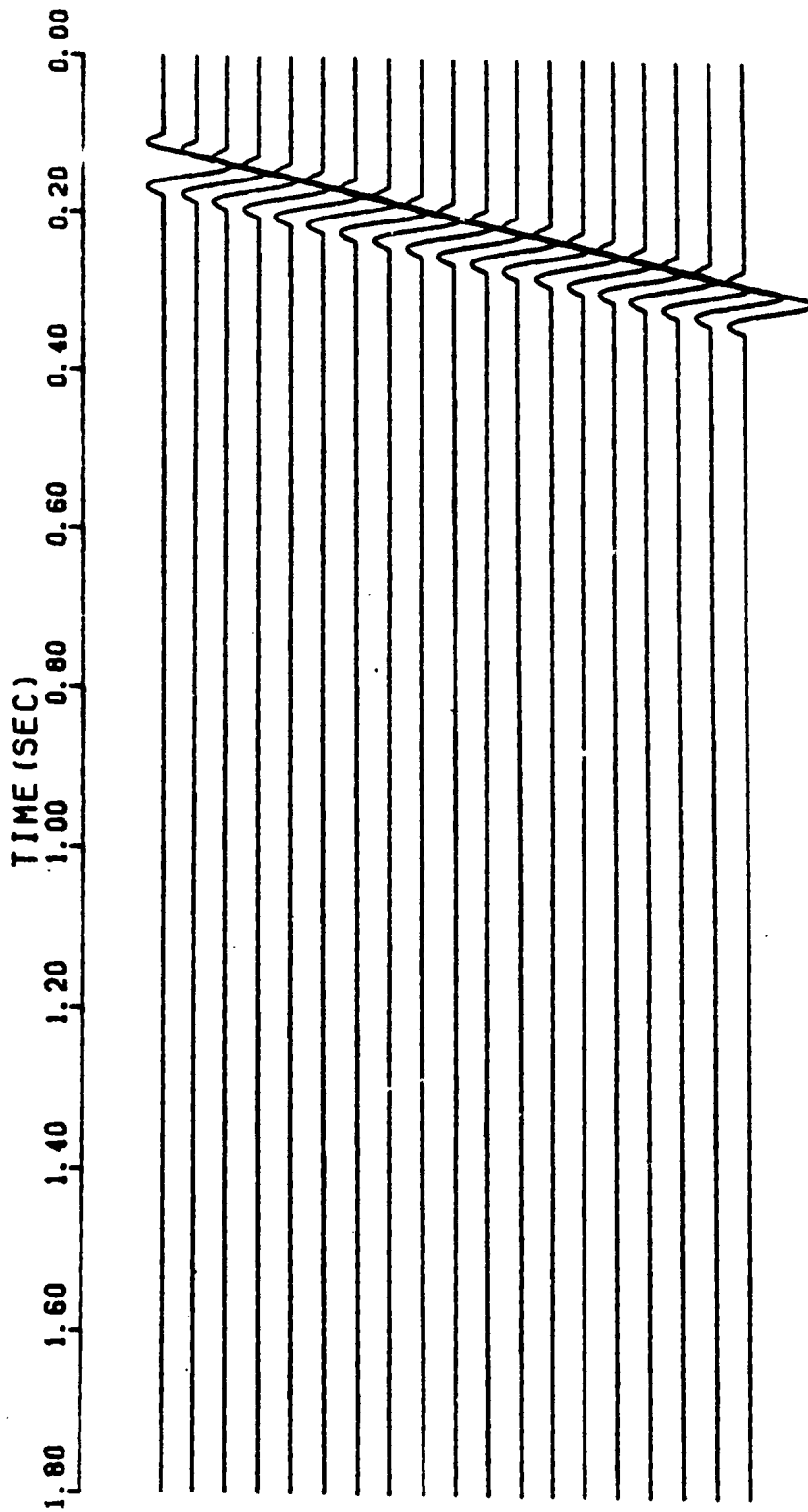
FIG.3.12 UNMIGRATED SECTION

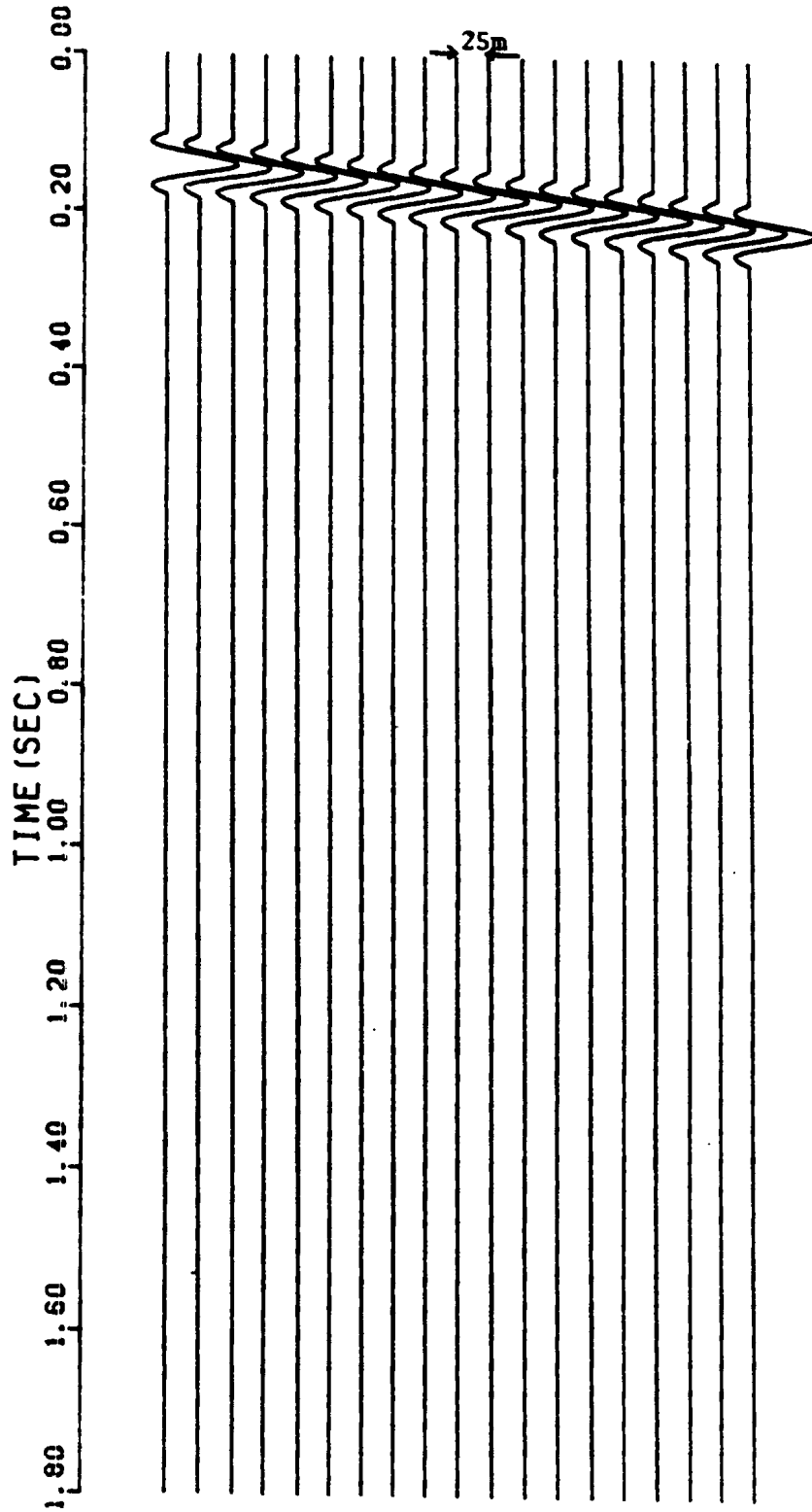DIP OF REFLECTOR=30DEGREES

TIME (SEC)
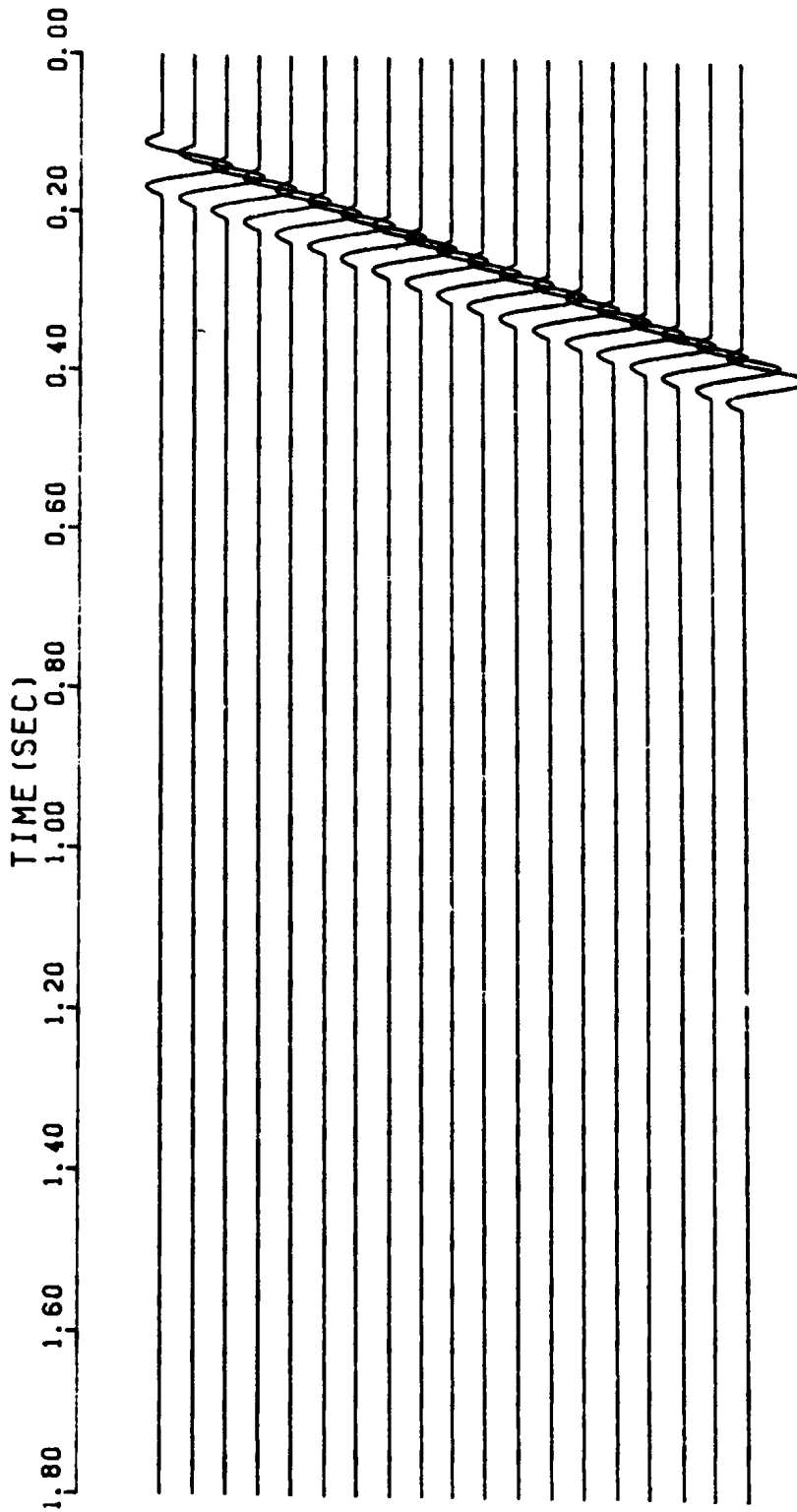
FIG.3.1.3 UNMIGRATED SECTION

DIP OF REFLECTOR=40DEGREES
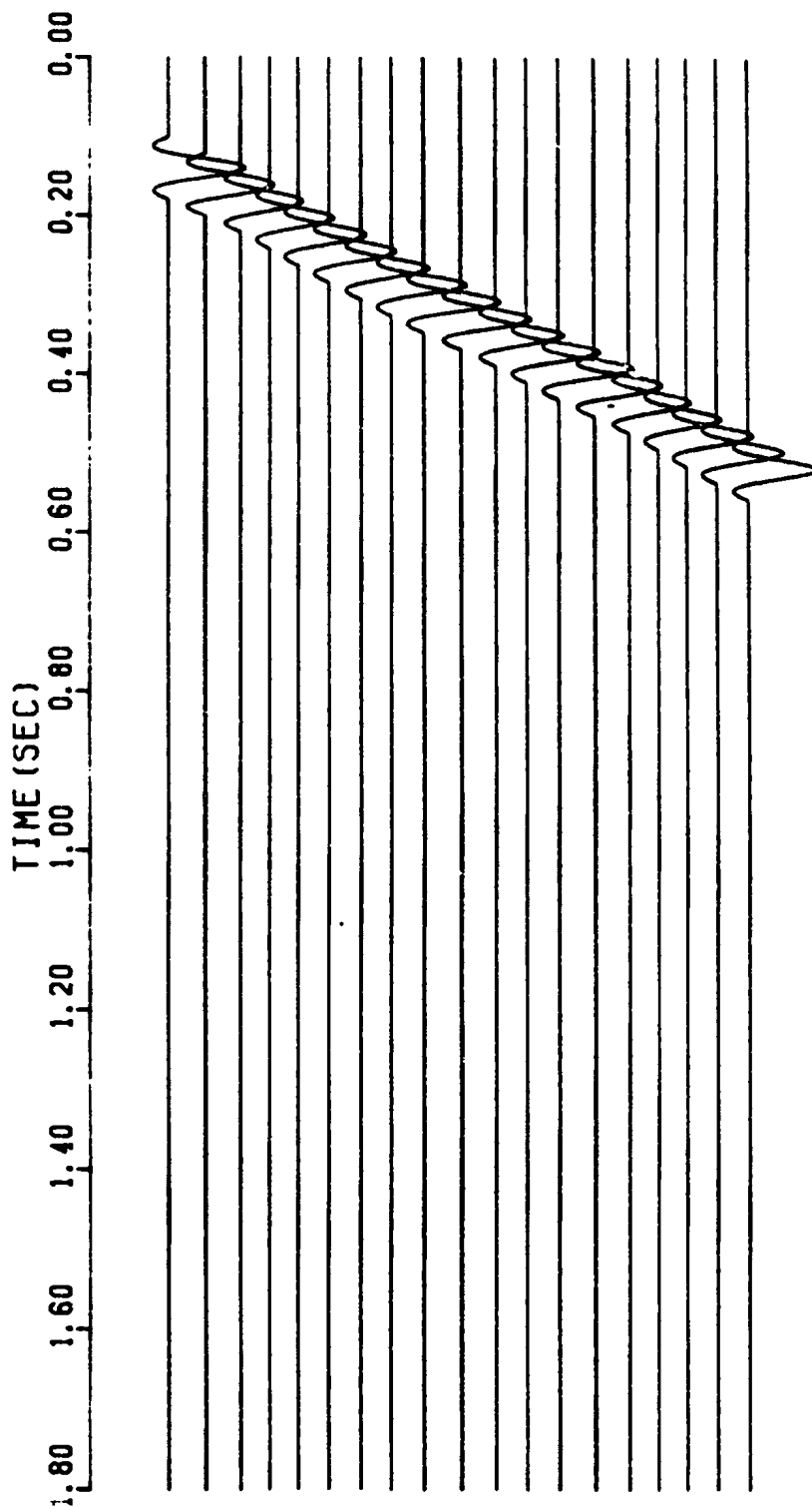
FIG.3.3.1.4 UNMIGRATED SECTION

DIP OF REFLECTOR=50DEGREES
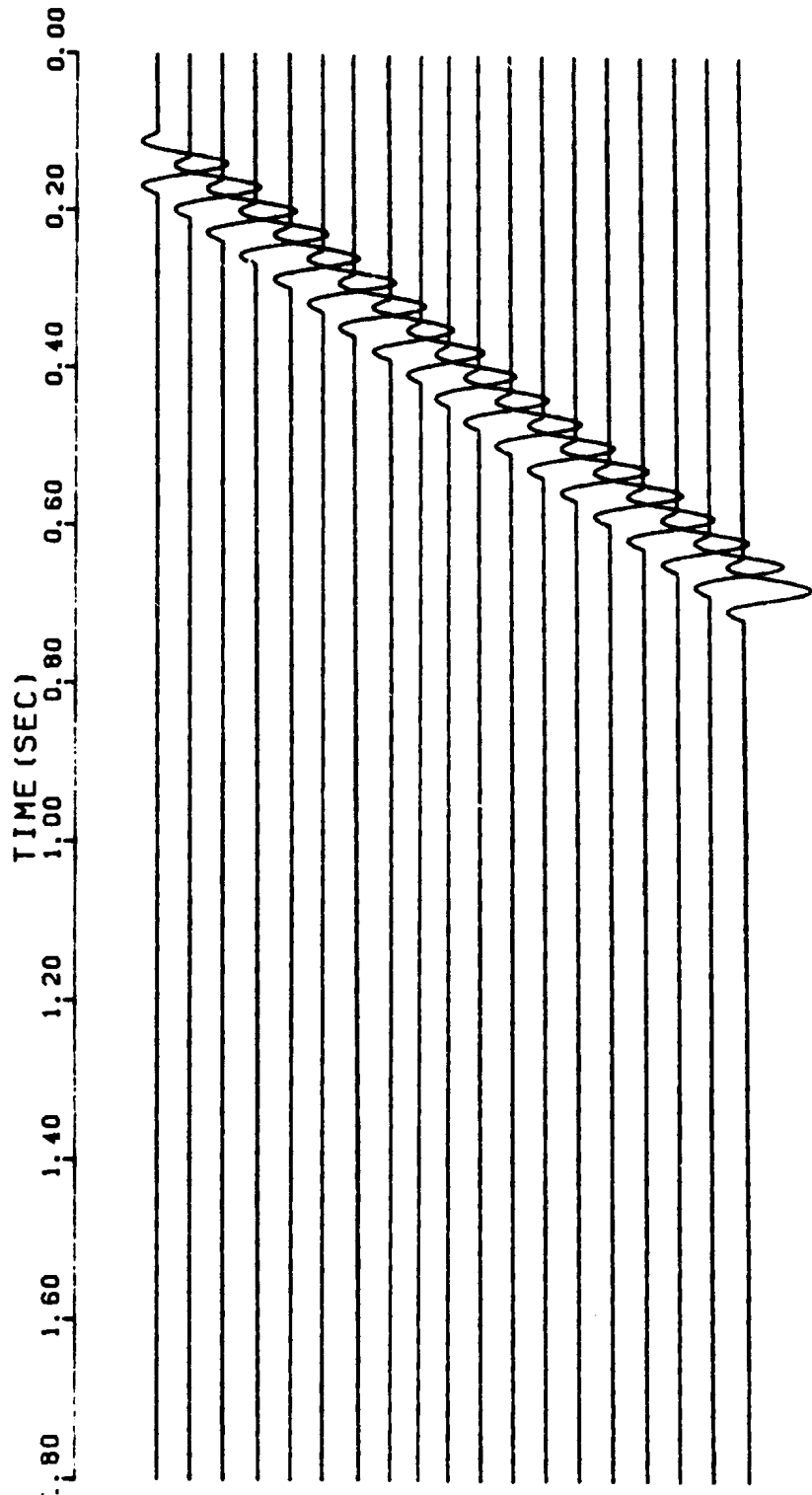
FIG.3.3.15 UNMIGRATED SECTION

DIP OF REFLECTOR=60DEGREES
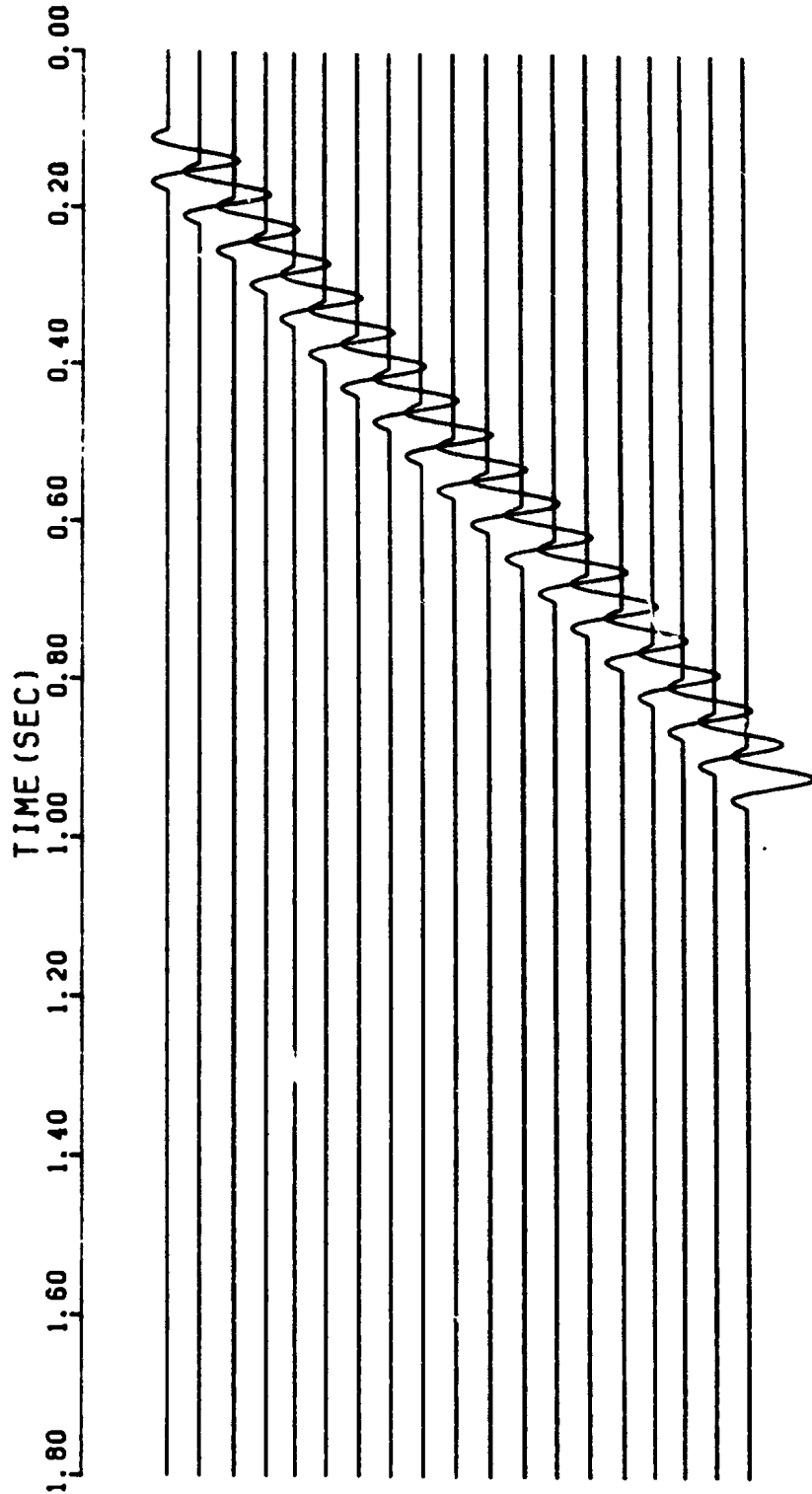
FIG.3.16 UNMIGRATED SECTION

MIGRATION VELOCITY=2000 M/S
REFLECTOR DIP=10DEGREES

TIME (SEC)

FIG.3.3.1.7 MIGRATED SECTION

MIGRATION VELOCITY=2000 M/S
REFLECTOR DIP=20DEGREES

FIG.3.18 MIGRATED SECTION

MIGRATION VELOCITY=2000 M/S
REFLECTOR DIP=30DEGREES

FIG.3.3.1.9 MIGRATED SECTION

FIG.33110 MIGRATED SECTION
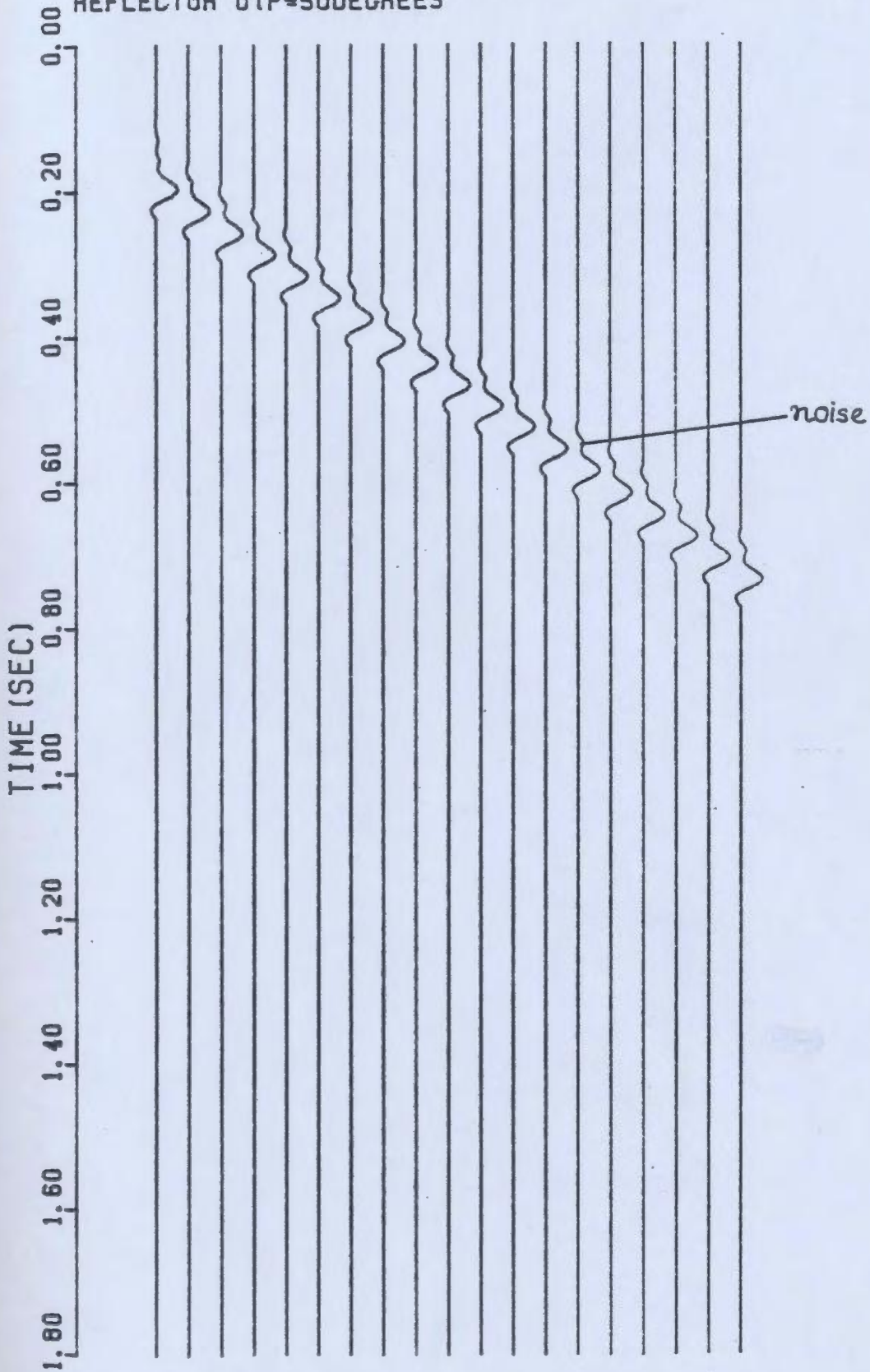
FIG.3.3.1.1 MIGRATED SECTION
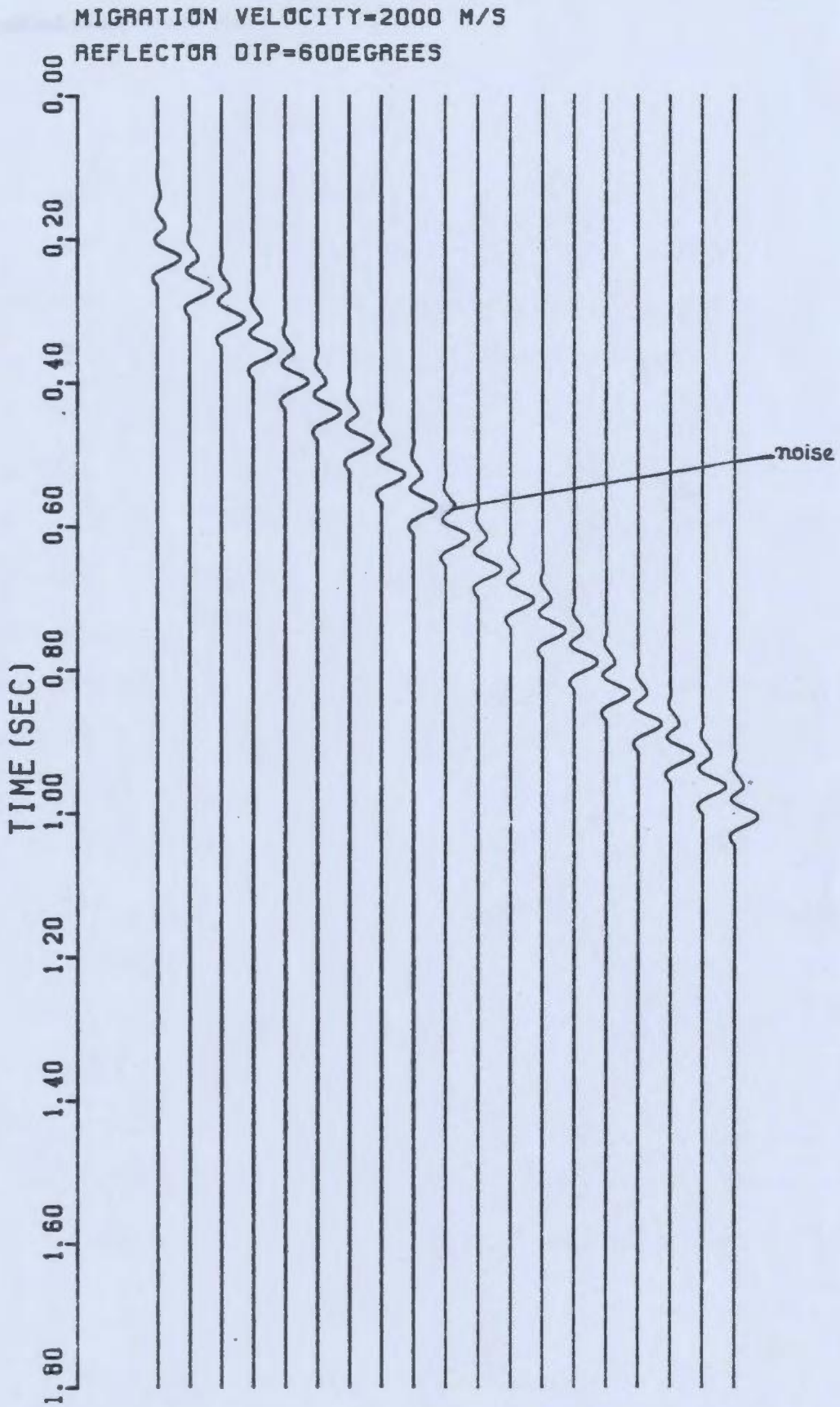
FIG.3.3.1.12 MIGRATED SECTION

The migrated sections (Figures 3.3.1.7 to 3.3.1.12) look better than the stacked (unmigrated) sections. Diffractions are migrated to their true positions. A reduction o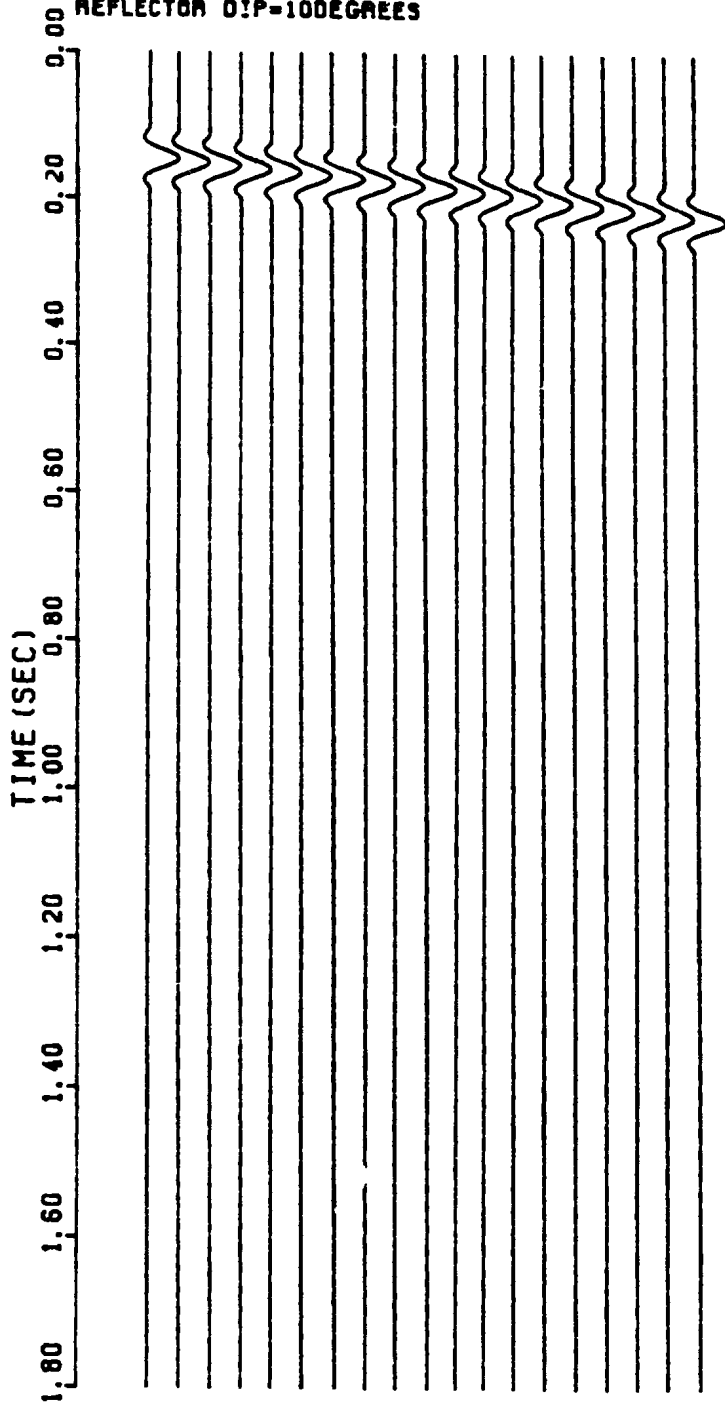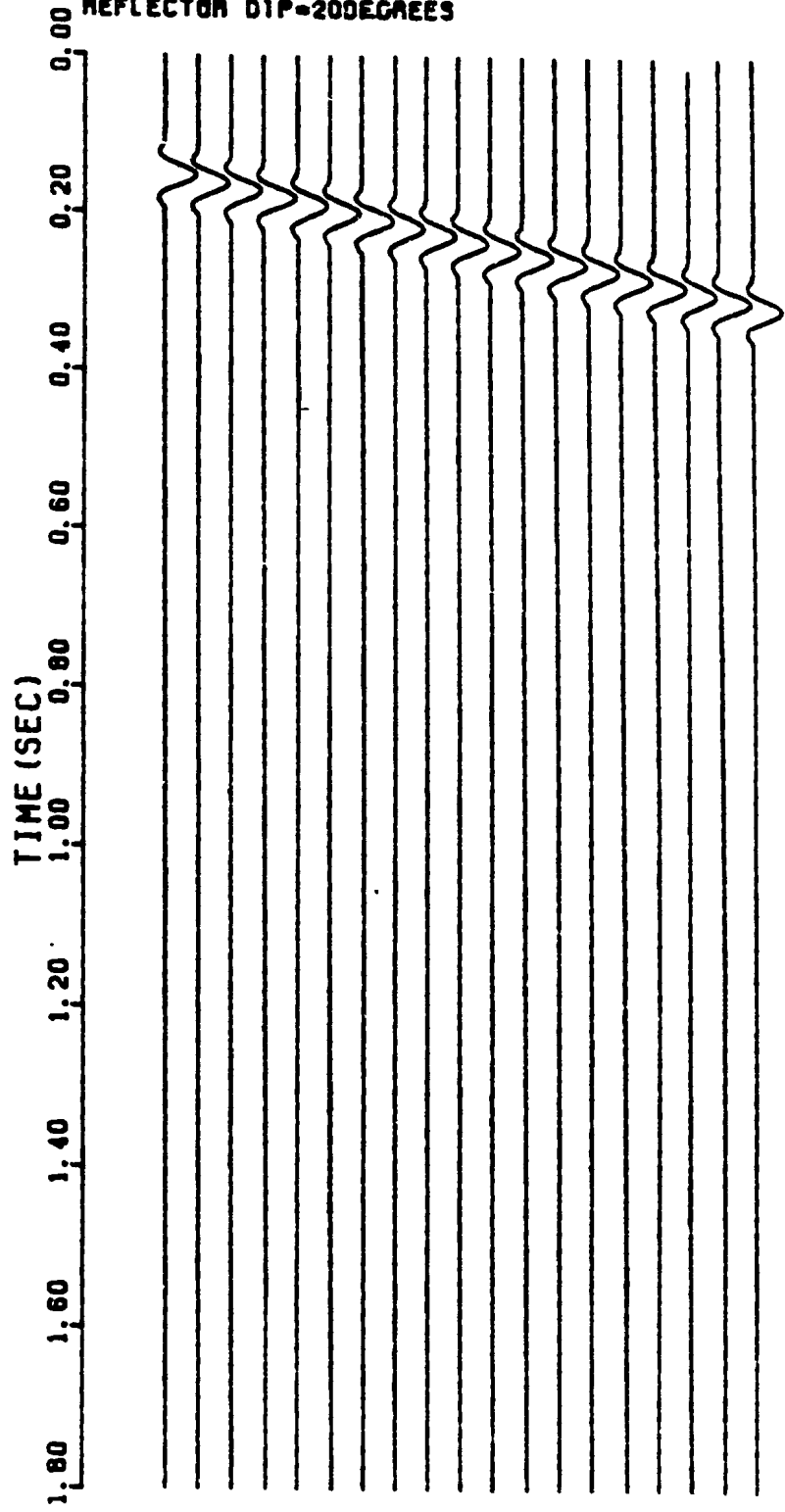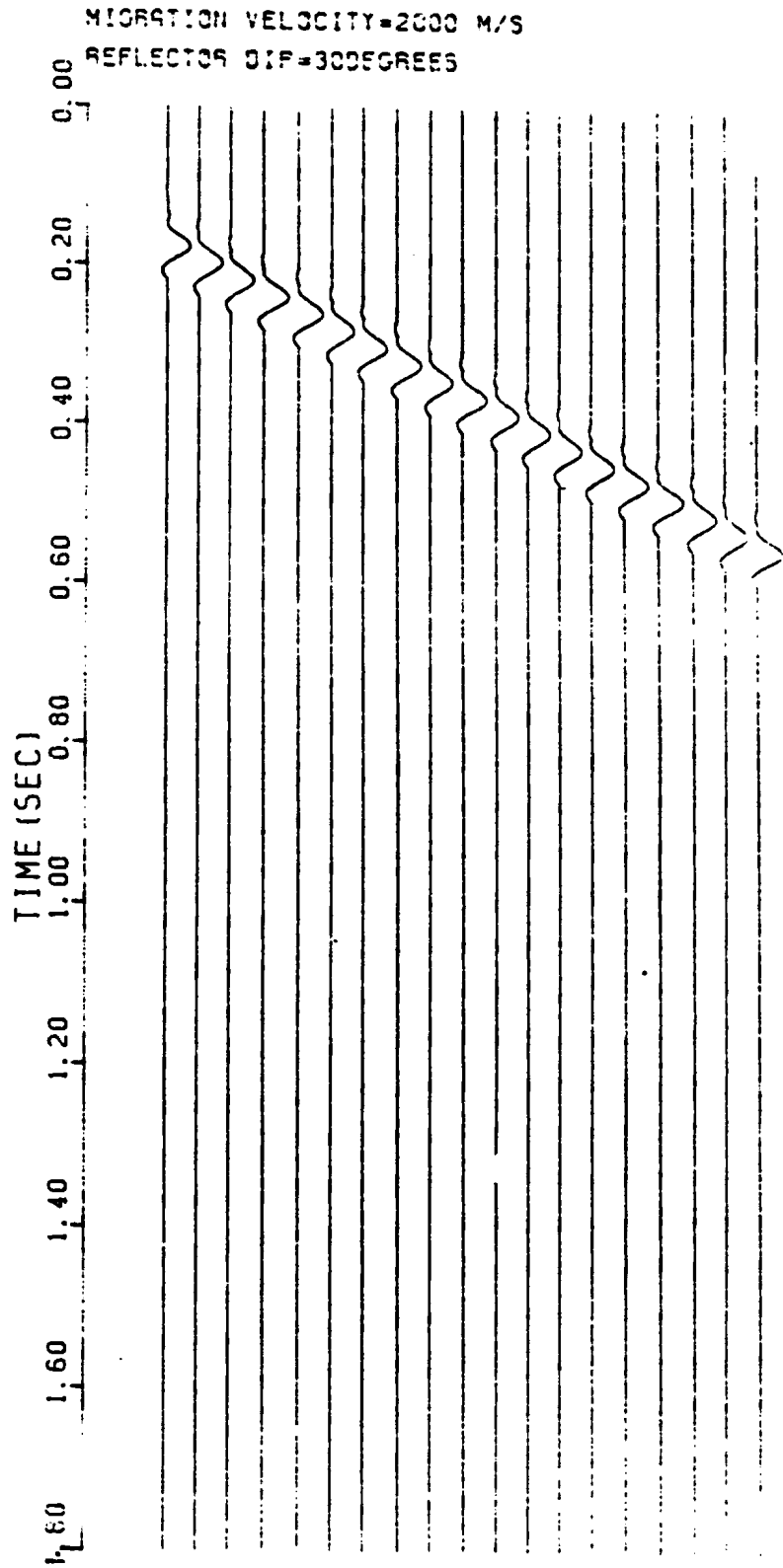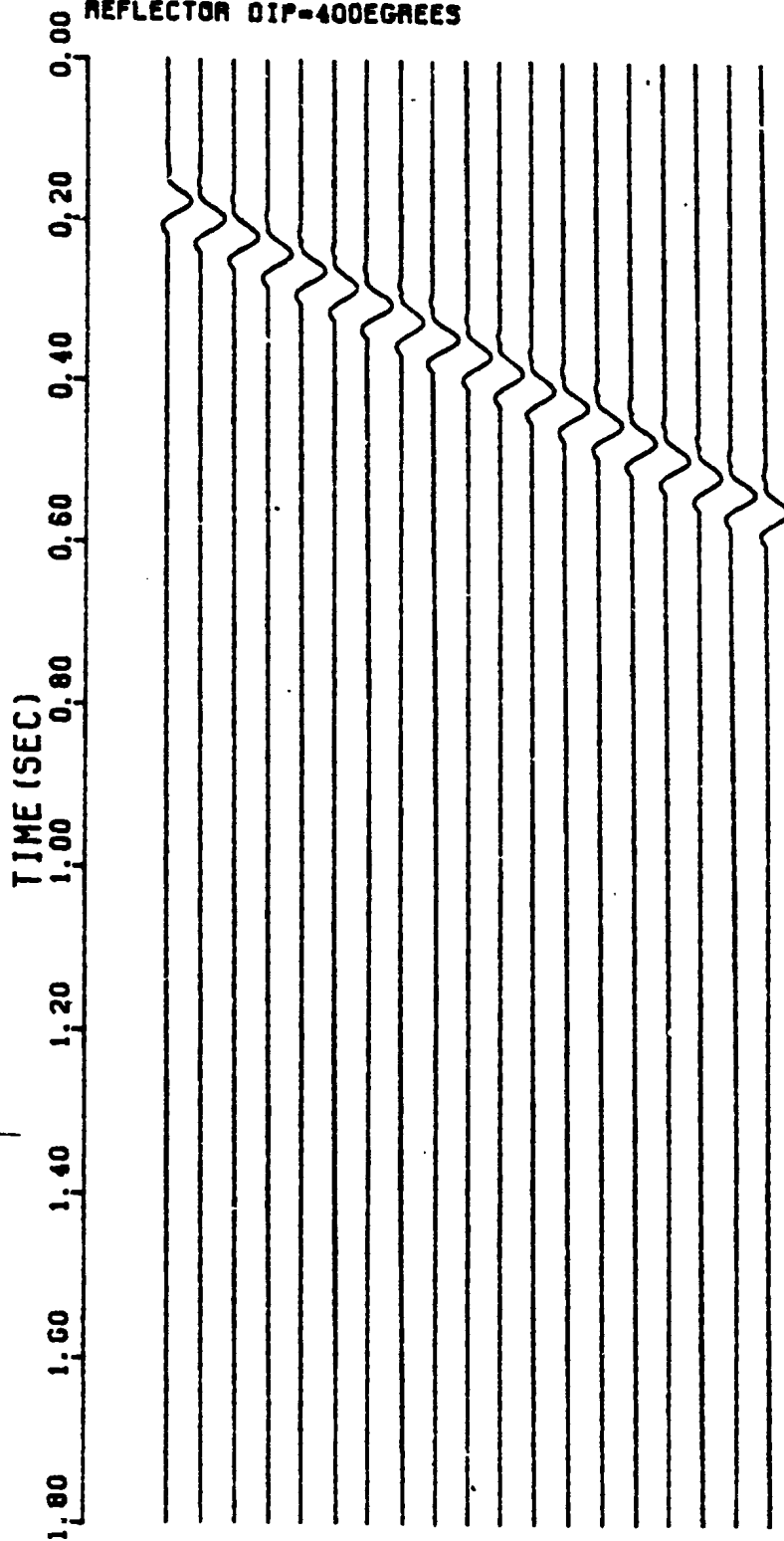f amplitude by a factor 2.0 was observed in all the migrated sections and pulse shapes were broadened due to loss of high frequency content in the reflected pulse. The highest frequency content in the reflected pulse in the migrated sections was in the range of 10 to 15 HZ showing a frequency shift from the original signal. It is observed that noise was introduced into the migrated sections with reflector dip greater than 40° (Figures 3.3.1.11 and 3.3.1.12). During the migration process a phase change was noticed which is shown in the Figure 3.3.1.13. A graph was plotted (Fig. 3.3.1.13) between time shift and offset distance taking different dip angles of the reflector. The time shift was calculated from the peak position of (considering the highest amplitude) the unmigrated and migrated pulse taking the same offset distance. It was evident from Figure 3.3.1.13 that phase change is independent of offset distance. The phase shift is constant for a particular dip angle of the reflector. There is a sudden jump in phase shift after the reflector dip equals to 30 degrees. This shows phase shift is dependent on increase of dip angle of the subsurface reflector. The data were fitted by a least-squares polynomial of the form $\Delta t = a\phi + b\phi^2 + c$. A Fortran subroutine for the least-squares fit of the polynomial was used to calculate the co-efficients (James et al., 1977). Figure 3.3.1.14 represents the least-square fit of the data obtained from the Table-3.3.1.
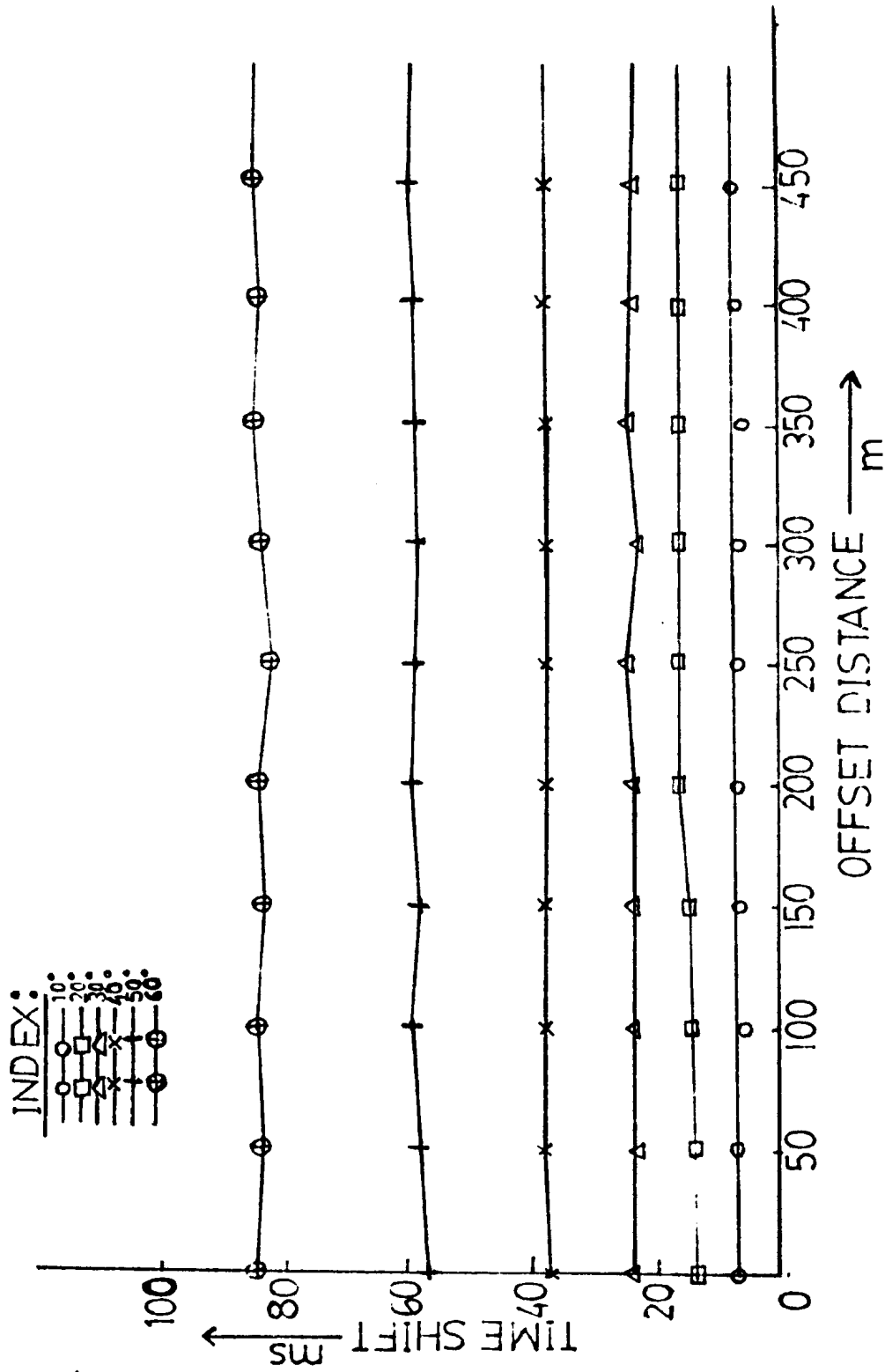
FIG. 3.3.1.13   TIME SHIFT-OFFSET DISTANCE CURVE

Serial Number	Angle of Dip 'ϕ' in (Degrees)	Average Time shift 'Δt' in (ms)	Remarks
1	10	6	A straight line relationship of
2	20	14	the type $\Delta t = a\phi$ (where a is a
3	30	24	constant quality) can be obtained
4	40	38	A nonlinear relationship of the type
5	50	60	$\Delta t = a\phi + b\phi^2$ (where a and b are
6	60	85	constant quantities) can be obtained

Table-3.3.1 Effect of dip angle on phase is shown.

The graph (Figure 3.3.1.14) was plotted between average time shift and dip angle. The average time shift was obtained from the individual time shift for different offset distances considering only one dip angle at a time. A linear straight line relationship can be obtained between angle of dip and average time shift up to reflector dip equals to 30 degrees (Table-3.3.1). As the dip increases, this linear relationship is no longer valid but replaced with a nonlinear relationship (Table-3.3.1). A break in the slope (Figure 3.3.1.14) indicates that the method is stable up to a reasonable amount of phase change i.e., up to dip angles equal to 30 degrees.

The effect of velocity on diffraction stack migration was examined on
synthetic data generated for an inclined reflector dipping at an angle 30
degrees. The velocity was varied from 1500 m/s to 2500 m/s in steps of
100 m/s. The best migration velocity was 2000 m/s which was same as the
material velocity considered for the inclined reflector model. Figures
3.3.1.15 to 3.3.1.25 represent the migrated time sections produced with
different migration velocities for the above model. In general, the
migrated time sections are much clarified than unmigrated synthetic
section (Figure 3.3.1.9) generated for the above model with material
velocity 2000 m/s. Two extreme cases were examined on taking two
migration velocities 1500 m/s and 2500m/s. It is observed that a change
in velocity of $\pm$ 500 m/s from the actual migration velocity 2000 m/s
resulted a time shift in the order of $\pm$ 1 ms. It shows that change in
velocity has an effect over phase shift in the migrated section. This
error in phase can be detected if the sampling interval is 1 ms in the
migrated section.

3.3.2 An Anticline

Figure 3.3.2.1 to 3.3.2.6 represent the stacked (unmigrated) synthetic
time sections for the anticline model for which the flanks have dip angles
10°, 20°, 30°, 40°, 50°, and 60° respectively. The
corresponding migrated sections are presented in figures 3.3.2.7 to
3.3.2.12. These synthetic sections were migrated with material velocity
2000 m/s which was used in constructing the above model. In the migrated

MIGRATION VELOCITY=1500 M/S
REFLECTOR DIP=30DEGREES

FIG.3.3.1.5 MIGRATED SECTION

MIGRATION VELOCITY=1500 M/S
REFLECTOR DIP=30DEGREES
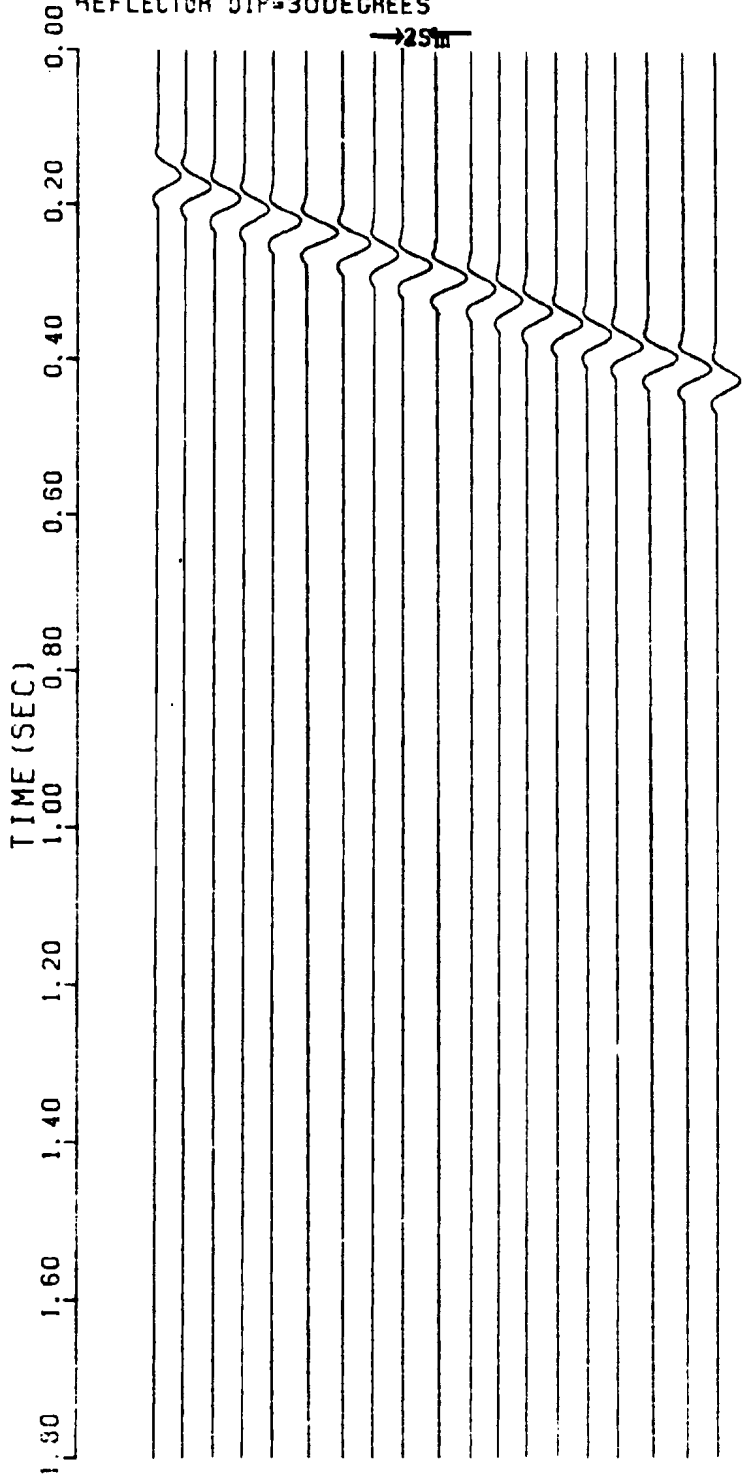
FIG.33115 MIGRATED SECTION

MIGRATION VELOCITY=1600 M/S
REFLECTOR DIP=30DEGREES
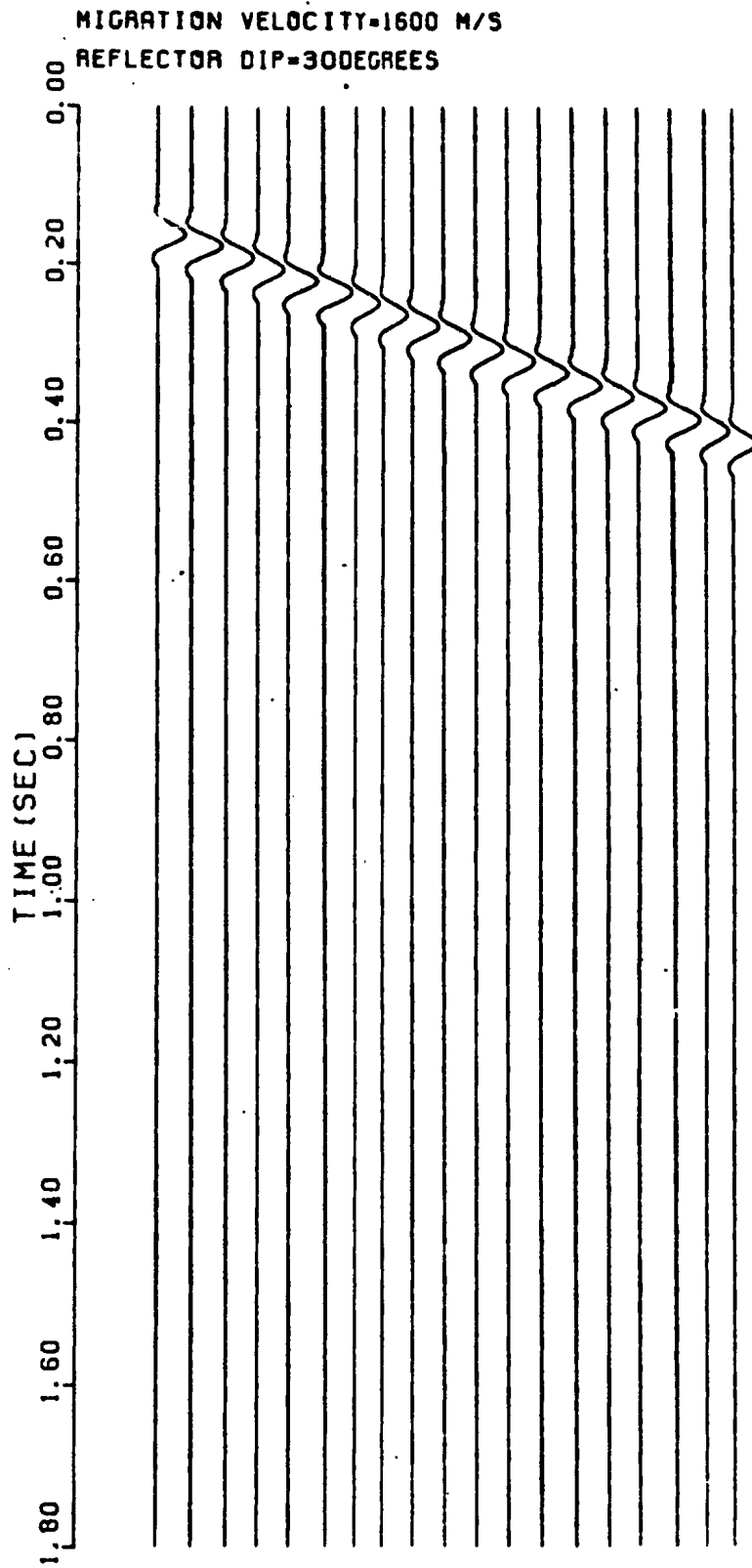
FIG.2.3.1 MIGRATED SECTION

MIGRATION VELOCITY=1700 M/S
REFLECTOR DIP=30DEGREES
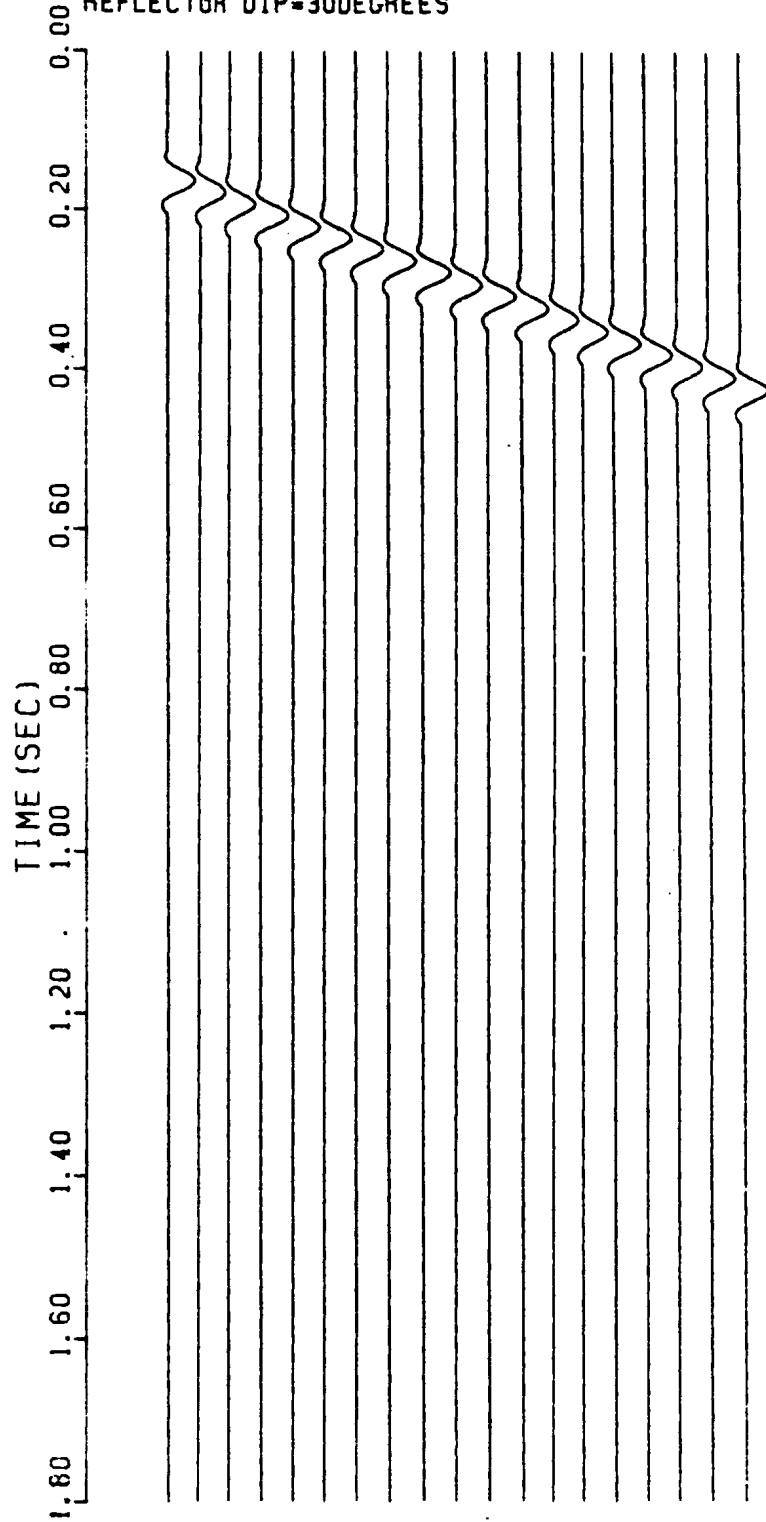
FIG.3.31.17 MIGRATED SECTION

MIGRATION VELOCITY=1800 M/S
REFLECTOR DIP=30DEGREES
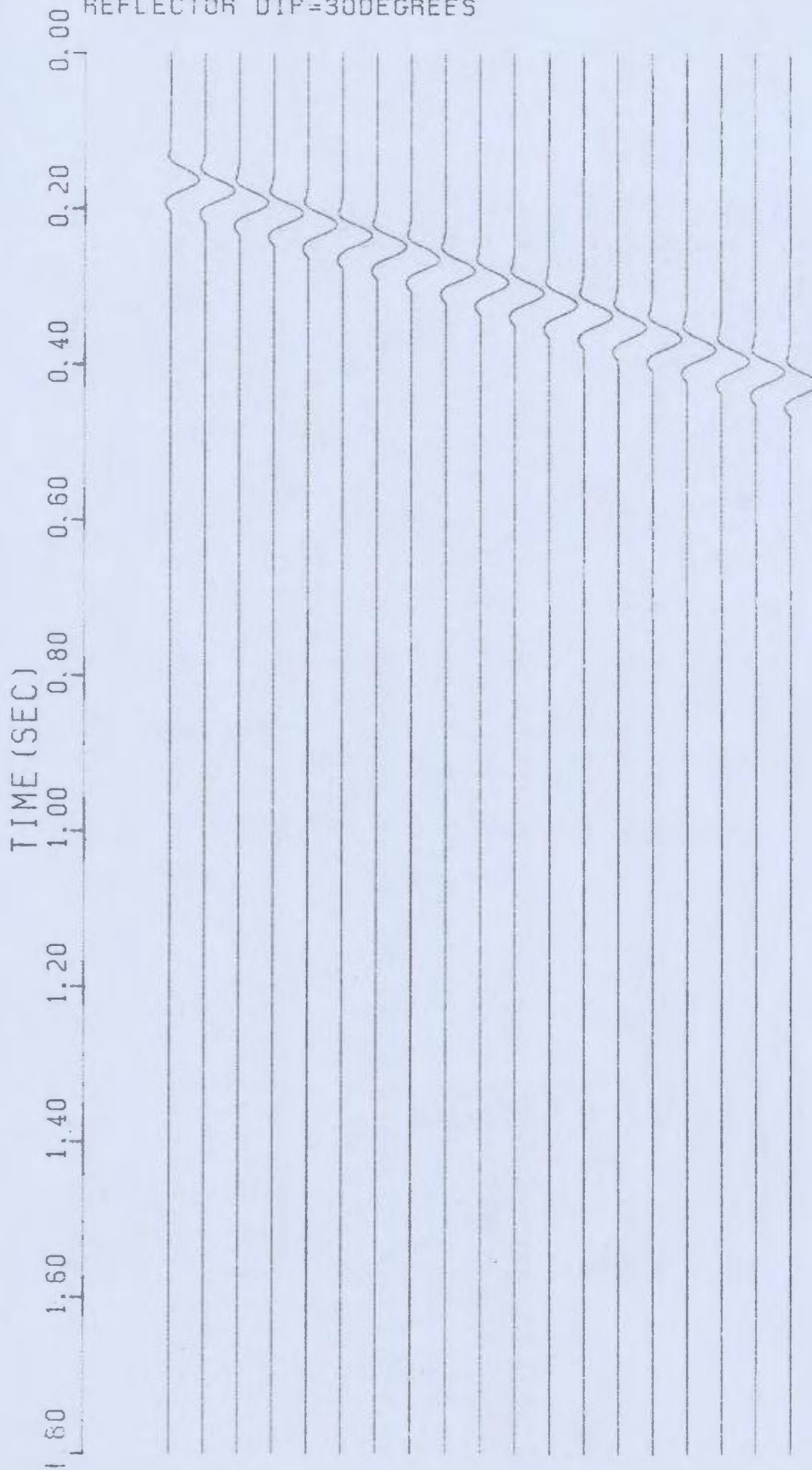
FIG.3.3.1.18 MIGRATED SECTION
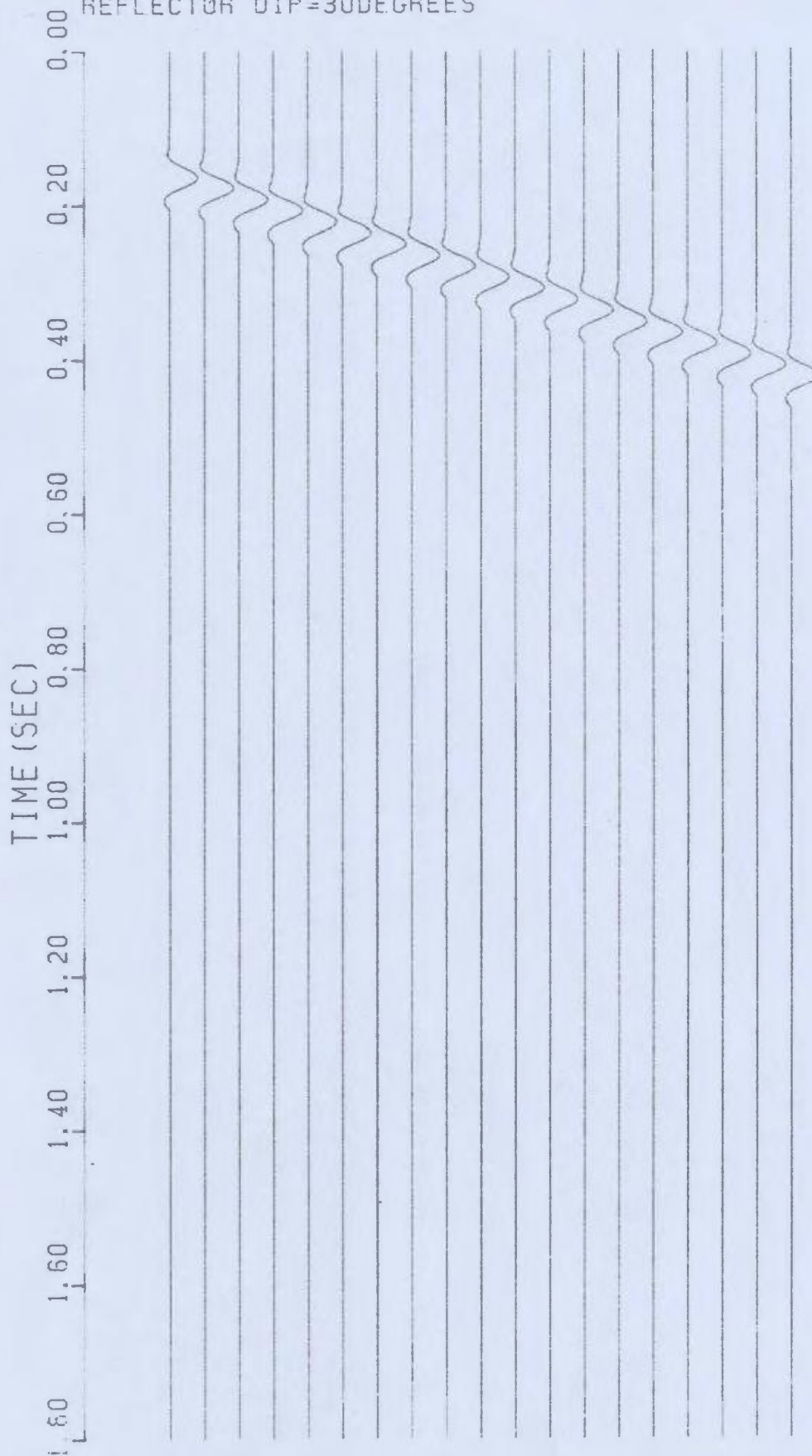
FIG. 3.3.1.19 MIGRATED SECTION

MIGRATION VELOCITY=2000 M/S
REFLECTOR DIP=30DEGREES
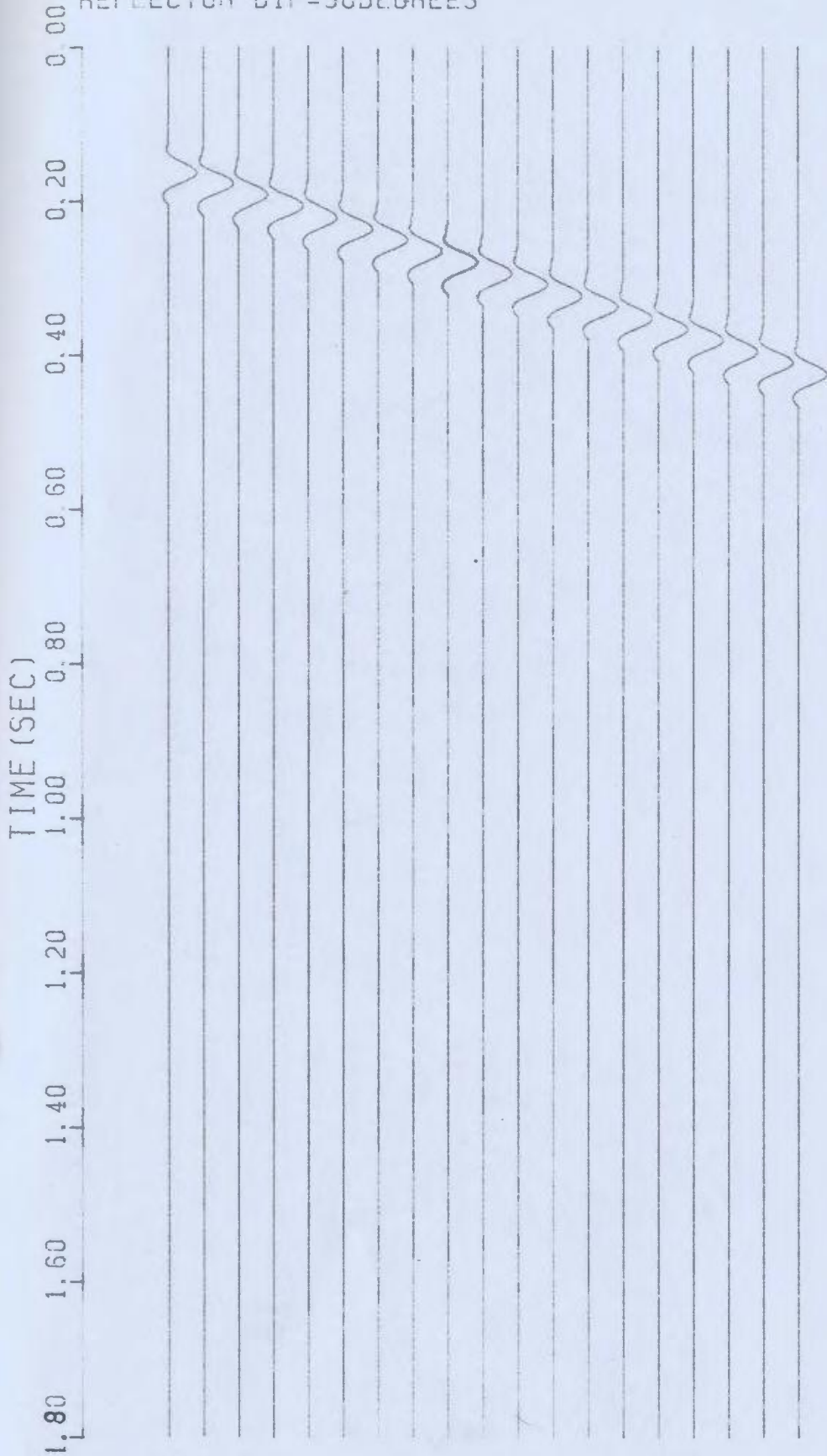
FIG.3.3.1.20 MIGRATED SECTION

MIGRATION VELOCITY=2100 M/S
REFLECTOR DIP=30DEGREES

TIME (SEC)
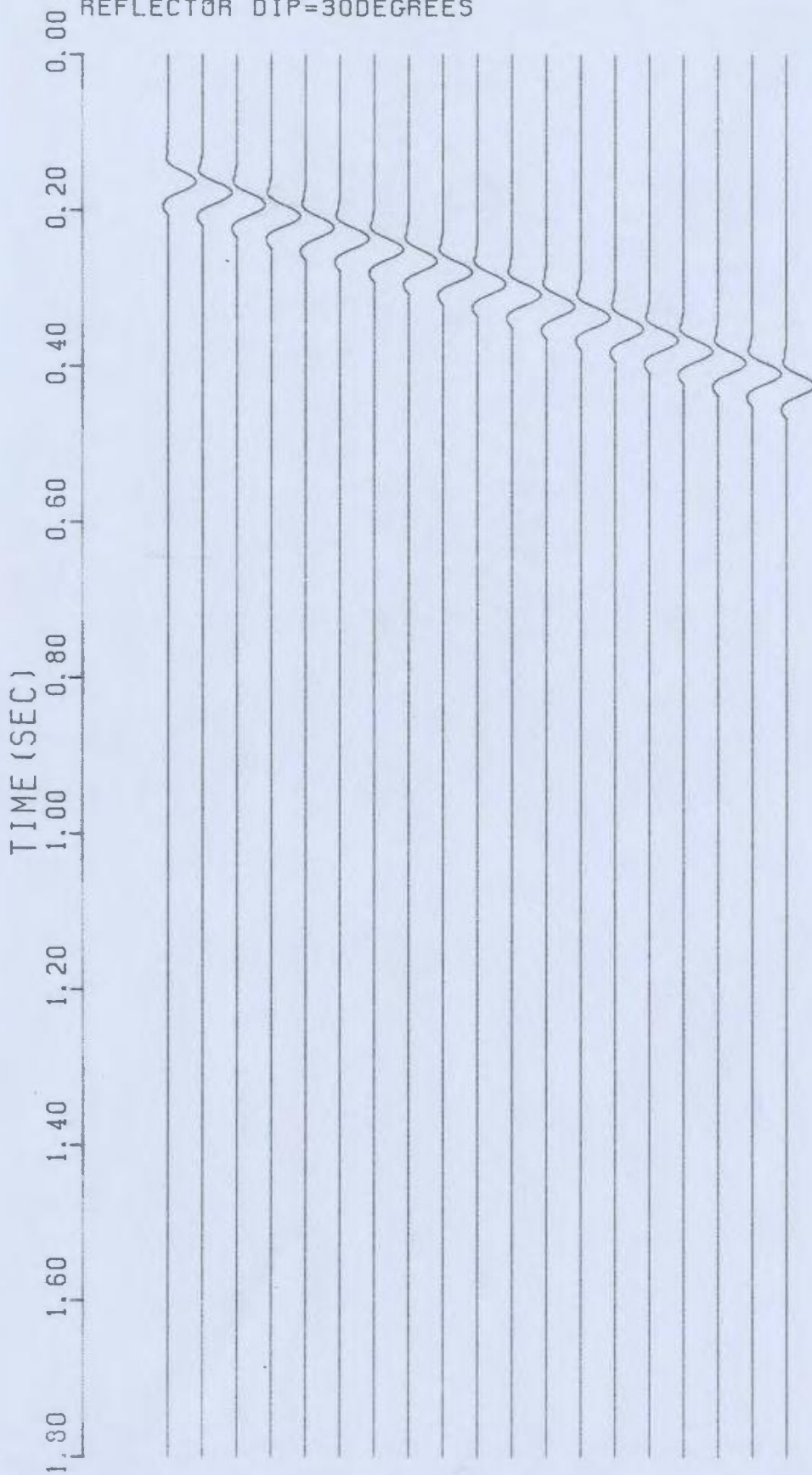
FIG.3.3.1.21 MIGRATED SECTION

MIGRATION VELOCITY=2200 M/S
REFLECTOR DIP=30DEGREES
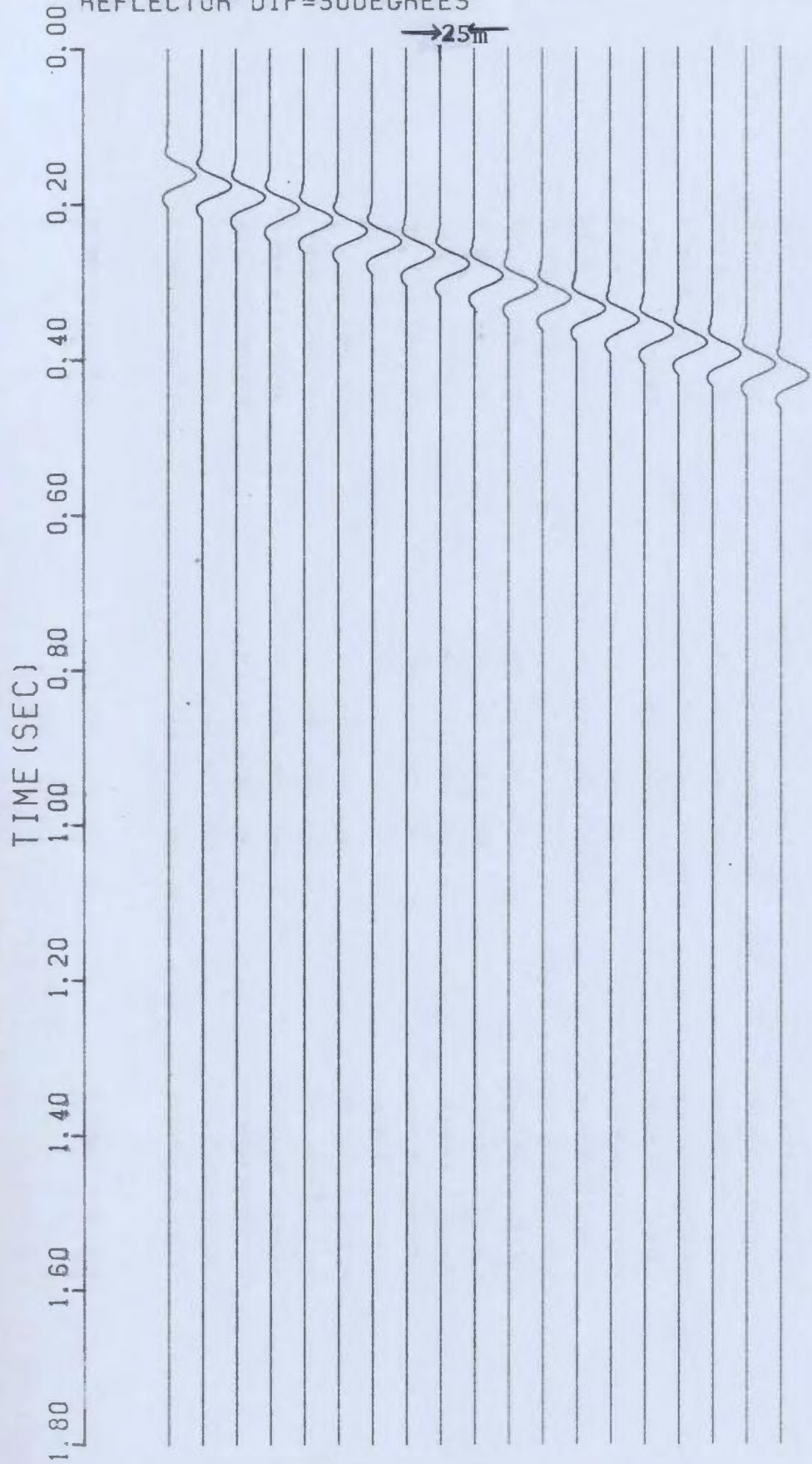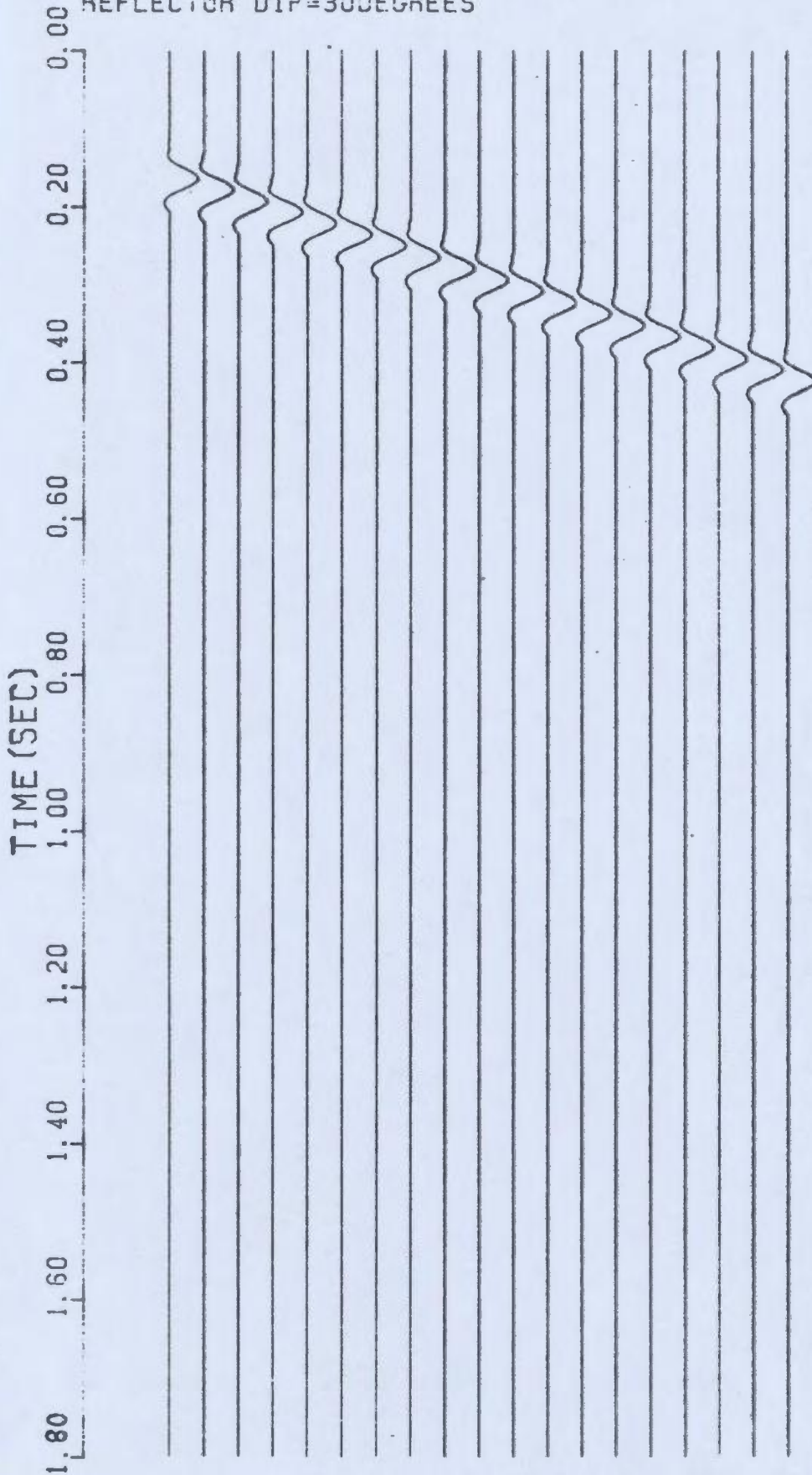
FIG.3.3.1.22 MIGRATED SECTION

MIGRATION VELOCITY=2300 M/S
REFLECTOR DIP=30DEGREES

TIME (SEC)
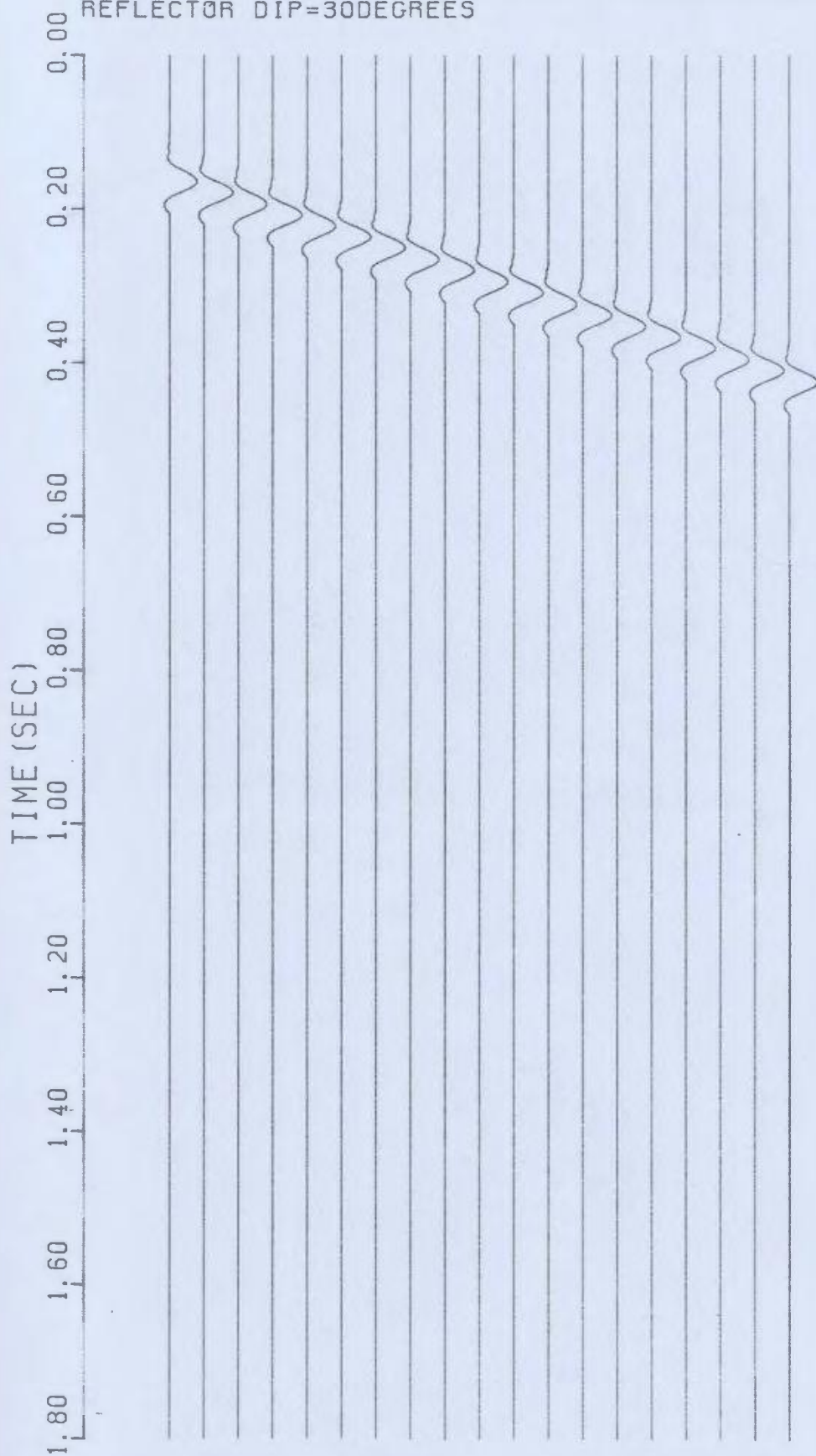
FIG.3.3.1.23 MIGRATED SECTION

MIGRATION VELOCITY=2400 M/S
REFLECTOR DIP=30DEGREES
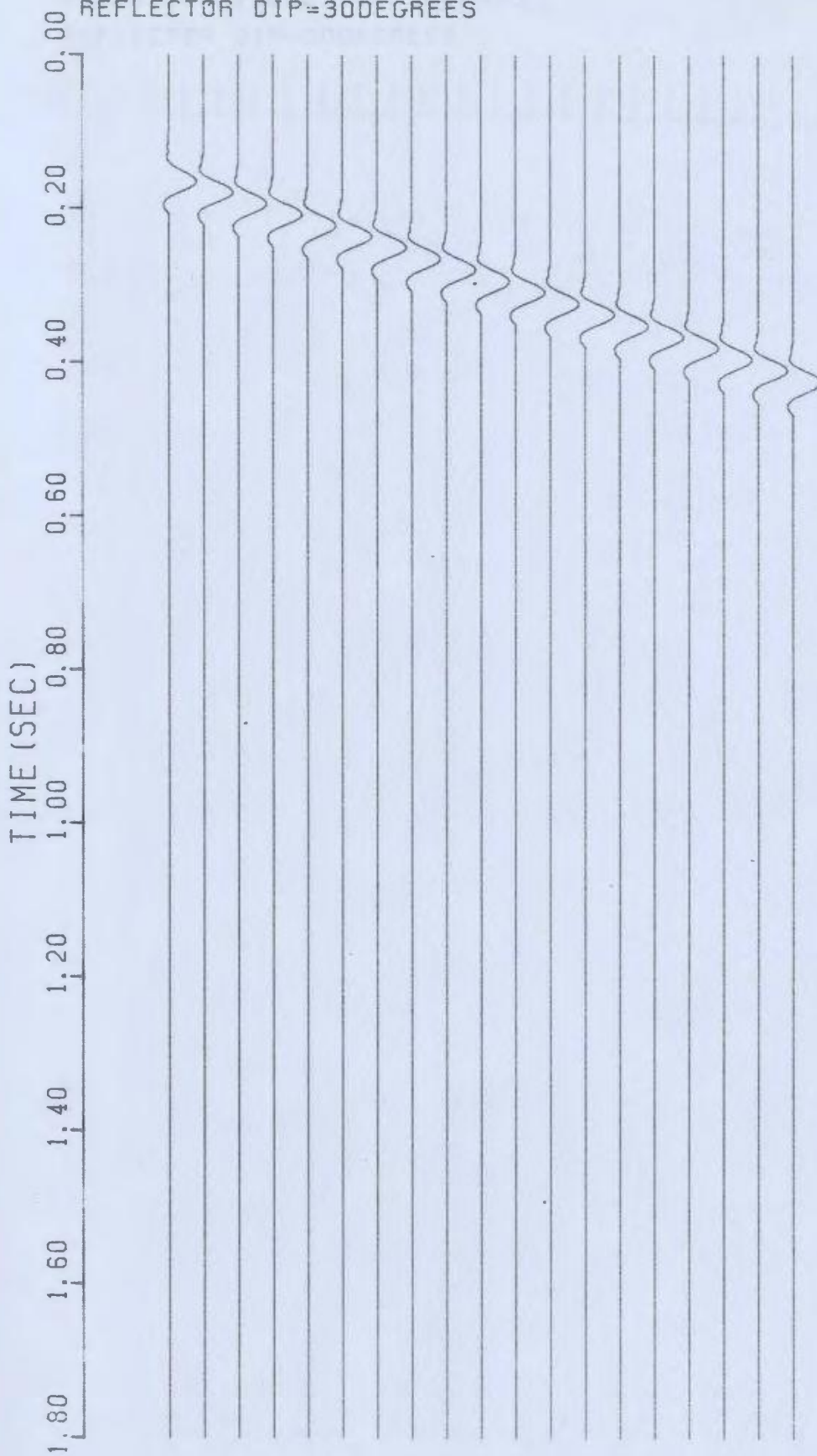
FIG.3.3.1.24 MIGRATED SECTION

MIGRATION VELOCITY=2500 M/S
REFLECTOR DIP=30DEGREES
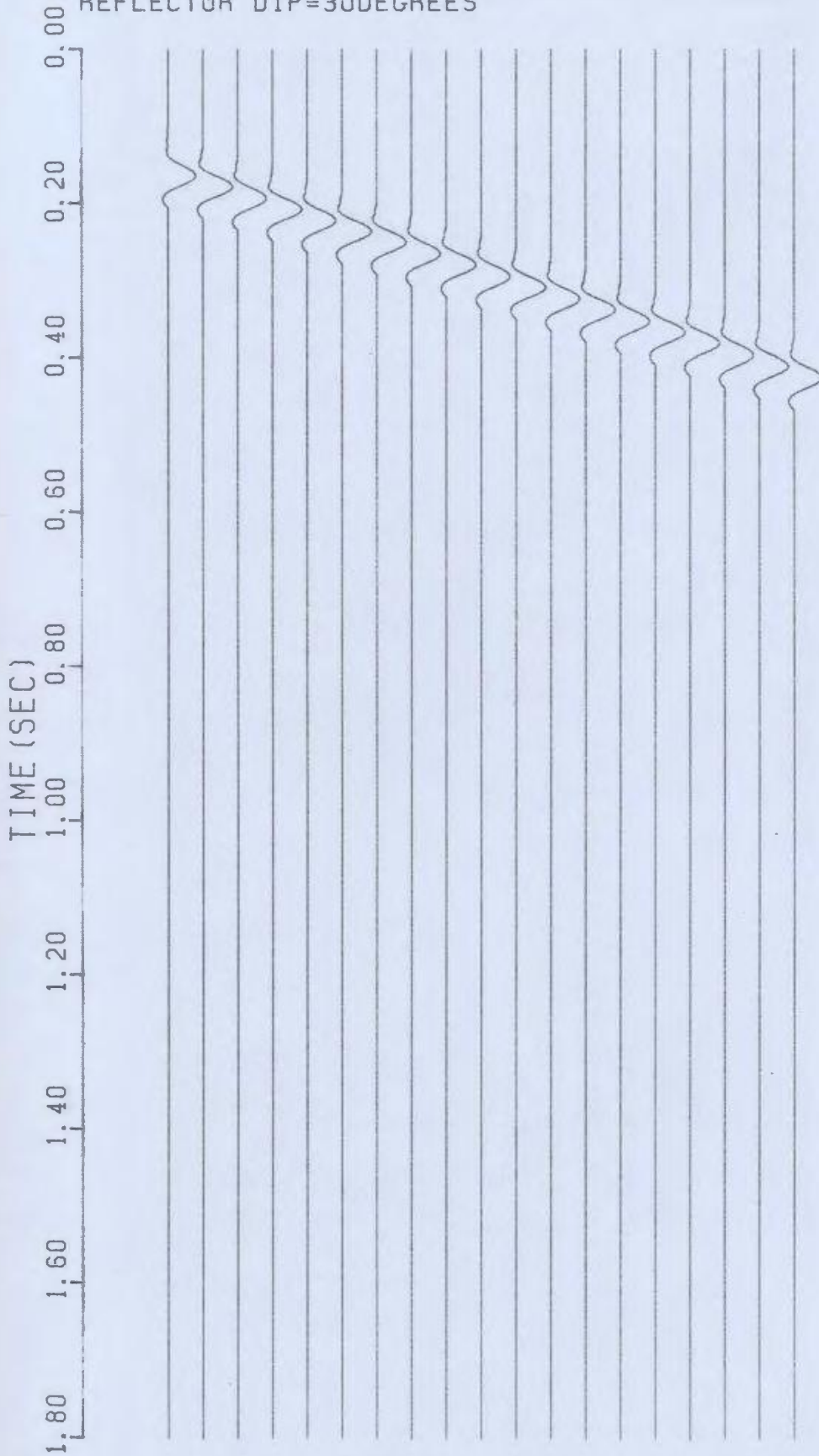
FIG.3.3.1.25 MIGRATED SECTION

sections, the anticline structure was better clarified than the unmigrated
sections. The diffraction patterns generated at the sharp boundaries of
the anticline were collapsed and breadth of anticline was reduced. The
amplitude was reduced by a factor of 3.0 in all the migrated sections of
the anticline portion compared to an amplitude reduction by a factor of
2.0 in the straight reflector portion of the anticline. The pulse shapes
were broadened due to the loss of high frequency content in the reflected
pulse. Noise was observed in the migrated sections (Figures 3.3.2.11 and
3.3.2.12) with their reflector dip angle 50° and 60° respectively.
This indicates that noise was introduced during the migration process from
steeply dipping events. The effect of velocity on diffraction stack
migration was not studied for this particular model.

DIP OF ANTICLINE=10DEGREES
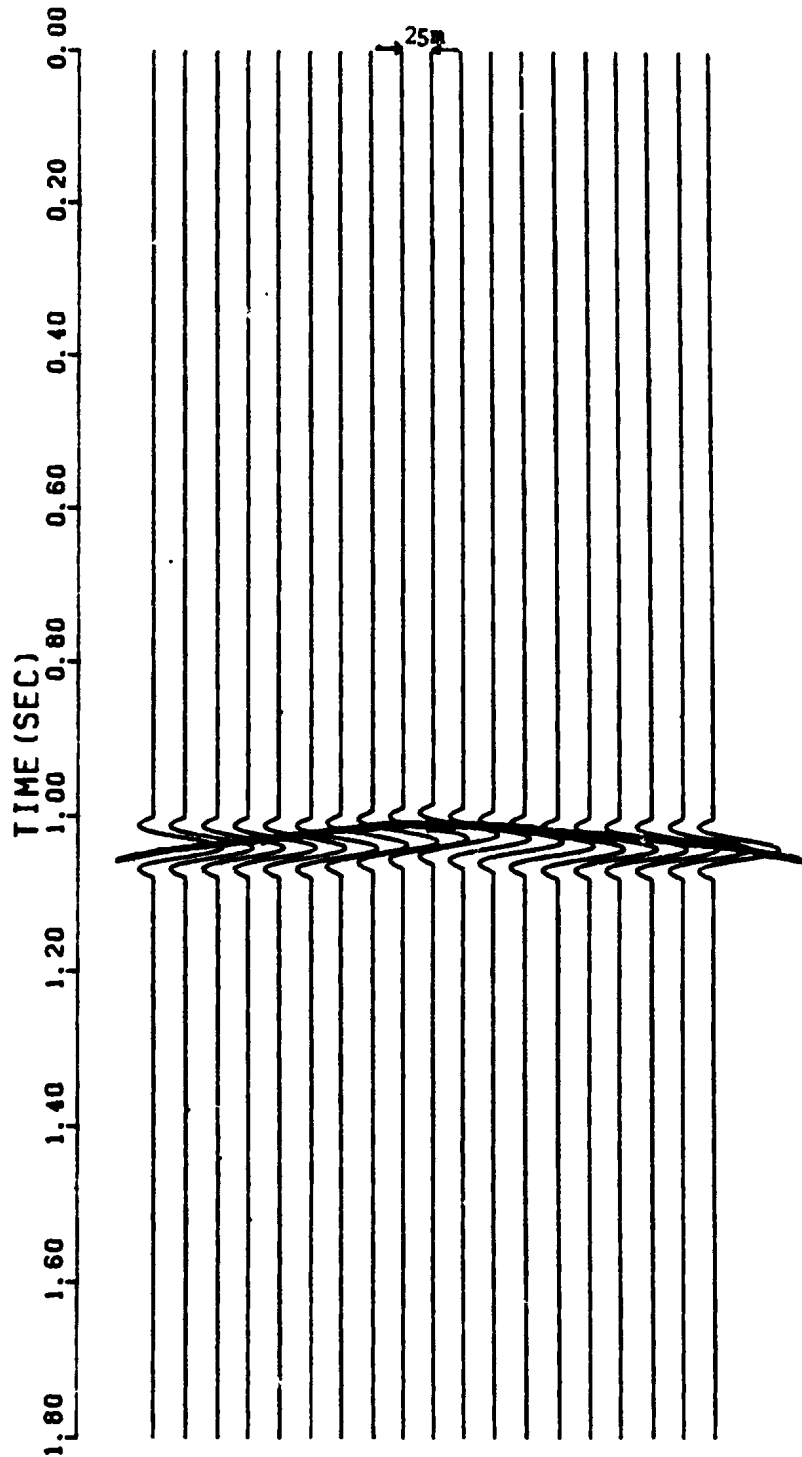
FIG.3.3.2.1 UNMIGRATED SECTION

DIP OF ANTICLINE=20DEGREES
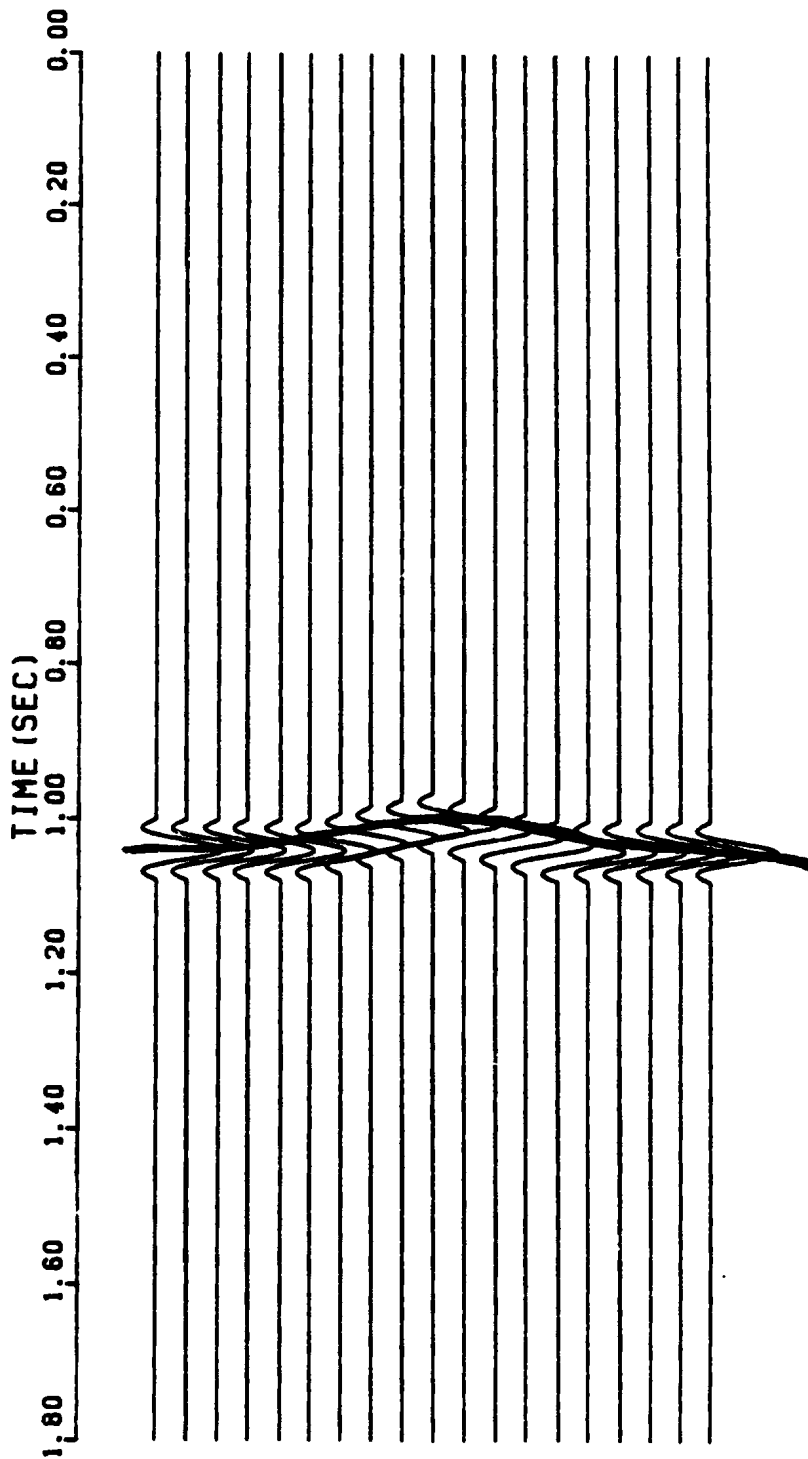
FIG.3.3.2.2.UNMIGRATED SECTION

DIP OF ANTICLINE=30DEGREES
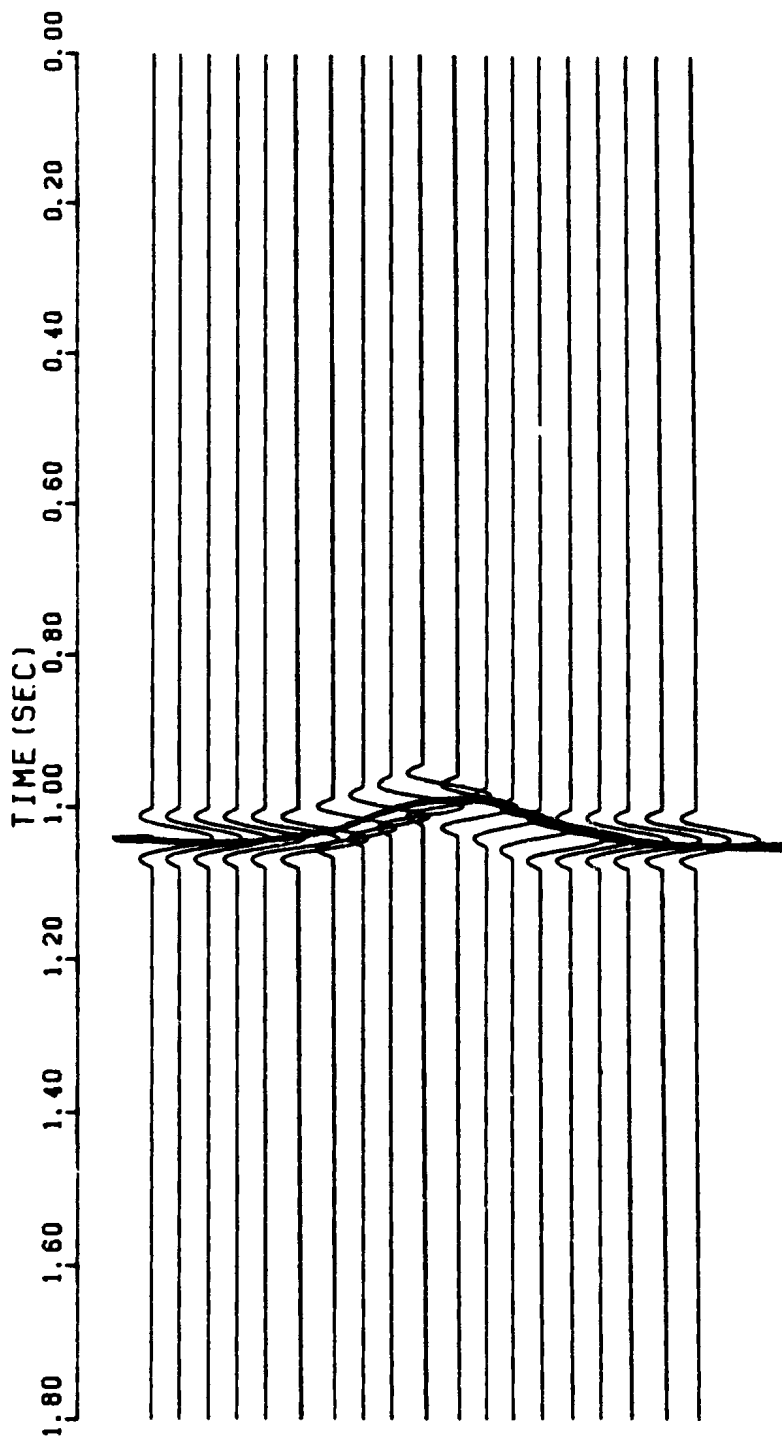
FIG.3.3.2.3 UNMIGRATED SECTION

DIP OF ANTICLINE=40DEGREES
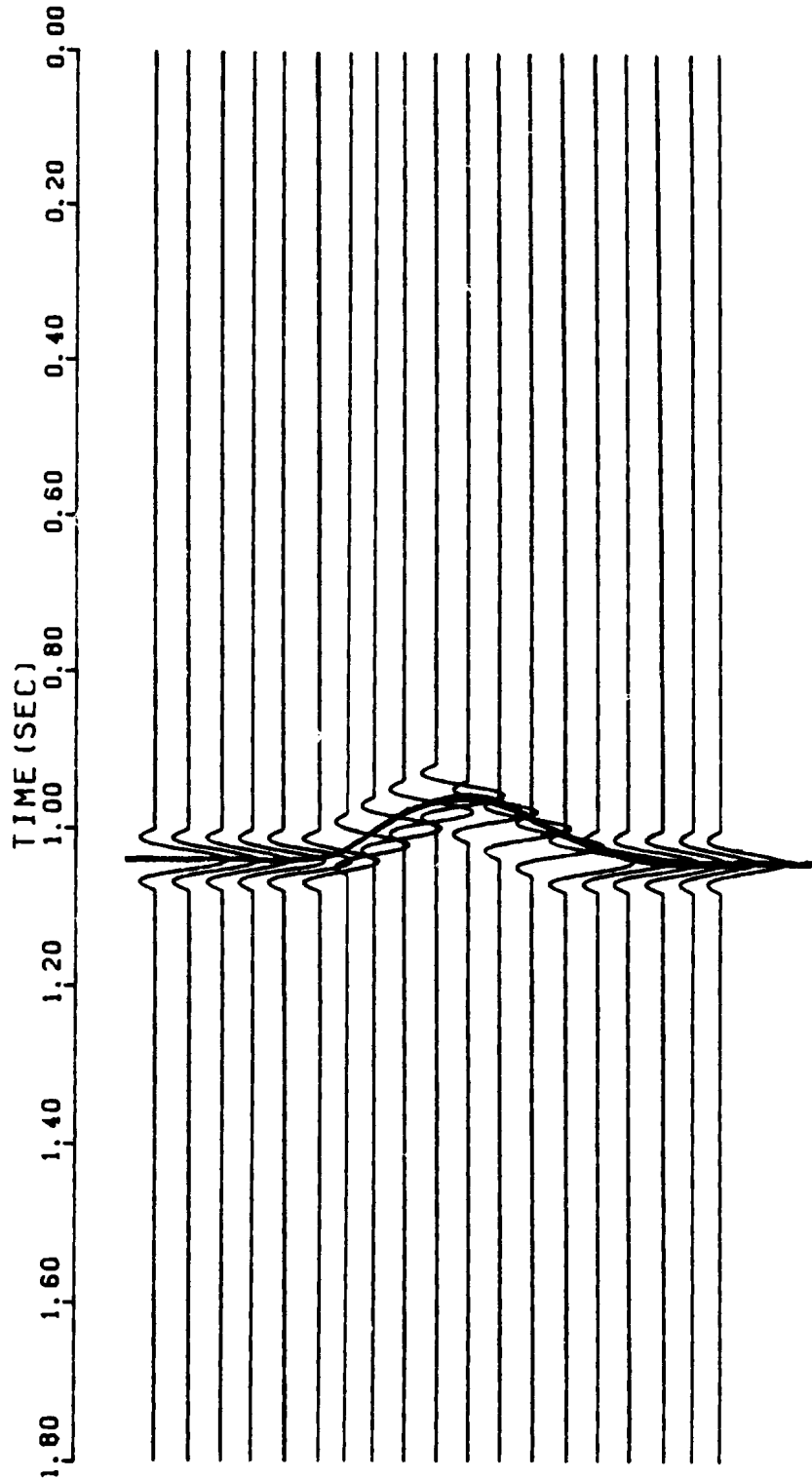
FIG.3.24 UNMIGRATED SECTION

DIP OF ANTICLINE=50DEGREES
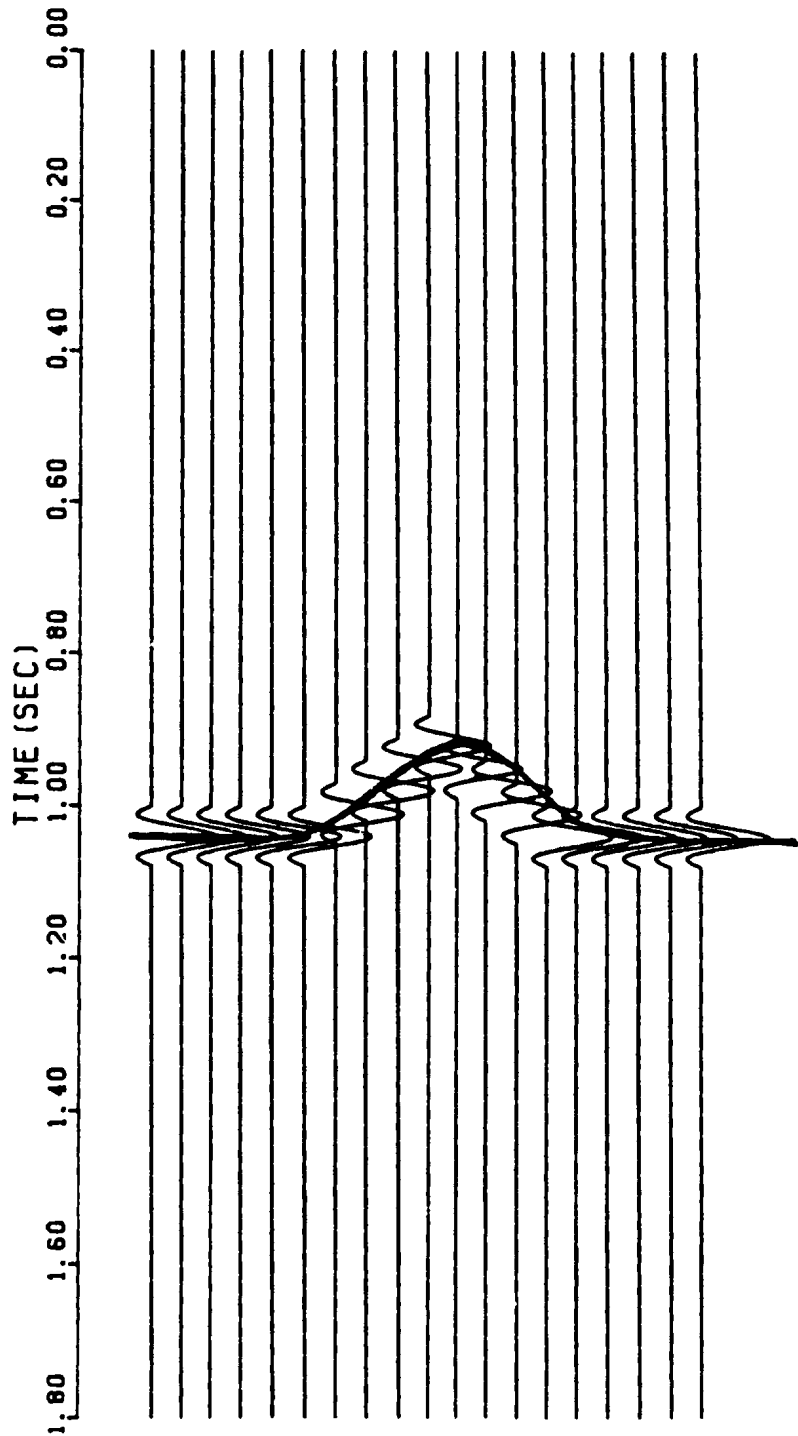
FIG.3.3.2.5 UNMIGRATED SECTION

DIP OF ANTICLINE=60DEGREES
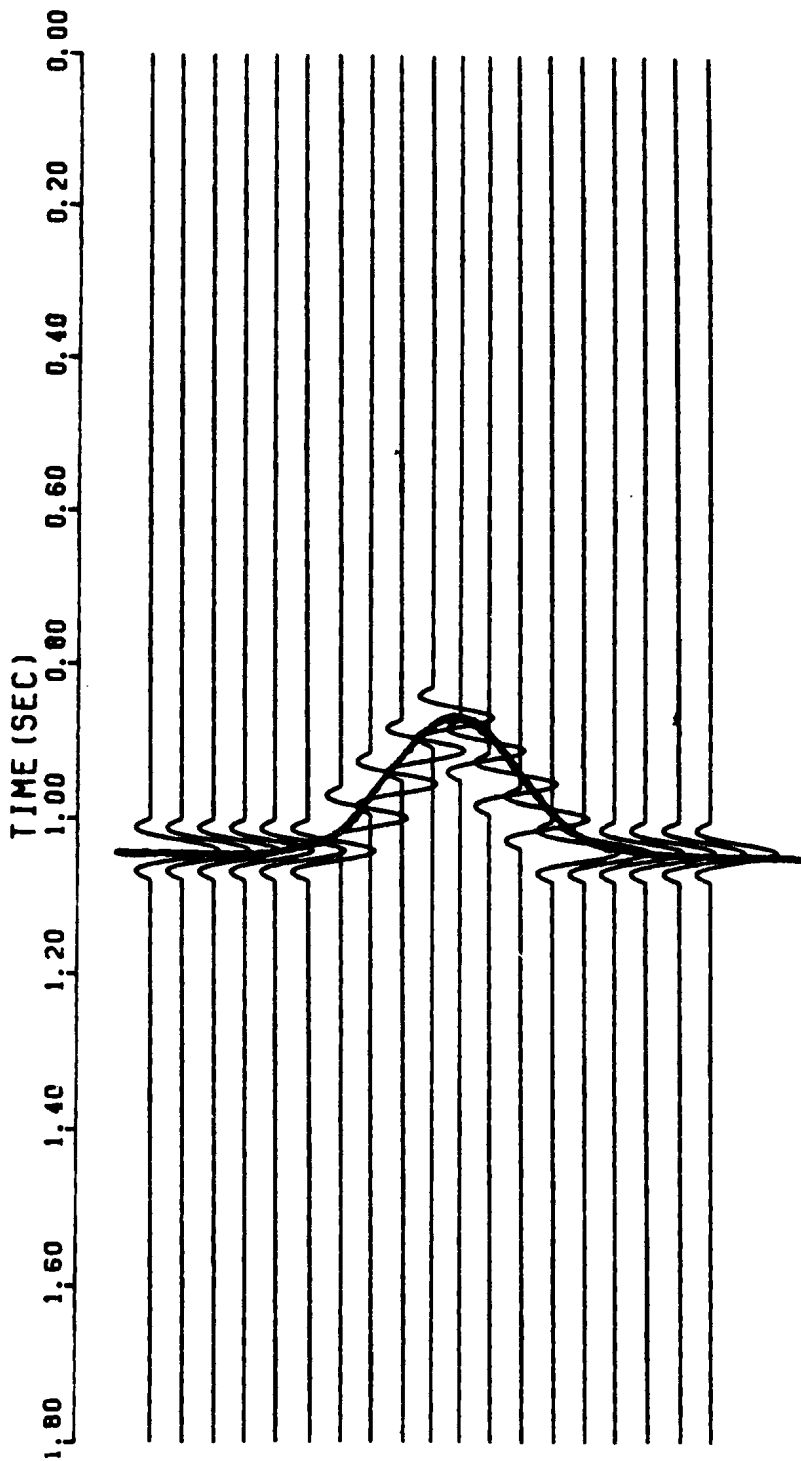
FIG.3.3.2.6 UNMIGRATED SECTION

DIP OF ANTICLINE=10DEGREES
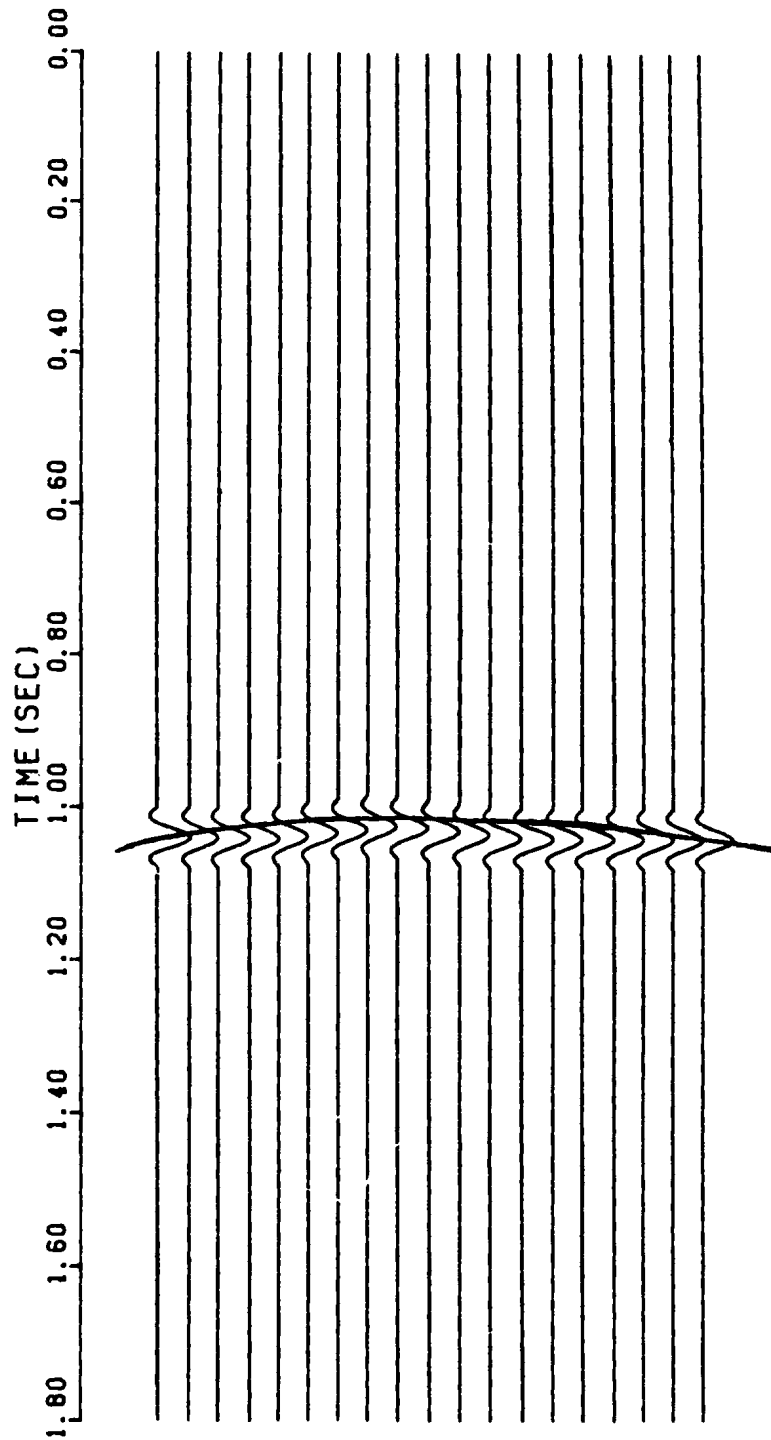
FIG.3.32.7 MIGRATED SECTION

DIP OF ANTICLINE=20DEGREES
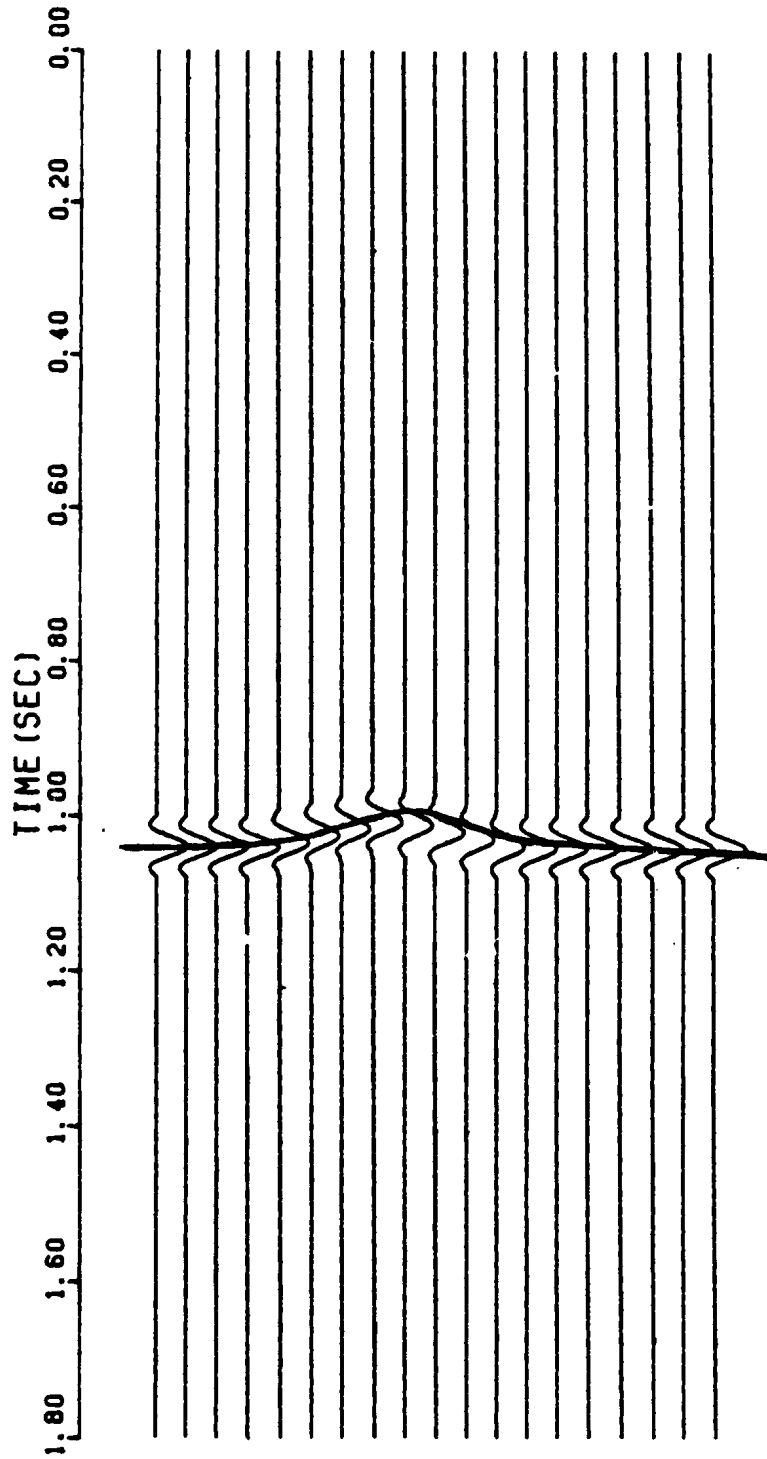
FIG.112.8 MIGRATED SECTION

DIP OF ANTICLINE=30DEGREES
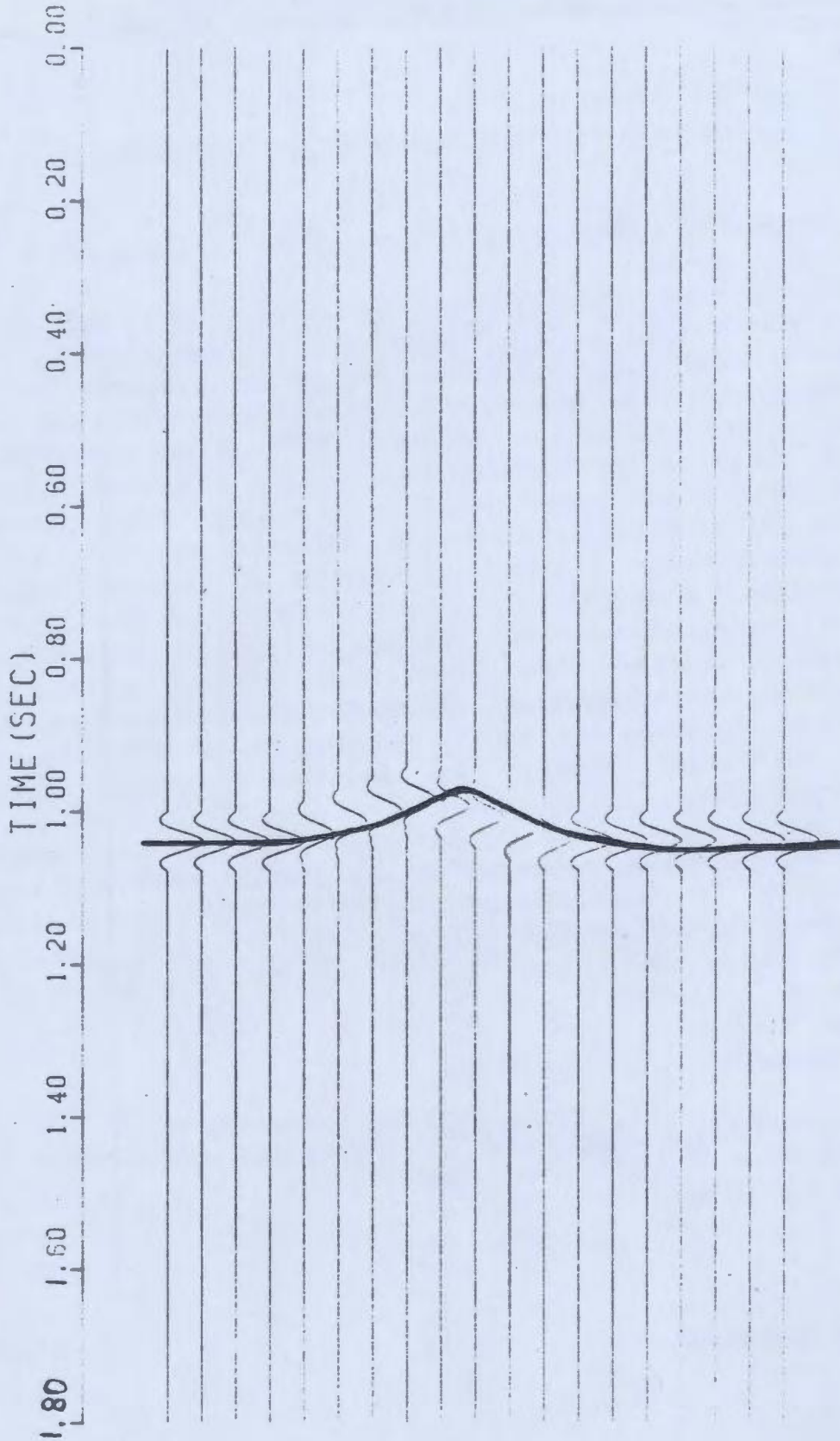
FIG.3.3.2.9 MIGRATED SECTION

DIP OF ANTICLINE=40DEGREES
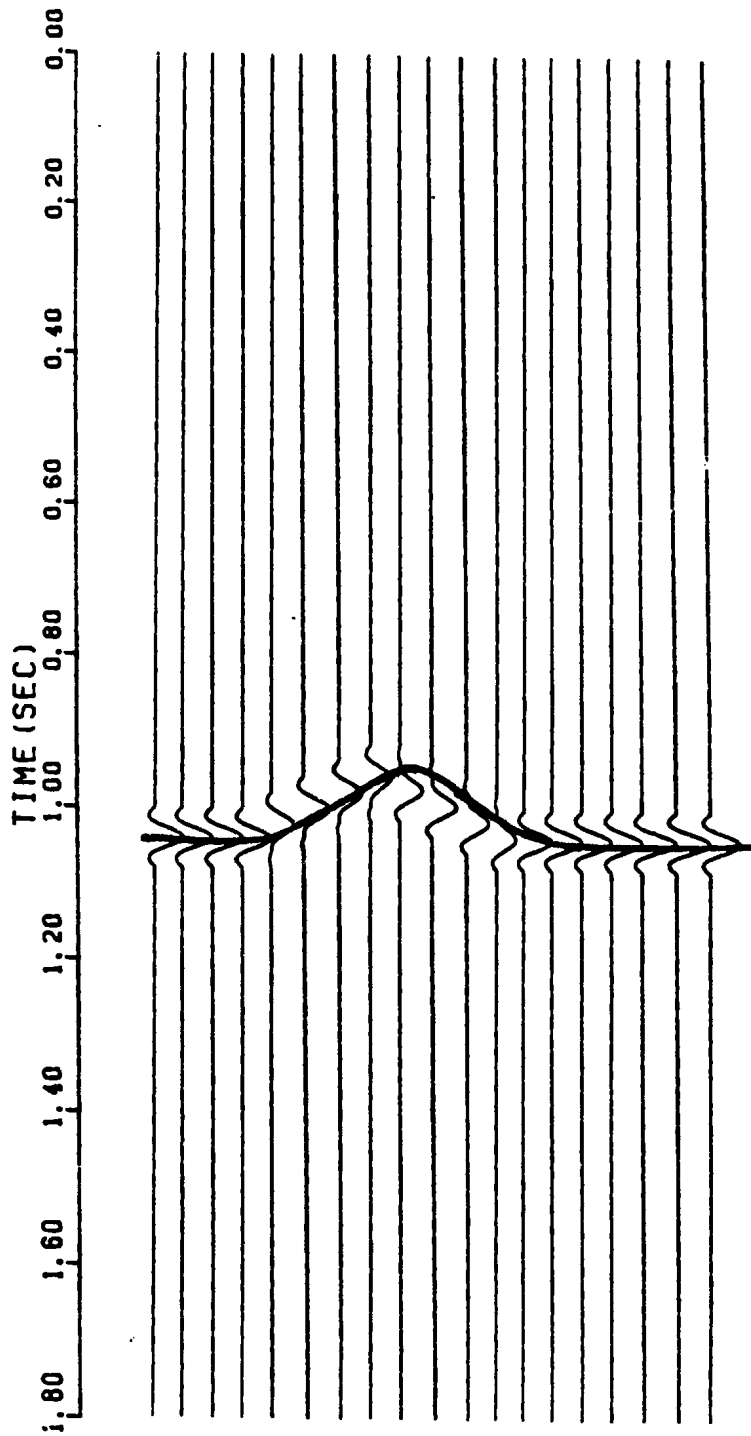
FIG.3.3.2.10 MIGRATED SECTION

DIP OF ANTICLINE=50DEGREES
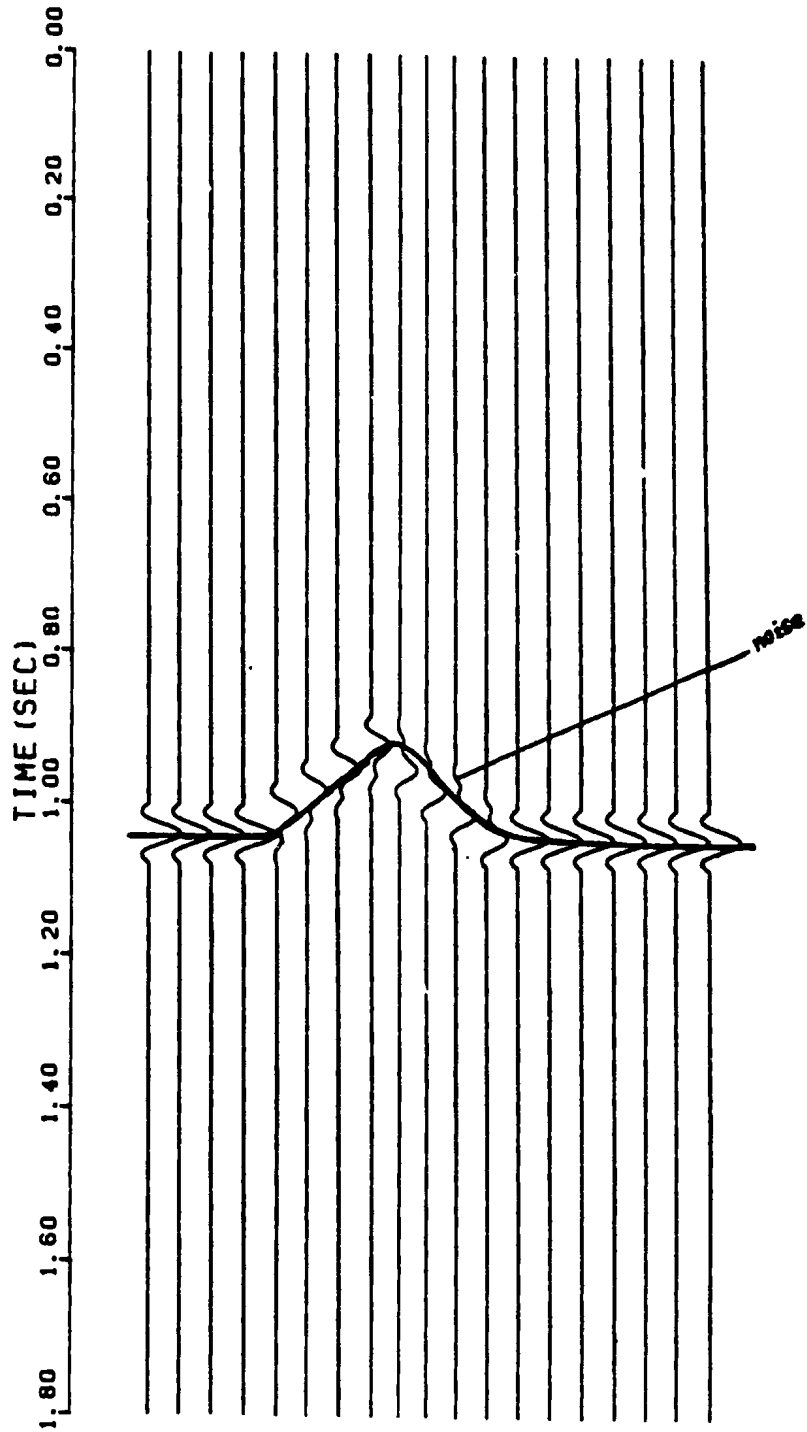
FIG.3.3.2.11 MIGRATED SECTION

- 77 -

DIP OF ANTICLINE=60DEGREES
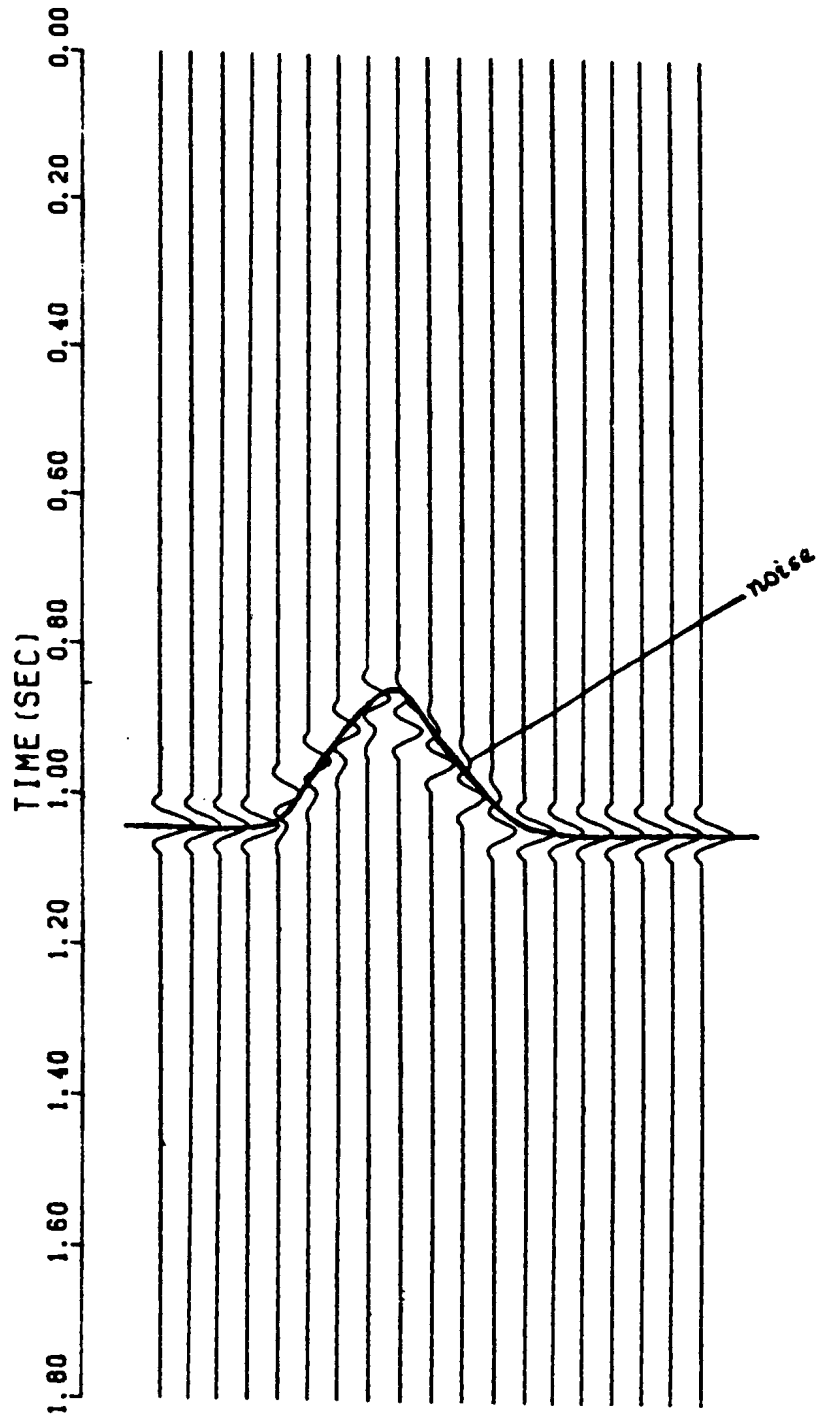
FIG.3.3.2.12 MIGRATED SECTION

CHAPTER 4

4.0 APPLICATION OF DIFFRACTION STACK METHOD TO FIELD DATA

In general, field reflection data are presented as record sections for
final interpretation of the subsurface structures. These record sections
display seismic traces side-by-side to show the continuity of reflection
events. Such record sections can be compared with geological cross
sections provided the following conditions are satisfied: (1) there
should not be any lateral variation in velocity; (2) no geometrical
bending of the ray paths away from the vertical. In steep dip areas the
ray paths bend away from the vertical causing distortions in actual
geometry of the subsurface structures. Migration is used in such cases to
construct the correct configuration of the dipping subsurface structures
for a more reliable interpretation than is possible from conventional
record sections. The existing field seismic data (stacked sections) were
used in implementing the diffraction stack migration scheme. The main
purpose of implementing the above technique is to improve the lateral
resolution over the dipping anticline structure after collapsing the
diffraction patterns generated at the sharp boundaries. In addition, the
actual boundary of the anticline structure can be delineated after
applying the migration technique.

4.1 Local Geology of the Adolphus Structure

The salt generated domal structure known as "Adolphus" is located
approximately 225 miles east of St. John's on the Grand Banks of
Newfoundland (Fig. 4.1). Geophysical investigations from Mobil's survey
indicated a number of favourable structures on the Grand Banks area which
led to three well locations on a salt piercement structure. Three wells,
Adolphus K-41, Adolphus 2K-41 and Adolphus D-50 were drilled in the Jeanne
d'Arc Subbasin to evaluate combined stratigraphic and structural traps in
the Tertiary and Cretaceous sandstones on a diapiric salt dome structure
(Well history report, Petroleum Directorate, Govt. of Newfoundland and
Labrador, 1975). Most of the lithological information of this structure
was obtained from the drilling cores of one wildcat well and two
exploratory wells.

First the K-41 wildcat well was drilled on the crest of a salt generated
domal structure on the Grand Banks of Newfoundland. The well was spudded
on November 16, 1972 and then abandoned at a total depth of 1239 m in the
Tertiary Banquereau formation. The K-41 well penetrated approximately
335 m of undifferentiated Quaternary and Tertiary, and 904 m of Tertiary
sediments. Between 0-352 m, no samples were collected from ditch
cuttings. The major rocks encountered in the subsequent ditch cuttings
were mudstones, siltstones and sandstones. Alternate layering of mudstone
and sandstone beds was observed in the ditch cuttings. Sometimes very
fine to coarse grained quartz and traces of pyrite were noticed along with
mudstone formation.
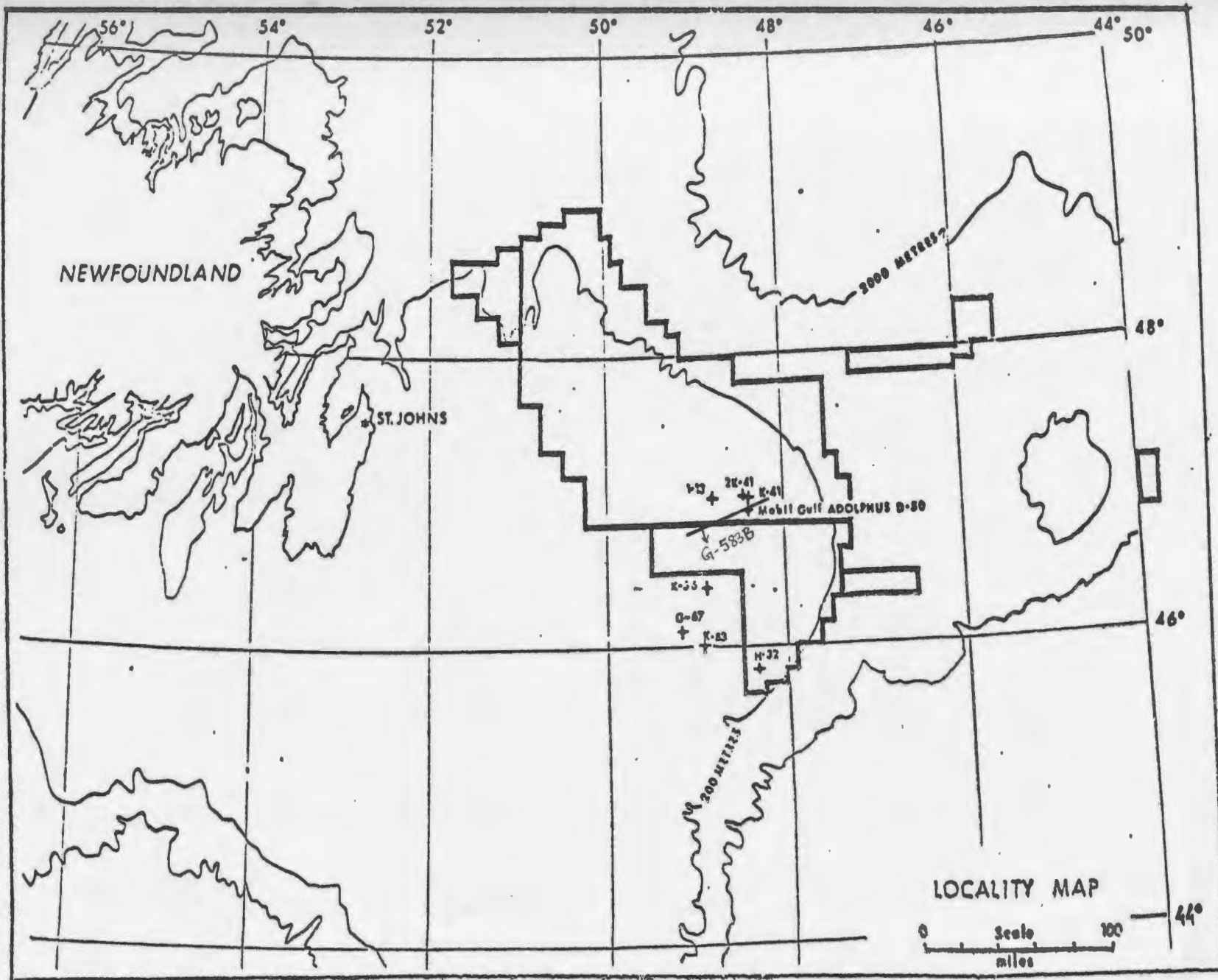
Figure 4.1 Map showing the Adolphus structure (From well history report, 1975).

Later two more exploratory wells were drilled on the Adolphus salt
structure. The first of these "Adolphus 2K-41" was drilled on the crest
of the salt dome structure followed by the second exploratory well
"Adolphus D-50" drilled on the flank of the same salt structure. The
major lithological units penetrated by these two exploratory wells are
presented in Table 4.1 (Rashid, 1978). In the first exploratory well,
3660m of sedimentary strata were penetrated along with a salt thickness of
800m. It is believed that the salt age ranges from Triassic to Lower
Jurassic. During the growth of diapiric structure, the salt pierced the
lower section of sedimentary strata (Jurassic and Lower Cretaceous
formations) and uplifted the upper sections of Dawson formations
(Rashid, 1978). An average uplift of 370m was noticed between Adolphus
2K-41 and D-50 formations (Table-4.1). Several production tests were run
in Adolphus 2K-41 in order to find commercial quantity of hydrocarbon
reserves. However, only minor flows of oil and gas from the upper
Cretaceous sandstones at depth 2610-2645m were observed. The flow rate
was 268 barrels of oil per day. A gas flow of 5664 cubic meters per day
was observed in the Adolphus 2K-41 well.

4.2 Data Translation from Consul Staked Reel

As a part of the analysis work, the diffraction stack migration technique
was applied to field seismic data (stacked data) collected over the
Adolphus structure on the Grand Banks of Newfoundland. These seismic data
were supplied in the form of consul staked reels by Mobil Oil Canada

Formation	Depth range (m)	Thickness (m)	Major lithology
Adolphus 2-k-41			
Banquereau	Down to 2381	—	Shales and mudstone
Wyandot Equivalent	2381-2432	51 m	Chalk and limestone
Dawson Canyon	2432-2554	122 m	Limestone, sandstone, mud, and shale
Logan Canyon Equivalent	2554-2853	299 m	Mud, sandstone, limestone, chalk, and shale
Top of salt	2853-3658	805 m	Mostly halite with thin interbeded red-brown shales and minor dolomites
Adolphus D-50			
Banquereau	Down to 2659	—	Mudstone and shales
Wyandot Equivalent	2659-2916	257 m	Limestone
Dawson Canyon	2916-3103	187 m	Limestone and siltstone
Logan Canyon Equivalent	3103-3686	583 m	Limestone and siltstone

Table 4.1   Details of geological formations penetrated by Adolphus wells. (After Rashid, 1978).

Limited, Calgary to undertake the present analysis. The stacked data were produced after applying the normal processing sequence (Fig. 1.4) and then stored in the magnetic tape as demultiplexed SEG Y Format. The stacked data over line G-583B were chosen for our present analysis because it cuts both sides of Adolphus anticline structure.

First the consul staked reel containing the data for line G-583B was transferred to the VAX/VMS 11/780 computing system using a computer programme developed (Appendix-1) in order to translate the data from demultiplexed SEG Y Format (Barry et al., 1975). The above computer programme was written to read the reel identification header as well as the trace data block (Fig 4.2) in SEG Y Format. A subroutine was incorporated in the above programme to translate the trace data samples correctly on VAX/VMS system because the original consul staked tape containing the data samples was written in IBM format.

4.3 Parameters for Migration of Field Data

Before implementing the migration, it was necessary to fix the three basic parameters; sampling interval, aperture aned migration velocity. As a rule of thumb, there should be at least two samples per cycle for the highest frequency (Nyquist frequency) present in the signal to be analysed. It was observed that most of the reflected energy in the unmigrated stack section (Fig. 4.4.1) was in the range of 10 to 50 HZ which was within Nyquist frequency range of the signal to be

Digital Tape Formats

Nine Track, 800 bpi NRZI or 1600 bpi Phase Encoded (PE) Demultiplex (Trace Sequential) Format
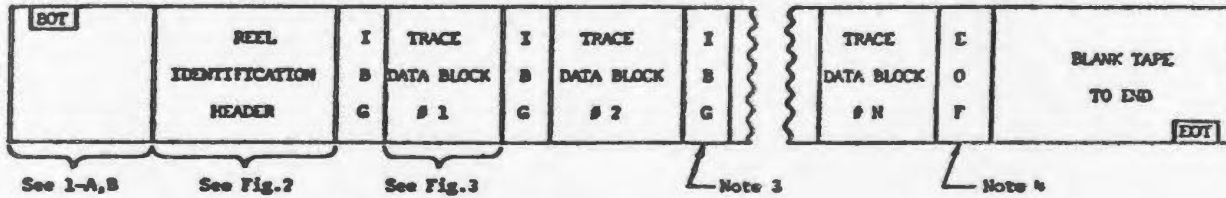
Tape Motion (Tape viewed oxide down)
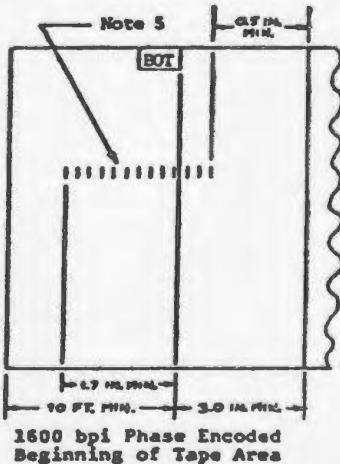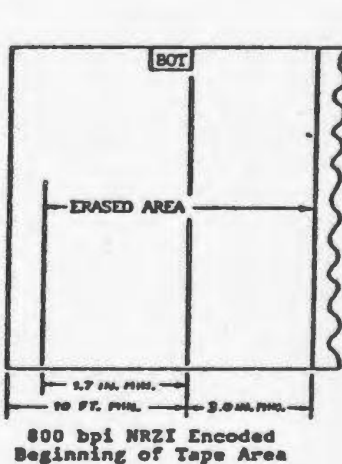
800 bpi NRZI Encoded Beginning of Tape Area — 1-A

1600 bpi Phase Encoded Beginning of Tape Area — 1-B

1-C

NOTES:

1. Preamble-Preceeds each of the 45 blocks within the reel identification header and each trace data block when 1600 bpi PE is used. Consists of 40 all-zero bytes followed by one all-ones byte.

2. Postamble-Follows each of the 45 blocks within the reel identification header and each trace data block when 1600 bpi PE is used. Consists of one all-ones byte followed by 40 all-zero bytes.

3. Interblock Gap (IBG)-Consists of 0.6" nominal, 0.5" minimum.

4. End of file (EOF)-Consists of an IBG followed by:
   (a) PE tape mark having 80 flux reversals at 3200 fci in bit numbers F,0,2,5,6, and 7. Bits 1,3, and 4 are dc-erased.
   or (b) NRZI tape mark having two bytes with one bits in bit numbers 3,6, and 7 separated by seven all-zero bytes.

5. PE Identification Burst-Consists of 1600 flux reversals per inch in bit number P; all other tracks are erased.

Figure 4.2   Recommended demultiplexed format (After Barry et al, 1975).

considered. An output sampling rate of 4 ms was used which gives a
Nyquest frequency of 125 Hz. This latter value is well above the highest
frequency observed in the seismic data and therefore there should be no
aliasing problems. The 4 ms interval also allowed a reasonable
computation time for the summation operation in the diffraction stack
method.

In the implementation of the above technique, only data from a finite
aperture are migrated. The seismic resolution can be improved by choosing
the correct aperture. It is essential to use only data falling within the
portion of the migration surface that contain the main contribution to the
image. The aperture for the stacked data was estimated by applying the
relation given in section 3.2.1. Three apertures were tried to migrate
the stacked data over Adolphus structure. Table-4.3 gives the apertures
used for three different migration velocities on stacked data.

Serial Number	Velocity of the medium 'm/s'	Frequency of the pulse 'HZ'	Maximum depth considered 'm'	Aperture value equivalent to no. of traces
1	2500	50	3750	12
2	3500	50	5250	17
3	4500	50	6750	22

Table 4.3   Different apertures values for different set of velocities
for field stacked data.

The most important parameter in diffraction stack migration is the
migration velocity. Velocity acts as a variable in defining the hyperbola

along which the summation is to be carried out. There are several choices
available in selecting the correct velocity for migration. The common
choices are interval velocity, average velocity and RMS velocity. Usually
velocity analysis is performed on unstacked reflection data to assign the
correct stacking velocity for migration. Stacking velocity can be
determined in various methods such as applying NMO corrections, with a
number of constant velocities, to the traces of a CDP gather; computing
coherent energy for the NMO-corrected traces; and mapping the coherency
obtained as a function of travel time and velocity (Sattlegger, 1975).
But the existing field seismic data over the Adolphus structure was
already stacked. So velocity analysis could not be attempted for our
present analysis. On the basis of available geological information from
three exploratory wells drilled on Adolphus structure, three different
constant velocities were chosen to perform the diffraction stack migration
method (Table-4.3).

4.4 Results of Migrated Sections

The diffraction stack algorithm (Appendix-1) was applied to the existing
stacked seismic data on the Adolphus structure after testing the method on
synthetic data. The implementation procedure has been discussed in
section 3.2.2. The results of the migrated sections are discussed here.
Figure 4.4.1 represents a 24-fold conventional stack seismic section
(unmigrated) on Adolphus structure in the Grand Banks of Newfoundland. A
sampling interval of 4 ms and trace spacing of 25m were used to plot the
stacked seismic section. The horizontal scale was taken to be about

64 traces to a mile whereas the vertical scale was 50 samples per inch. A 3 sec record equivalent to 750 samples was used for diffraction stack migration. Three different constant velocities 2500 m/s, 3500 m/s and 4500 m/s were used to migrate the whole stacked section. These velocities were chosen on trial and error method on examining the coherency energy at the apex of diffraction hyperbola. A total of 504 traces were migrated covering about 12.6 km length along the profile. A trace interval of 25m was used for all three migrated sections.

Figures 4.4.1 to 4.4.4 represent the unmigrated and migrated time sections with migration velocities 2500 m/s, 3500 m/s and 4500 m/s respectively. These migrated sections were plotted with the amplitude scale multiplied by a factor of two relative to that for the unmigrated section. Figures 4.4.2 to 4.4.4. are the migrated-time sections across a medium-piercement salt dome (see Table-4.1). Three major reflectors D, E and F have been identified very clearly in the migrated sections. These three reflectors D, E and F are correlated with local geology (section 4.1) of the Adolphus structure as top of Cretaceous, limestone and unconformity beds respectively. These beds were penetrated by three exploratory wells drilled on the Adolphus structure confirming the above seismic markers. The top of Cretaceous marked as 'D' is clearly identified in all the three migrated sections. The second reflector 'E' is identified clearly on both sides of the salt structure except on the top of salt dome. The reflections are terminated at the salt top indicating the presence of a major unconformity. Pre-unconformity reflections above box A are better identified in the migrated sections than the unmigrated section. There is

clear gap between reflectors E and F showing the upliftment of sedimentary strata. This upliftment sedimentary strata were confirmed from the results of exploratory drilling on Adolphus 2K-41 and Adolphus D-50 wells (Table-4.1).

In all the migrated sections, the general structure was better clarified than in the original stacked section (Fig. 4.4.1). Weak diffractions are almost unnoticiable in the migrated section due to the focussing effect. Majority of the strong diffractions (along the salt dome flank) are migrated to their true positions. In regions indicated by box A, B and C on both sections, we notice that considerable energy has been moved to their true spatial positions in reducing the breadth of the anticline.

The amplitude was not preserved properly. A reduction of amplitude by a factor 2 was observed in all three migrated time sections and pulse shapes were changed. During the migration process, high frequency content of the reflection pulse was lost and probably phase lag was introduced. The reflection character of flat event is nearly identical with that of unmigrated data indicating the medium to be nearly homogeneous. The highest frequency of the reflected pulse in the migrated sections were in the range of 20 to 30HZ. The scattered reflections within the salt are partly removed in the migrated sections. The salt dome flank was better delineated than the unmigrated section. The dimension of the salt structure was delineated properly.

Finally, migration noise was introduced from dipping events. Multiple-branched reflections at the flank of the anticline structure could not be removed totally. These reflections might have generated the noise during the diffraction stack process. On comparing the three migrated sections, it is observed that the section with migration velocity 3500m/s was migrated better than other two migrated sections. The above velocity was found suitable as it gave the maximum energy of coherence at the apex of the diffraction hyperbola curve. In other words, it gave the best migration stack by assigning the maximum energy at the apex of the diffraction curve.

CHAPTER 5

5.0 CONCLUSIONS

This thesis has presented the results of an investigation of the diffraction stack migration scheme applied to both stacked synthetic and field seismic data.

In order to implement the migration technique, computer programmes were developed. This migration scheme was applied to the zero offset synthetic data generated for two simple models. Zero offset (equivalent to stacked data) single fold synthetic seismograms were constructed for various reflector dips considering two models - an inclined reflector and an anticline. The effect of dip angle and migration velocity were examined for the first model in carrying out the diffraction stack migration process. Later the diffraction stack migration algorithm was applied to the anticline model. Only the effect of dip angle was considered in the above model while implementing the migration scheme.

After testing the diffraction stack migration technique on synthetic data, the same algorithm was applied to the field seismic data collected over Adolphus anticline structure located in the Grand Banks of Newfoundland. These field seismic data were provided to us from Mobil Oil Canada Limited, Calgary in form of a consul staked tape.

On the basis of synthetic and field data interpretation, the following conclusions were drawn:

1) The diffraction stack migration algorithm has clarified the general structure of the subsurface even though the velocity field was not known   accurately.

2) The diffraction patterns were properly collapsed in the synthetic migrated sections as the velocity function was correctly assigned. The strong diffractions were not collapsed completely in the field seismic migrated section as the velocity function was not well known. Part of the record section was undermigrated as the velocity used is too low whereas part of the record section were overmigrated as a result of high velocity.

3) In general, amplitude reduction was observed in all migrated time sections both in synthetic and field data. The amplitude reduction was more prominent in the field migrated sections. The reflection character was maintained nearly identical for the flat event of the unmigrated field section indicating the medium to be nearly homogeneous.

4) Pulse shapes were broadened in all the migrated sections due to the loss of high frequency content in the reflected pulse.

5) Phase lag was observed in the synthetic migrated sections for an inclined reflector model. The results show that phase shift is independent of offset distance. As the dip increases the amount of phase change will increase. From the general character of the field migrated sections, phase lag was probably introduced during migration process.

6) Noise was observed in synthetic migrated sections for both geological models in the case of steep dip angles. This noise was introduced during the migration process due to the presence of dipping events. Appreciable noise was observed in the field migrated sections due to the presence of multiply-branched reflections at the flank of anticline structure. Noise is also introduced in the field migrated sections due to overmigration phenomena of the part of the record section. These noise were produced in form of a 'smiles' pattern as the limbs of hyperbolas migrate through the point reflector into smiles.

7) In general, the geological markers D, E and F are better clarified in the migrated sections than in the unm..grated section for the field seismic data. The salt flank was delineated better than in the original stacked section. The dimension of the salt structure was delineated better than the unmigrated section in reducing the breadth of the anticline. The above features are also observed in the synthetic anticline model.

8) From observations of migrated sections on two models, it is confirmed
that the diffraction stack method works efficiently for steep dip
reflectors up to dip angle 40 degrees.

5.1 Limitations and Suggestions for Further Work

These are the following limitations of the present investigation:

1) The diffraction stack migration method is an expensive method. The
computational cost increases with sampling rate as it does summation
along generated diffraction hyperbola for each sampling interval.

2) It does not preserve amplitude and frequency of the pulse properly
during the migration process.

3) It cannot handle lateral velocity variations without a ray tracing
programme.

4) It produces 'break-up' noise and smiles pattern during the migration
process due to overmigration phenomena.

To overcome the above problems, it is suggested that the wave equation
(finite-difference) migration technique should be applied to both
synthetic and field data. The Frequency-wavenumber method based on the

FFT algorithm should be applied to this data to reduce the computational cost during the migration process. Corrections for amplitude and frequency can be incorporated during the diffraction atack process by applying Newman filter and Hubral correction.

Appendix 1: Computer Programmes

```
C                            ----------
C                             TAPEREAD
C                            ----------
C      PROGRAM TO TRANSLATE MOBIL'S DATA FROM
C      THE DEMULTIPLEXED SEG Y FORMAT
C      THIS PROGRAM READS REEL IDENTIFICATION HEADER
C      AND TRACE DATA BLOCK
C      THIS DATA IS FROM GRAND BANKS SEISMIC LINE-G583B
C      PROGRAM TO READ TAPE_EBC_ASC CONVERSION
       CHARACTER*3200CARD,EBCARD,LINE*80
       INTEGER*2 HEAD2
       INTEGER*4 HEAD1
       INTEGER*4TH1,TH3,TH5
       INTEGER*2TH2,TH4,TH6
       INTEGER*2 ITRAC(1500)
       DIMENSION TRACE(1500)
C
       COMMON/ONE/ HEAD1(3),HEAD2(194)
       COMMON TH1(7),TH2(4),TH3(8),TH4(2),TH5(4),TH6(76)
C      BYTE I1,I2,I3,I4,I5,I6,I7,I8,I9,I10,I11
C
       OPEN(UNIT=10,FILE='[GEOPH]MOBIL.DAT;1',STATUS='OLD')
       READ(10,10) EBCARD
  10   FORMAT(A)
       CALL LIB$TRA_EBC_ASC(EBCARD,CARD)
       DO 20 I=1,3200,80
       LINE=CARD(I:I+79)
       WRITE(6,10) LINE
  20   CONTINUE
C      PROGRAM TO READ REEL IDENTIFICATION HEADER-PART2
       READ(10,15) ((HEAD1(I),I=1,3),(HEAD2(K),K=1,194))
  15   FORMAT(3A4,194A2)
       CALL SW1
       CALL SW2
       CALL WRT
 999   CONTINUE
C      THIS IS A PROGRAM TO READ TRACEHEAD AND DATA SAMPLE
       DO 19K=1,50
       DO 19J=1,24
       READ (10,16) TH1,TH2,TH3,TH4,TH5,TH6,ITRAC
  16   FORMAT(7A4,4A2,8A4,2A2,4A4,76A2,1500(A2,2X))
       CALL SW3
       CALL SW4
       CALL SW5
       CALL SW6
       CALL SW7
       CALL SW8
       CALL WRT2
       DO 18 I=1,1500
       CALL IBMVAX(ITRAC(I),TRACE(I))
       IF(TRACE(I).LE.-300.0) TRACE(I)=-300.0
  18   IF(TRACE(I).GE.300.0) TRACE(I)=300.0
       IF(K.GT.29) WRITE(4,80) (TRACE(I),I=1,750)
  80   FORMAT(10F8.3)
  19   CONTINUE
```

```
        STOP
        END
        SUBROUTINE SW1
        COMMON/ONE/ H1(12),H2(388)
        BYTE H2,H1,I1,I2,I3,I4
        DO 30 I=4,12,4
        I1=H1(I)
        I2=H1(I-1)
        I3=H1(I-2)
        I4=H1(I-3)
        H1(I)=I4
        H1(I-1)=I3
        H1(I-2)=I2
        H1(I-3)=I1
30      CONTINUE
        RETURN
        END
        SUBROUTINE SW2
        COMMON/ONE/ H(3),H1(388)
        BYTE H2,H1
        DO 30 I=2,388,2
        H2=H1(I)
        H1(I)=H1(I-1)
        H1(I-1)=H2
30      CONTINUE
        RETURN
        END
        SUBROUTINE WRT
        COMMON/ONE/ HEAD1(3),HEAD2(194)
        INTEGER HEAD1
        INTEGER*2 HEAD2
        WRITE(6,14) (HEAD1(I),I=1,3)
14      FORMAT(1X,3I10)
        WRITE(6,15) HEAD2
15      FORMAT(1X,8I10)
        RETURN
        END
        SUBROUTINE SW3
        COMMON T1(28),T2(8),T3(32),T4(4),T5(16),T6(152)
        BYTE T6,T5,T4,T3,T2,T1,I1,I2,I3,I4
        DO 40 I=4,28,4
        I1=T1(I)
        I2=T1(I-1)
        I3=T1(I-2)
        I4=T1(I-3)
        T1(I)=I4
        T1(I-1)=I3
        T1(I-2)=I2
        T1(I-3)=I1
40      CONTINUE
        RETURN
        END
        SUBROUTINE SW4
        COMMON T(7),T1(8),T2(32),T3(4),T4(16),T5(152)
        BYTE T5,T4,T3,T2,T1,I2,I1
        DO 40  I=2,8,2
        I2=T1(I)
        T1(I)=T1(I-1)
```

```fortran
        T1(I-1)=I2
40      CONTINUE
        RETURN
        END
        SUBROUTINE SW5
        COMMON A(7),B(2),T1(32),T2(4),T3(16),T4(152)
        BYTE T4,T3,T2,T1,I1,I2,I3,I4
        DO 40 I=4,32,4
        I1=T1(I)
        I2=T1(I-1)
        I3=T1(I-2)
        I4=T1(I-3)
        T1(I)=I4
        T1(I-1)=I3
        T1(I-2)=I2
        T1(I-3)=I1
40      CONTINUE
        RETURN
        END
        SUBROUTINE SW6
        COMMON C(7),D(2),E(8),T1(4),T2(16),T3(152)
        BYTE T3,T2,T1,H2,H1
        DO 40 I=2,4,2
        H2=T1(I)
        T1(I)=T1(I-1)
        T1(I-1)=H2
40      CONTINUE
        RETURN
        END
        SUBROUTINE SW7
        COMMON F(7),G(2),H(8),R(1),T1(16),T2(152)
        BYTE T2,T1,I1,I2,I3,I4
        DO 40 I=4,16,4
        I1=T1(I)
        I2=T1(I-1)
        I3=T1(I-2)
        I4=T1(I-3)
        T1(I)=I4
        T1(I-1)=I3
        T1(I-2)=I2
        T1(I-3)=I1
40      CONTINUE
        RETURN
        END
        SUBROUTINE SW8
        COMMON S(28),U(2),V(8),W(1),X(16),T1(152)
        BYTE G2,G1,T1,S,X
        DO 40 I=2,152,2
        G2=T1(I)
        T1(I)=T1(I-1)
        T1(I-1)=G2
40      CONTINUE
        RETURN
        END
        SUBROUTINE WRT2
        COMMON TH1(7),TH2(4),TH3(8),TH4(2),TH5(4),TH6(76)
        INTEGER*4 TH1,TH3,TH5
        INTEGER*2 TH2,TH4,TH6
```

```fortran
      WRITE(6,14) TH1,TH2,TH3,TH4,TH5,TH6
14    FORMAT(1X,10I10)·
      RETURN
      END
C     THIS SUBROUTINE WAS PROVIDED BY DR. J.A.WRIGHT
C     DEPT.OF EARTH SCIENCES,MUN,ST.JOHN'S
      SUBROUTINE IBMVAX(IIVAL,VAL)
C     INPUT IIVAL AN INTEGER*2 VARIABLE IN IBM FORMAT
C     OUTPUT VAL A REAL*4 VARIABLE IN VAX FORMAT
      INTEGER*2 IIVAL
C     TEST FOR 0.0
      IF (IIVAL.NE.0) GO TO 1
      VAL=0.
      RETURN
C     PERFORM BYTE SWAP
1     IVAL=IIVAL
      IF (IVAL.LT.0) IVAL=IVAL+65536
      LSB=(IVAL/256)
      MSB=(IVAL-(LSB*256))*256
      IVAL=MSB+LSB
C     DETERMINE POLARITY POL=+/-1.
      POL=+1.
      IF (IVAL.GE.32768) POL=-1.
C     DETERMINE CHARACTERISTIC ICHAR
      IF (IVAL.GE.32768) IVAL=IVAL-32768
      ICHAR=(IVAL/256)-64
C     CALCULATE FRACTION
      FRACT=(LSB/256.)
C     FORM NUMBER POL*FRACT*(16**ICHAR)
      CALL LIB$FLT_UNDER(0)
      VAL=POL*FRACT*(16.**ICHAR)
      RETURN
      END
```

```
C                      ----------------
C                         SYNSEISGRAM
C                      ----------------
C        THIS IS A PROGRAM TO GENERATE SYNTHETIC SEISMOGRAM
C        FOR AN INCLINED REFLECTOR
C        DIP OF THE REFLECTOR=60 DEGREES
C        SYNTHETIC SEISMOGRAM FOR 19 TRACES
C        DELTA=SAMPLING INTERVAL
C        VARIABLE PP IS THE INPUT
C        REFLECTIVITY RR=.13
         DIMENSION RR(1721),X(40),Y(40),ZZ(80),T1(40),PP(19)
         PARAMETER DIM=1800
         DIMENSION A(DIM),B(DIM),C(DIM),PROD(DIM)
         DATA (PP(I),I=1,19)/100,143,187,230,273,317,360,403,446
     3   ,490,533,576,620,663,706,750,793,836,879/
         DELTA=.001
         N=PP(1)
         DO 15 K=1,19
         DO 16 I=1,N
16       RR(I)=0
         RR(N+1)=.13
         OPEN(UNIT=4,FILE='A.DAT',STATUS='OLD')
         OPEN(UNIT=2,FILE='A.STO',STATUS='NEW')
         OPEN(UNIT=51,FILE='RIC25.DAT',STATUS='OLD')
         OPEN(UNIT=3,FILE='RIC25.STO',STATUS='NEW')
         OPEN(UNIT=9,FILE='SY257.OUT',STATUS='NEW')
         WRITE(2,71) (RR(I),I=1,1721)
15       IF(K.LT.19)N=PP(K+1)
         CLOSE(UNIT=2,STATUS='SAVE')
71       FORMAT(10F8.3)
C        PROGRAM TO GENERATE RICKER WAVELET(25HZ)
         W=2*3.1416*25
         DO 18 I=1,40
         T1(I)=I*DELTA
         X(I)=SIN(W*T1(I))
18       Y(I)=X(I)/(W*T1(I))
         DO 19 I=1,80
         IF (I.LE.40)THEN
         J=41-I
         ZZ(I)=Y(J)
         ELSE
         K=I-41+1
         ZZ(I)=Y(K)
         END IF
19       CONTINUE
         WRITE(3,71) ZZ
         CLOSE(UNIT=3,STATUS='SAVE')
C        THIS IS A PROGRAM TO DO CONVOLUTION
         N=1721
         M=80
         J=N+M-1
         READ(51,71) (B(L),L=1,M)
         KK=1
2        READ(4,71) (A(L),L=1,N)
         DO 6 JJ=(N+1),J
6        A(JJ)=0
         DO 8 JJ=(M+1),J
8        B(JJ)=0
```

```
        DO 29 JJ=1,J
29      C(JJ)=0
        DO 39 L=1,J
        DO 39 K=1,M
        IF((L-K+1).LE.0) GO TO 39
        PROD(L)=B(K)*A(L-K+1)
        C(L)=C(L)+PROD(L)
39      CONTINUE
        WRITE(9,71)  (C(L),L=1,J)
        KK=KK+1
        IF(KK.LT.20) GO TO 2
        CLOSE(UNIT=9,STATUS='SAVE')
        STOP
        END
```

```
C
C                           ----------
C                             DFRST
C                           ----------
C
C
C       PROGRAM TO DO DIFFRACTION STACK MIGRATION USING SYNTHETIC DATA
C       ZERO OFFSET SYNTHETIC DATA WAS GENERATED
C       FOR AN INCLINED REFLECTOR
C       DIP OF REFLECTOR=10 DEGREES
C       APERTURE SIZE=FIVE INPUT TRACES
C       INPUT AND OUTPUT SAMPLING INTERVAL=1MS
C       MIGRATION VELOCITY=2000 M/S
C       TRACE INTERVAL=25M
C       THIS PROGRAM WILL GENERATE MIGRATED OUTPUT FOR 19 TRACES
        DIMENSION DSAM(1800,29),TSAM(1800),X(29),A1(1800)
        DIMENSION TAM(1800),P(29)
C       THIS A PROGRAM TO GENERATE TIME INTERVAL
        SI=.001
        DO 13 I=1,1800
13      TAM(I)=SI*FLOAT(I)
        OPEN(UNIT=8,FILE='TS.DAT',STATUS='NEW')
        WRITE(8,7) TAM
        CLOSE(UNIT=8,STATUS='SAVE')
7       FORMAT(10F8.3)
C
C
C       THIS IS A PROGRAM TO GENERATE OFFSET DISTANCES
        DELTAX=25.0
        DO 14 I=1,29
14      P(I)=DELTAX*(I-1)
        OPEN(UNIT=9,FILE='OFFSET.DAT',STATUS='NEW')
        WRITE(9,11) P
        CLOSE(UNIT=9,STATUS='SAVE')
11      FORMAT(10F8.0)
C
C
C       THIS PROGRAM DOES DIFFRACTION STACK MIGRATION
C       SY252.DAT IS THE ZERO OFFSET SYNTHETIC DATA
        OPEN(UNIT=3,FILE='SY252.DAT',STATUS='OLD')
        OPEN(UNIT=4,FILE='TS.DAT',STATUS='OLD')
        OPEN(UNIT=5,FILE='OFFSET.DAT',STATUS='OLD')
        READ(3,51) ((DSAM(I,J),I=1,1800),J=1,29)
        READ(4,52) (TSAM(I2),I2=1,1800)
51      FORMAT(10F8.3)
52      FORMAT(10F8.3)
        SIT=.001
        V=2000.00
        XZERO=125
        READ(5,53) (X(I),I=1,29)
53      FORMAT(10F8.0)
        J=1
55      DO 10 IX=1,1800
        TST=SIT*FLOAT(IX)
        DO 20 IY=J,J+10
        TX=SQRT(((TST)**2)+((2*(X(IY)-XZERO)/V)**2))
        DO 30 IZ=1,1800
        TT=TX
        TZ=ABS(TT-TSAM(IZ))
        IF(TZ.LT..0005) GO TO 36
        GO TO 30
36      A1(IY)=DSAM(IZ,IY)
```

```
30         CONTINUE
20         CONTINUE
           AB=0.0
           DO 40 I=J,J+10
           AB=AB+A1(I)
           AB=AB/11.0
40         CONTINUE
           DSAM(IX,J+5)=AB
45         FORMAT(10F8.3)
10         CONTINUE
           XZERO=XZERO+25
           J=J+1
           IF(J.LT.25) GO TO 55
           OPEN(UNIT=20,FILE='MIGRT.DAT',STATUS='NEW')
           WRITE(20,45) ((DSAM(I,J),I=1,1800),J=6,24)
           CLOSE(UNIT=20,STATUS='SAVE')
           STOP
           END
```

```fortran
C                              ---------
C                              TRATIME
C                              ---------
C       THIS IS A PROGRAM TO GENERATE TRAVEL TIME
C       FOR AN INCLINED REFLECTOR
C       IT CALCLULATES TRAVEL TIME FOR REFLECTOR
C       WITH DIP=0 TO 85 DEGREES
C       TOTAL NO. OF OFFSET DISTANCES=21
        REAL T,DELTAX,THETA,D,VINT
C
        DIMENSION T(21,18),DELTAX(21),THETA(18),D(21,18),VINT(21,18)
C       V STANDS FOR VELOCITY OF THE MEDIUM
C       Z STANDS FOR DEPTH AT ZERO OFFSET DISTANCE
        V=2000.0
        Z=100.0
        DATA DELTAX/0.0,25.0,50.0,75.0,100.0,125.0,150.0,175.0
     3  ,200.0,225.0,250.0,275.0,300.0,325.0,350.0,375.0,400.0
C    2  ,425.0,450.0,475.0,500.0/
C
        DATA THETA/0.0,5.0,10.0,15.0,20.0,25.0,30.0,35.0,40.0,45.0,50.0
     4  ,55.0,60.0,65.0,70.0,75.0,80.0,85.0/
        DO 15 J=1,18
        DO 15 I=1,81
        T(I,J)=(2*(Z+DELTAX(I)*TAND(THETA(J))))/V
        D(I,J)=(T(I,J)*2000.00)/2.0
15      VINT(I,J)=2*D(I,J)/T(I,J)
        WRITE(6,213)
213     FORMAT(' INTERVAL VELO. OF DIFF. DEPTHS FOR A SINGLE INCLREFL')
        WRITE(6,210) VINT
        WRITE(6,212)
212     FORMAT(' DEPTH VALUES OF DIFFERENT TWO-WAY REFLECTIONTIME')
        WRITE(7,210) D
        WRITE(11,211)
211     FORMAT(' TWO-WAY REFLECTIONTIME IN SEC')
        WRITE(11,214) T
210     FORMAT(10F8.3)
214     FORMAT(10F8.3)
        STOP
        END
```

```
C                           -----------
C                           ANTRATIME
C                           -----------
C
C      THIS IS A PROGRAM TO GENERATE TRAVEL TIME FOR AN ANTICLINE
C      DIP OF THE ANTICLINE=10 DEGREES
C      TOTAL NO. OF OFFSET DISTANCES=21
C
       REAL T,DELX,THETA
C
       DIMENSION DELX(21),THETA(21)
C      V STANDS FOR VELOCITY OF THE MEDIUM
C      Z STANDS FOR DEPTH AT ZERO OFFSET DISTANCE
       V=2000.0
       Z=1000.0
       DATA THETA/0.,0.,0.,0.,0.,0.,10.,10.,10.,10.
     3 ,-10.,-10.,-10.,-10.,0.,0.,0.,0.,0.,0.,0./
       DATA DELX/0.,25.,25.,25.,25.,25.,25.,25.
     2 ,25.,25.,25.,25.,25.,25.,25.,25.
     4 ,25.,25.,25.,25./
       I=1
14     T=(2*(Z-DELX(I)*TAND(THETA(I))))/V
       Z=Z-DELX(I)*TAND(THETA(I))
       OPEN(UNIT=7,FILE'ANTRAT.DAT',STATUS='NEW')
       WRITE(7,211) T
       I=I+1
       IF(I.LT.22) GO TO 14
       CLOSE(UNIT=7,STATUS='SAVE')
211    FORMAT(10F8.3)
       STOP
       END
```

```
C                       ----------.
C                         FLDPLOT
C                       ----------
C       THIS IS A PROGRAM TO PLOT 504 MIGRATED SEISMIC TRACES
C       SEISMIC LINE-G583B IS LOCATED IN GRAND BANKS,NFLD.
        REAL DSAM(750,504),TRACE(752),TIME(752)
        OPEN(UNIT=10,FILE='FOR012.DAT',STATUS='OLD')
        READ(10,15) ((DSAM(I,J),I=1,750),J=1,504)
   15   FORMAT(10F8.3)
C       THE AMLITUDE IS ENHANCED BY A FACTOR OF 2.0
C       DF=DIVIDING FACTOR
C       DF=0.16666667
        TRACE(751)=-300.0
        TRACE(752)=3600.0
        TIME(751)=0.0
        TIME(752)=.2
        TIME(1)=3.0
        DO 20 I=2,750
        TIME(I)=TIME(I-1)-.004
   20   TRACE(I)=DSAM(I,1)
        CALL PLOTS(53,0,-1)
C       CALL FACTOR(1.0)
        CALL SCALE(TIME,15.0,750,1)
        CALL PLOT(2.,2.,-3)
        CALL AXIS(0.0,0.0,9HTIME(SEC),9,15.,90.,3.0001,-0.2)
        CALL PLOT(0.25,0.,-3)
        CALL SYMBOL(1.0,16.,.2,30HGRAND BANKS SEISMIC LINE-G583B,0.,30)
        CALL SYMBOL(1.0,15.5,.1,27HMIGRATION VELOCITY=3500 M/S,0.,27)
        CALL SYMBOL(0.,-1.,.1,39HFIG.    SEISMIC SECTION AFTER MIGRATION
      4 ,0.,39)
        DO 100 I1=1,504
        CALL LINE(TRACE,TIME,750,1,0,2)
        CALL PLOT(.04,0.,-3)
        IF(I1.EQ.504) GO TO 100
        DO 120 I2=1,750
  120   TRACE(I2)=DSAM(I2,I1+1)
  100   CONTINUE
        CALL PLOT(8.0,-.5,999)
        STOP
        END
```

Appendix 2: Calculation of Reflectivity for two Synthetic Models

Two synthetic models were considered - an inclined reflector and an anticline (Figures A2.1 and A2.2) respectively to calculate the reflectivity at the reflecting interface. Both models consist of a single reflecting surface overlain by a material of constant velocity 2000 m/s with density value 2.2 gm/c.c. The layer below the first reflecting surface has velocity and density values of 3000 m/s and 2.3 gm/c.c respectively. The reflectivity or reflection co-efficient of the single reflecting surface (Waters, 1981, p. 26) can be obtained from the simple relationship.
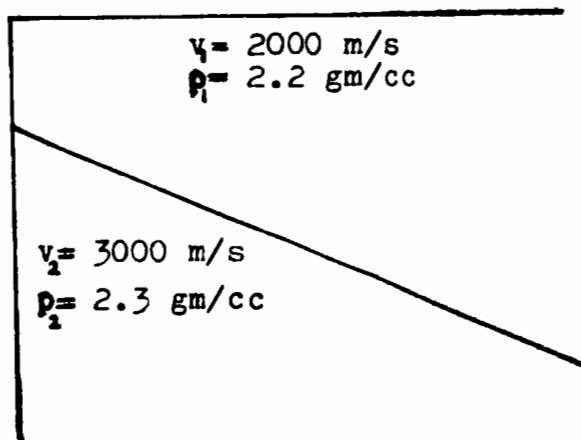
Fig. A2.1 An Inclined Reflector Model   Fig. A2.2 An Anticline Model
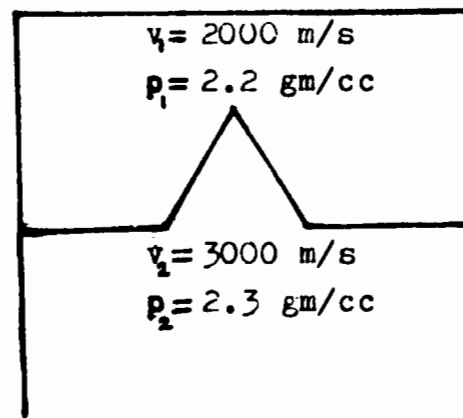
$$R_i = (P_{i+1}V_{i1} - P_iV_i)/(P_{i+1} + P_iV_i) \qquad \text{A2.1}$$

$$i = 1$$

where P_i and V_i denote the density and velocity. Using the values of P's and V's in the equation A2.1, the reflectivity $R_1 = 0.13$ is obtained.

ACKNOWLEDGEMENTS

REFERENCES

Al-Sadi, N.H., 1980, Seismic Exploration Technique and Processing,
Birkhauser Verlag, Basel.

Amoco and Imperial Oil, 1973, Regional Geology of the Grand Banks, Bull.
Can. Pet. Geol. v. 21, p. 479-503.

Anstey, N.A., 1977, Seismic Interpretation: The Physical Aspects, IHRDC
Publications, Boston.

Barry, K.M., Cavers, D.A., and Kneale, C.W., 1975, Recommended standards
for digital tape formats, Geophysics, v. 40, p. 344-352.

Bentley, C.R. and Worzel, J.L., 1956, Geophysical investigations in the
emerged and submerged Atlantic Coastal Plain, Part X: Continental
Slope and Continental Rise south of the Grand Banks, Geol. Soc.
America Bull., v. 67, p. 1-18.

Bower, M.E., 1962, Sea magnetometer surveys of the Grand Banks of
Newfoundland, Burgeo Bank, and St. Pierre Bank, Geol. Surv. Canada,
Paper 61-30, 11p.

Claerbout, J.F., 1970, Coarse grid calculations of waves in inhomogeneous
media with application to dilineation of complicated seismic
structure, Geophysics, v. 35, p. 407-418.

Dobrin, M.B., 1976, Introduction to Geophysical Prospecting, 3rd Edition, McGraw-Hill Publishing Co., New York.

Dohr, G., 1981, Applied Geophysics, 2nd Edition, Ferdinand Enke Verlag, Stuttgart.

Ewing, J., and Ewing, M., 1959, Seismic refraction measurements in the Atlantic Ocean Basins, in the Mediterranean Sea, on the Mid-Atlantic Ridge and in the Norwegian Sea, Geol. Soc. America Bull., v. 70, p. 291-318.

French, W.S., 1975, Computer migration of oblique seismic reflection profiles, Geophysics, v. 40, p. 961-980

Hagedoorn, J.G., 1954, A process of seismic reflection interpretation, Geophys. Prosp., v. 2, p. 85-127.

Hood, P., and Godby, E.A., 1965, Magnetic profile across the Grand Banks and Flemish Cap off Newfoundland, Can. J. Earth Sciences, v. 1, p. 85-92.

James, M.L., Smith, G.M., and Wolford, J.C., 1977, Applied Numerical Methods for Digital Computation With Fortran and CSMP, 2nd Edition, Harper and Row, Publishers, New York.

Lilly, H.D., 1965, Submarine examination of the Virgin Rocks area, Grand
Banks, Newfoundland, Preliminary note, Geol. Soc. America Bull.,
v. 76, p. 131.

McMillan, N.J., 1982, Canada's east coast: the new super petroleum
province, Journal of Canadian Petroleum Technology, v. 21, no. 2,
p. 1-15.

Owusu, K., Gardner, G.H.F., and Massell, W.F., 1981, Velocity estimates
derived from three-dimensional seismic data, presented at 51st Ann.
International Mtg. of SEG, Los Angeles.

Pelletier, B.R., 1971, A granodioritic drill core from Flemish Cap,
eastern Canadian continental margin, Can. J. Earth Sciences, v. 8,
p. 1499-1503.

Peterson, R.A., Fillippone, W.R., and Coker, F.B., 1955, The synthesis of
seismograms from Well Log Data, Geophysics, v. 20, p. 516-538.

Petroleum Directorate Information Kit, 1984, Government of Newfoundland
and Labrador, St. John's, Canada.

Press, F., and Beckmann, W., 1954, Geophysical investigations in the
emerged and submerged Atlantic Coastal Plain, Part VIII, Grand Banks
and adjacent shelves, Geol. Soc. America Bull., v. 65, p. 299-314

Proctor, R.M., Taylor, G.C., and Wade, J.A., 1983, Oil and Natural Gas
    Resources of Canada, Geological Survey of Canada - Open file 966,
    Ottawa, Canada.

Rashid, M.A., 1978, The influence of salt dome on the diagenesis of
    organic matter in the Jeanne d'Arc Subbasin of the northeast Grand
    Banks of Newfoundland Organic Geochemistry, v. 1, p. 67-77.

Robinson, E.A., and Silvia, M.T., 1977, Digital Foundations of Time Series
    Analysis: Wave-Equation Space-Time Processing, Holden-Day, Inc.,
    San Francisco.

Robinson, E.A., 1983, Migration of geophysical data, IHRDC Publications,
    Boston.

Rockwell, D.V., 1971, Migration stack aids interpretation, Oil and
    Gas J., April 19, p. 202-218.

Sattlegger, J.W., 1975, Migration velocity determination, Part I.
    Philosophy, Geophysics, v. 40, p. 1-5.

Stolt, R.H., 1978, Migration by Fourier transform, Geophysics, v. 43, p.
    23-48.

Waters, K.H., 1981, Reflection Seismology, John-Wiley and Sons, Inc., New York.

Well History Report, 1975, Mobil Gulf Adolphus D-50, Petroleum Directorate, Government of Newfoundland and Labrador, St. John's, Canada.

Well location map, 1984, Petroleum Directorate, Government of Newfoundland and Labrador, St. John's, Canada.
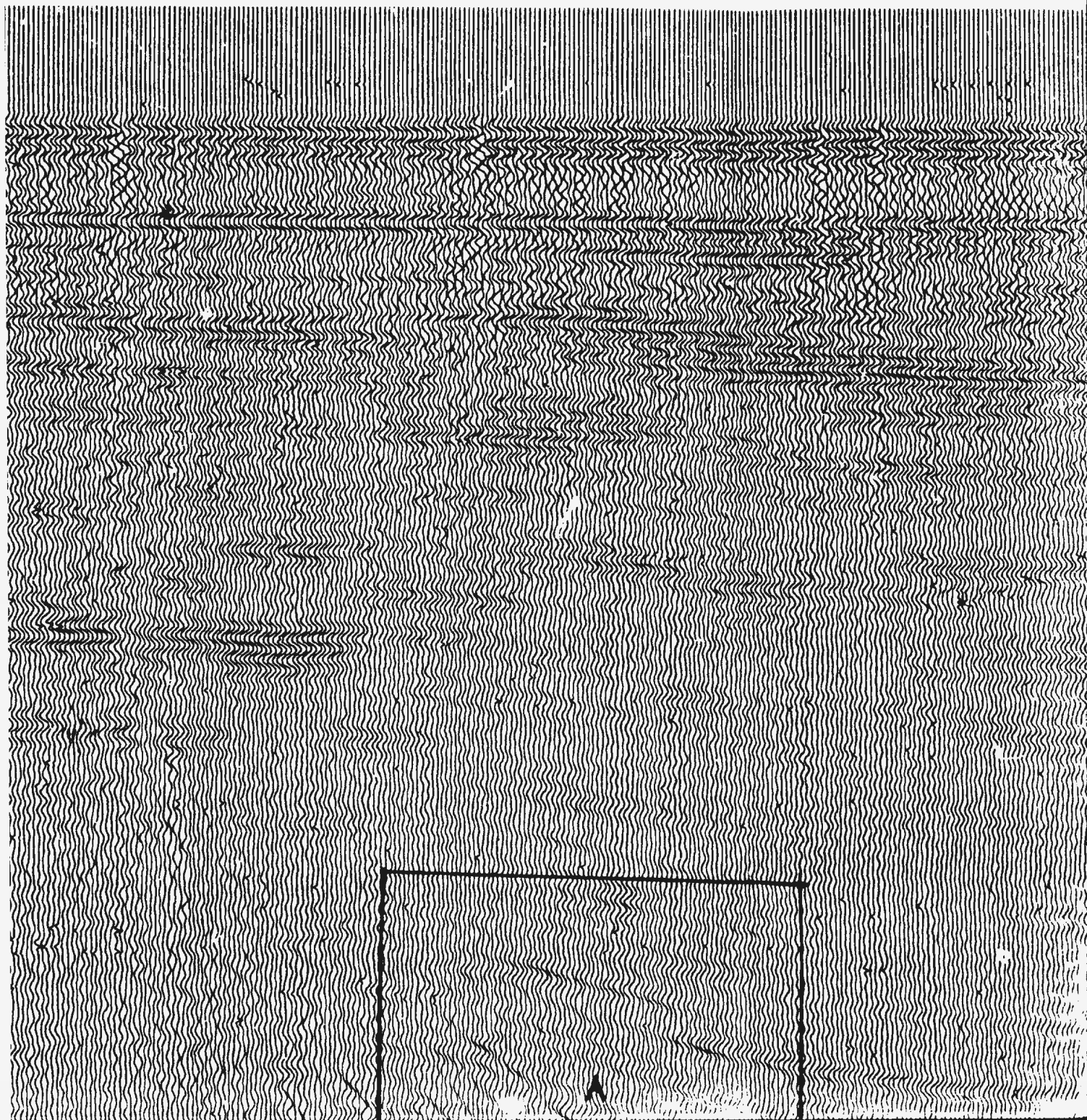
PLOT OF GRANDBANKS
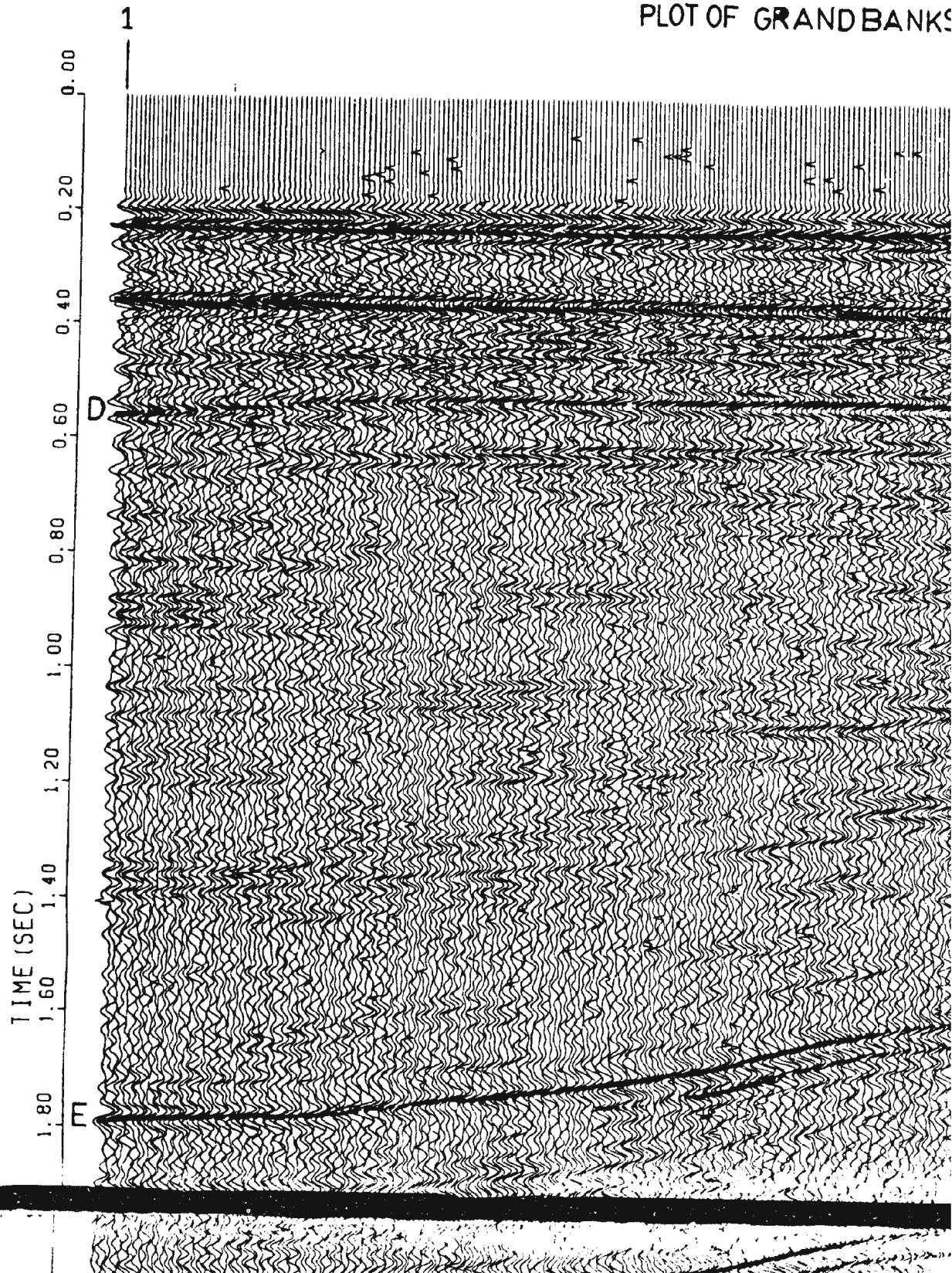
504

D

E
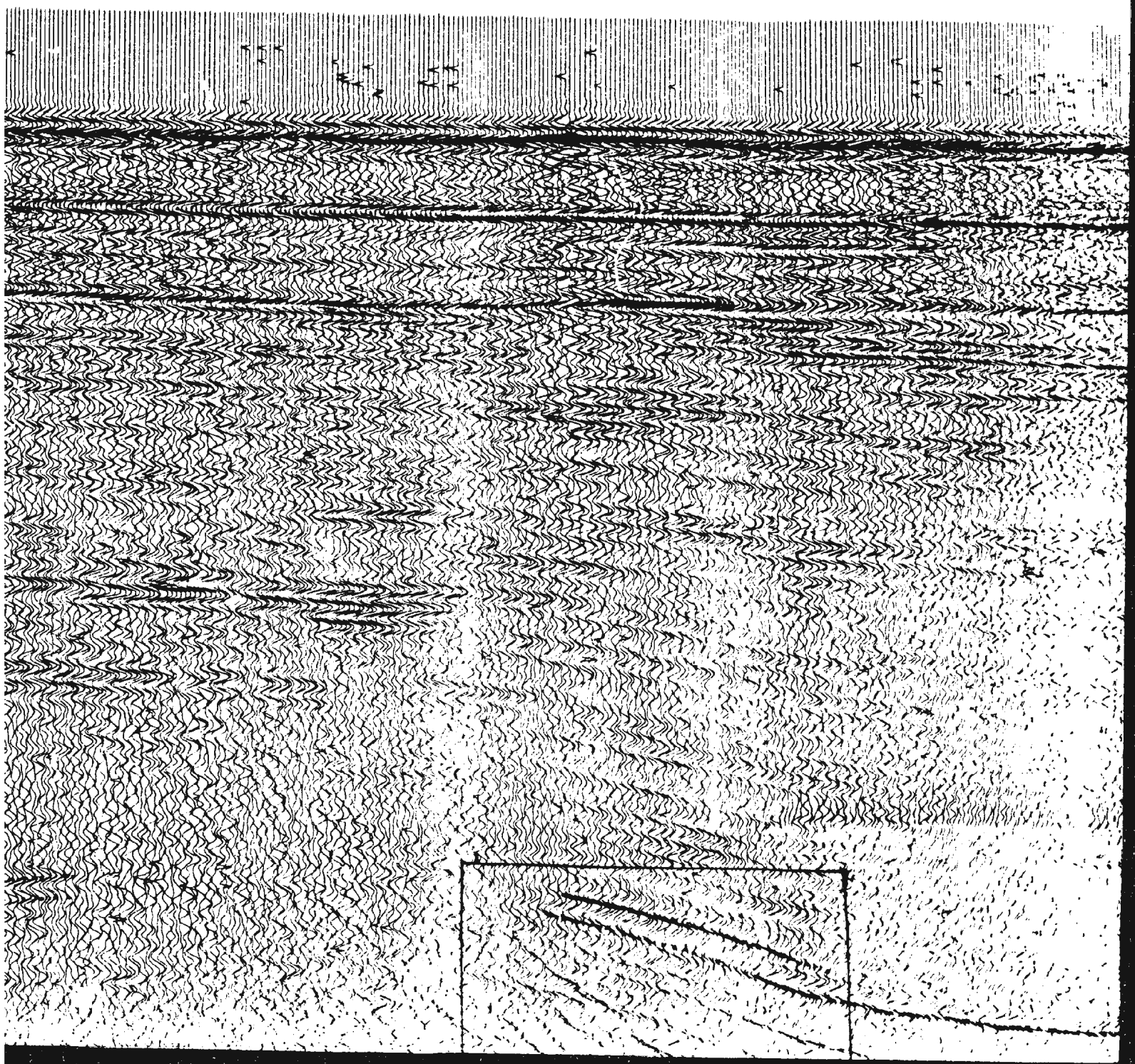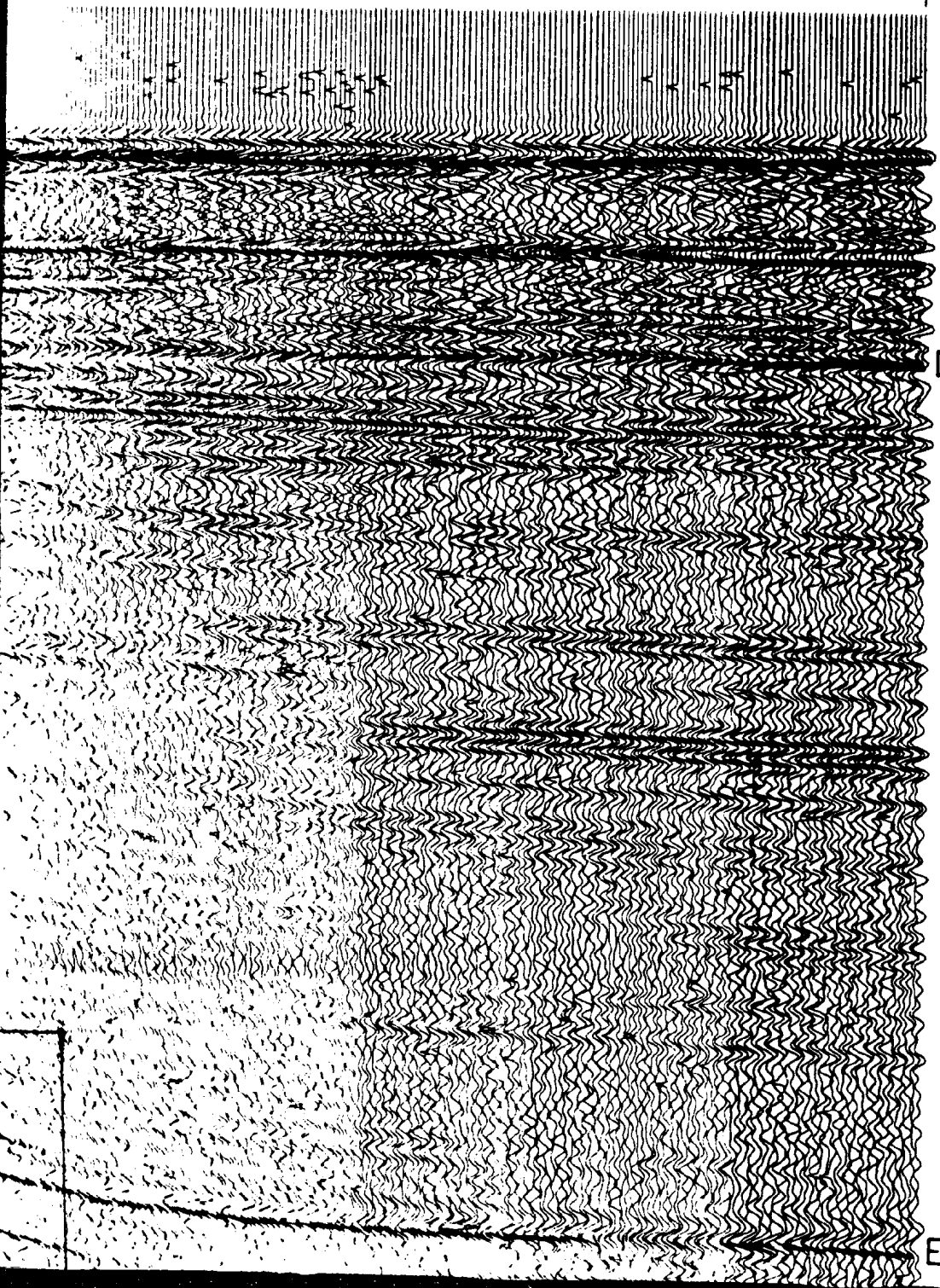
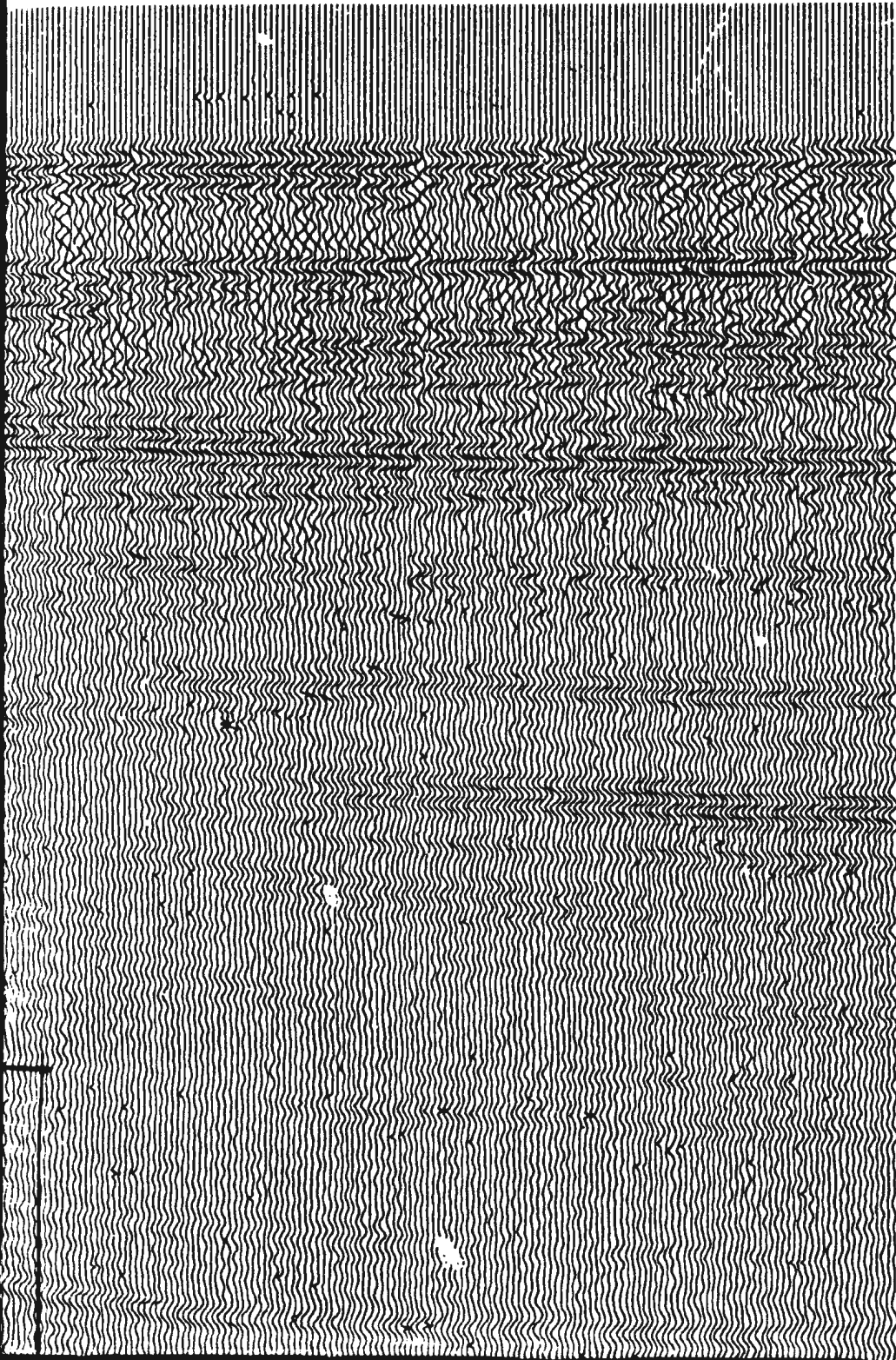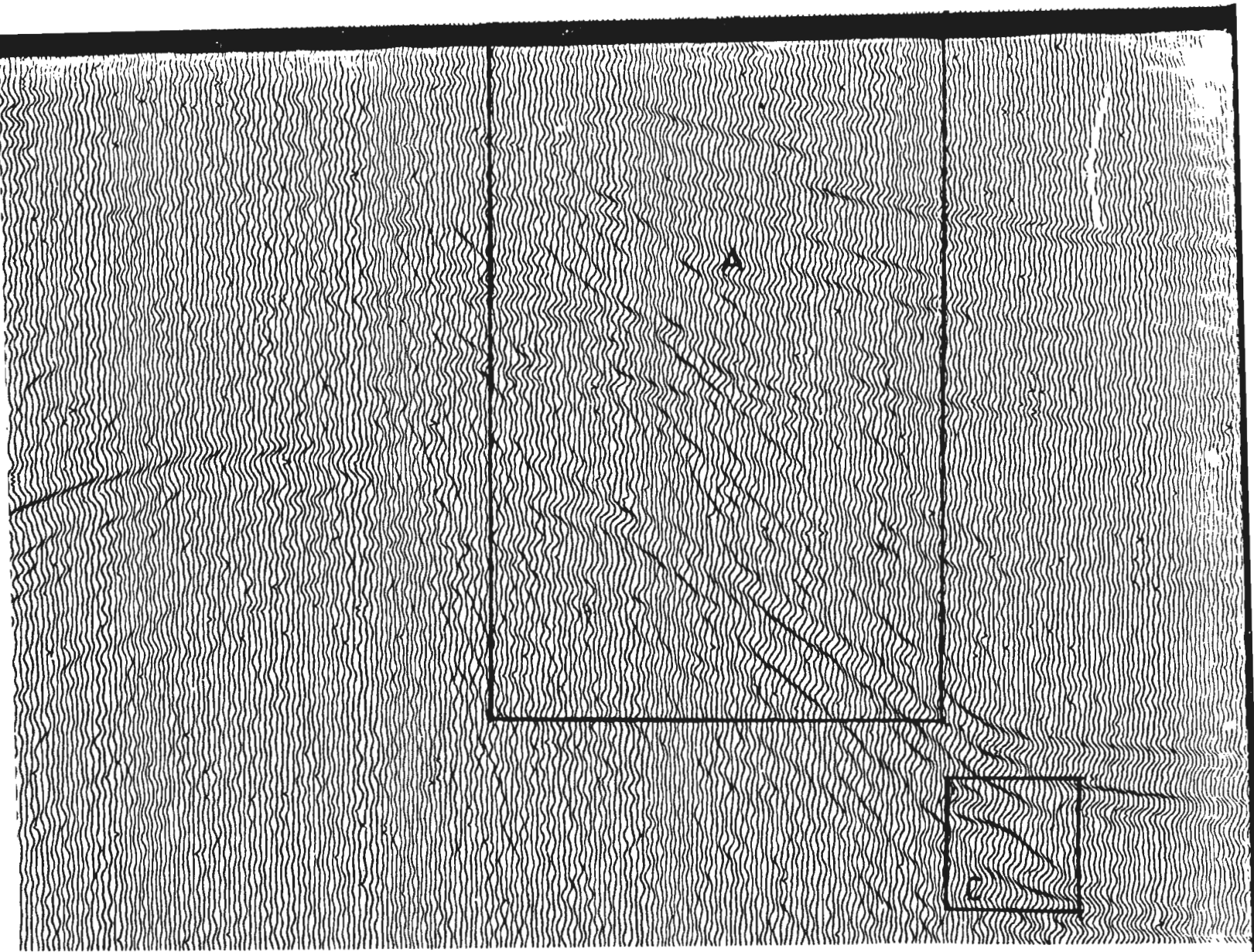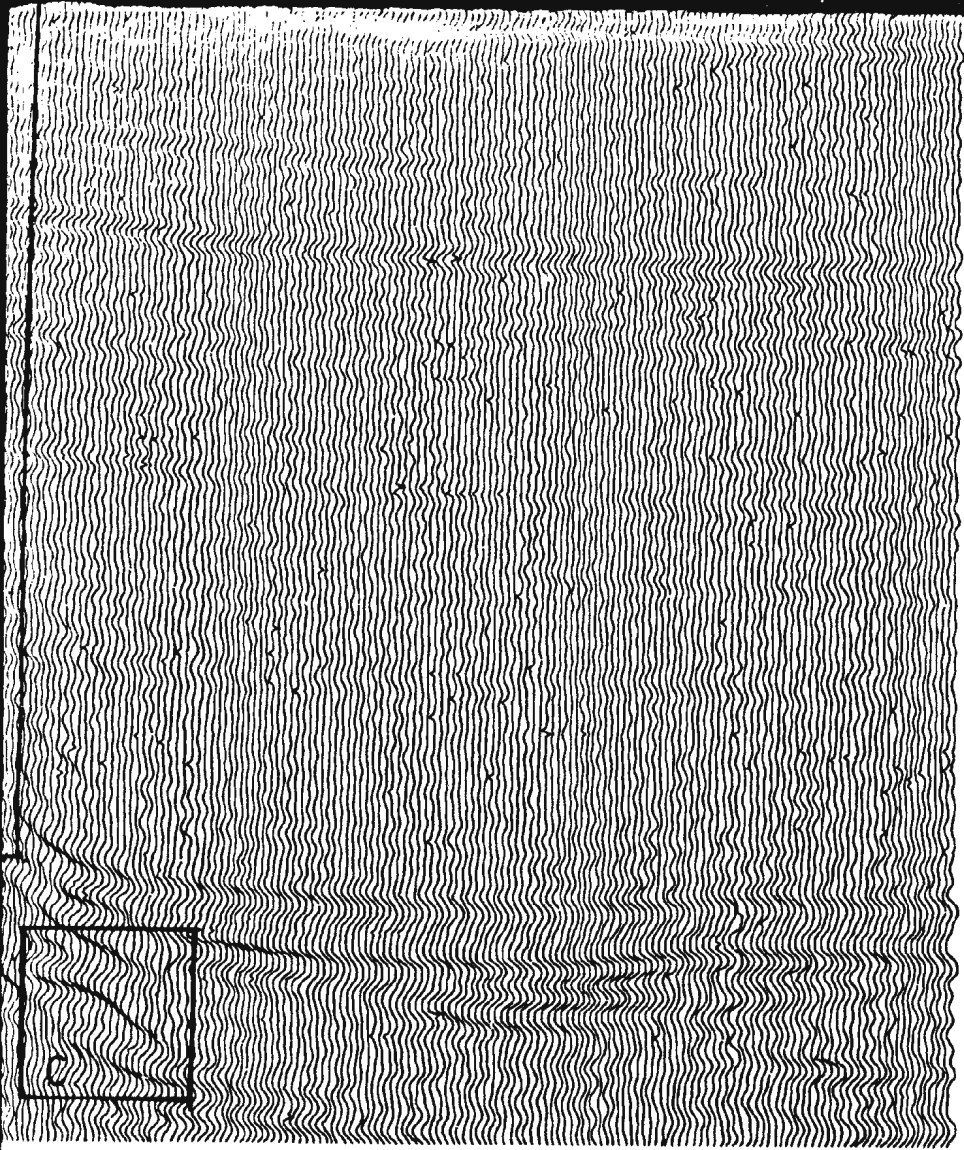# GRAND BANKS SEISMIC LINE-G583B
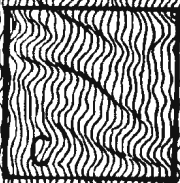
MIGRATION VELOCITY=2500 M/S

504

D

E
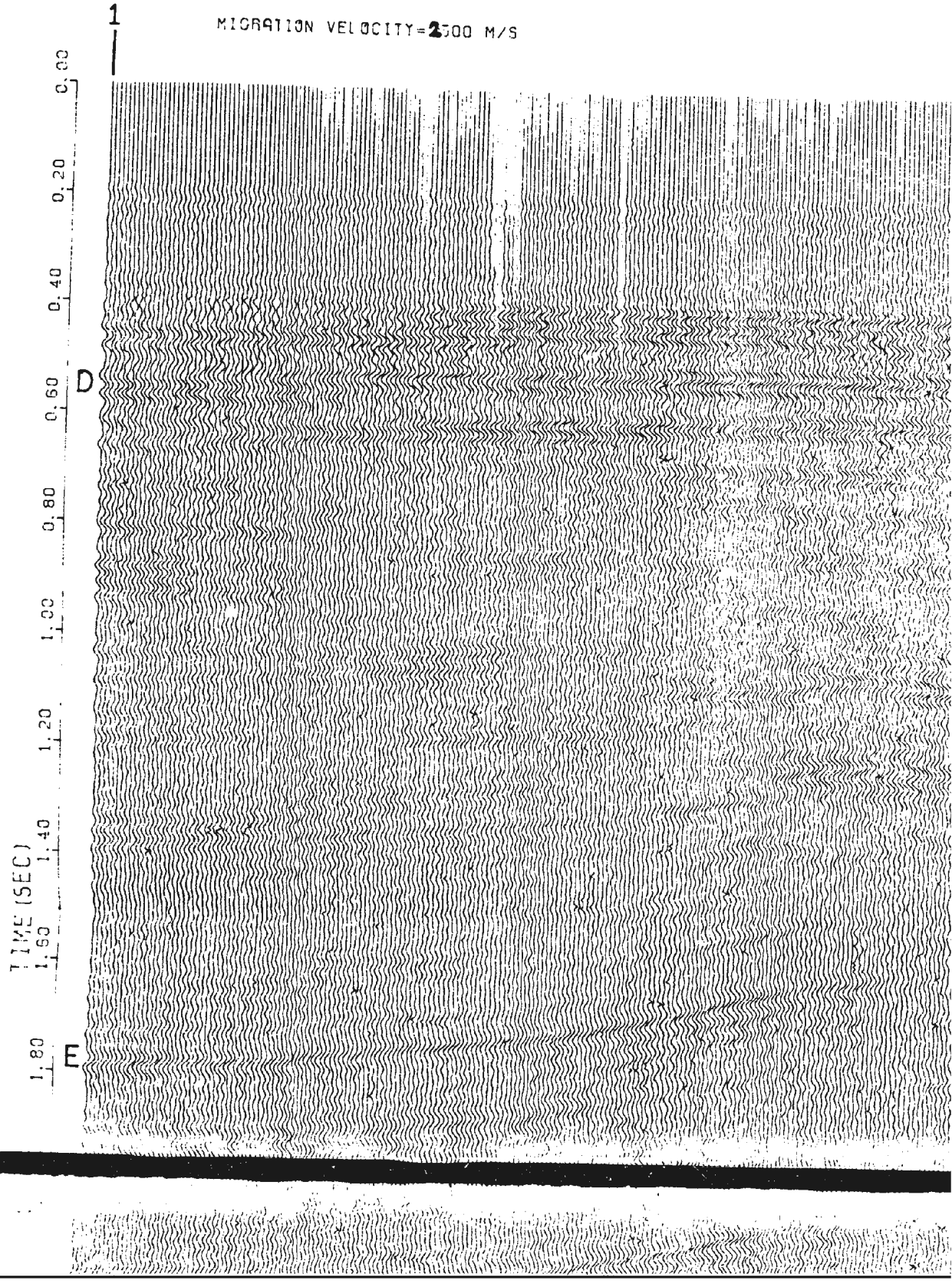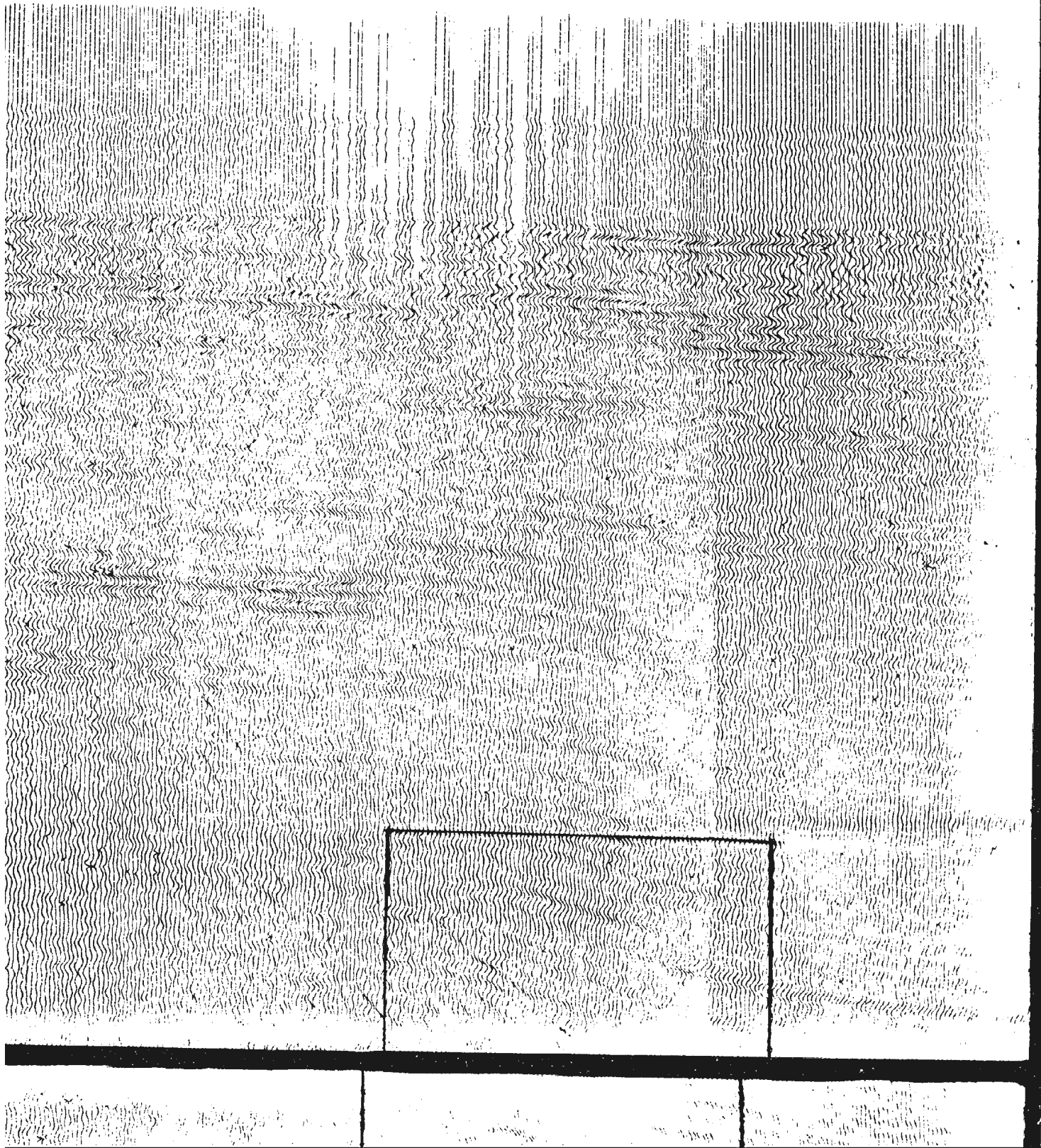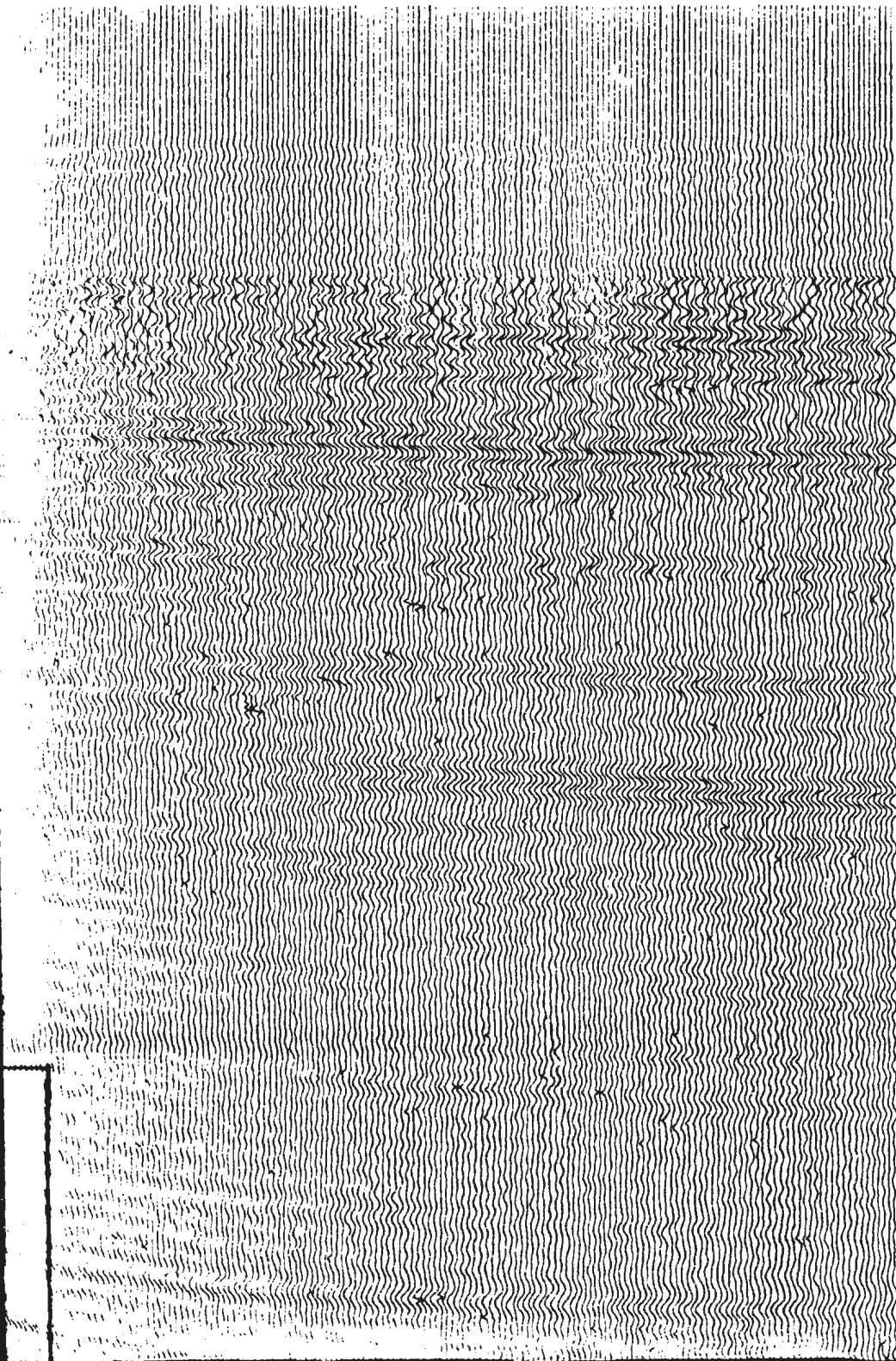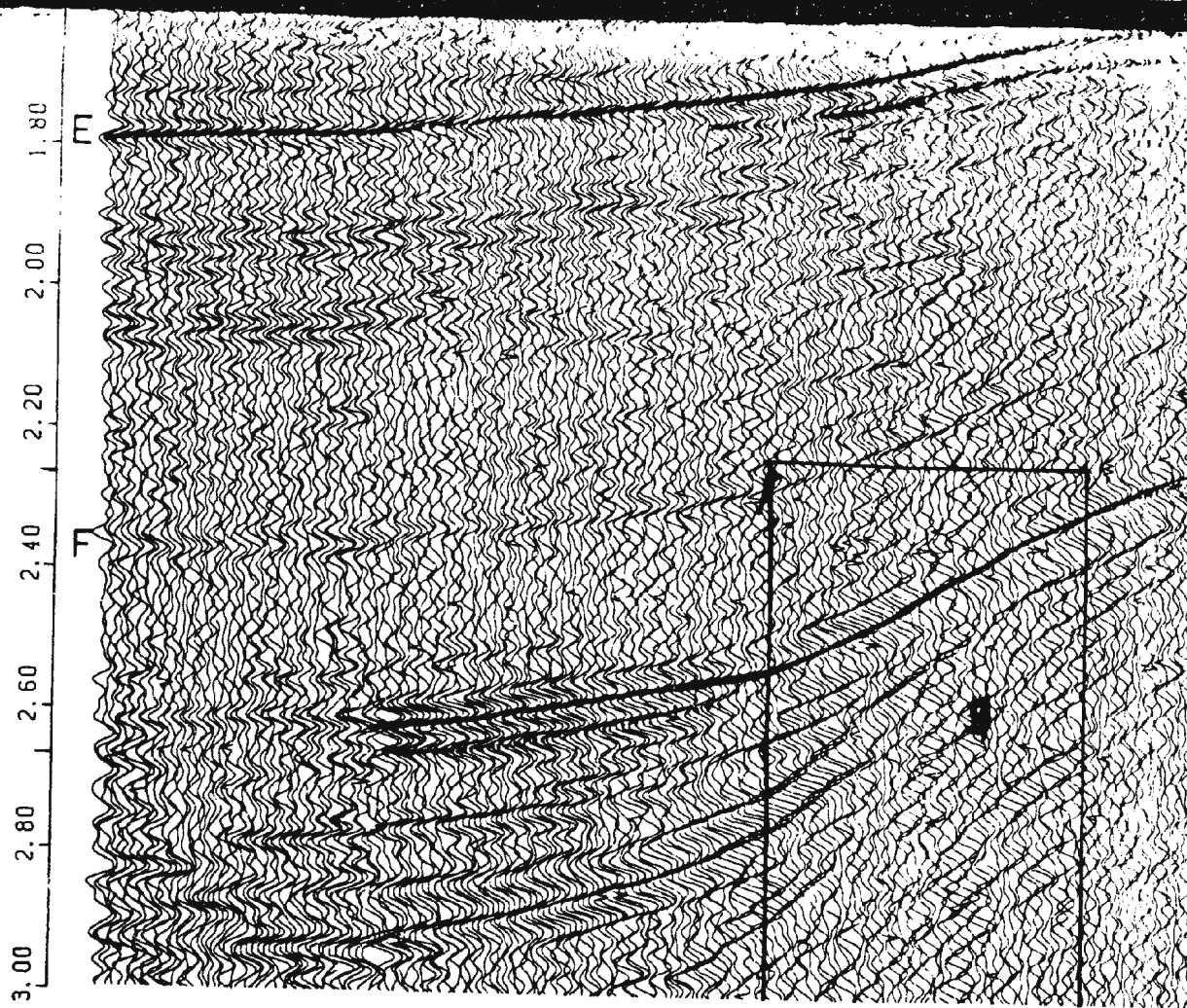
FIG.441 SEISMIC SECTION BEFORE MIGRATION
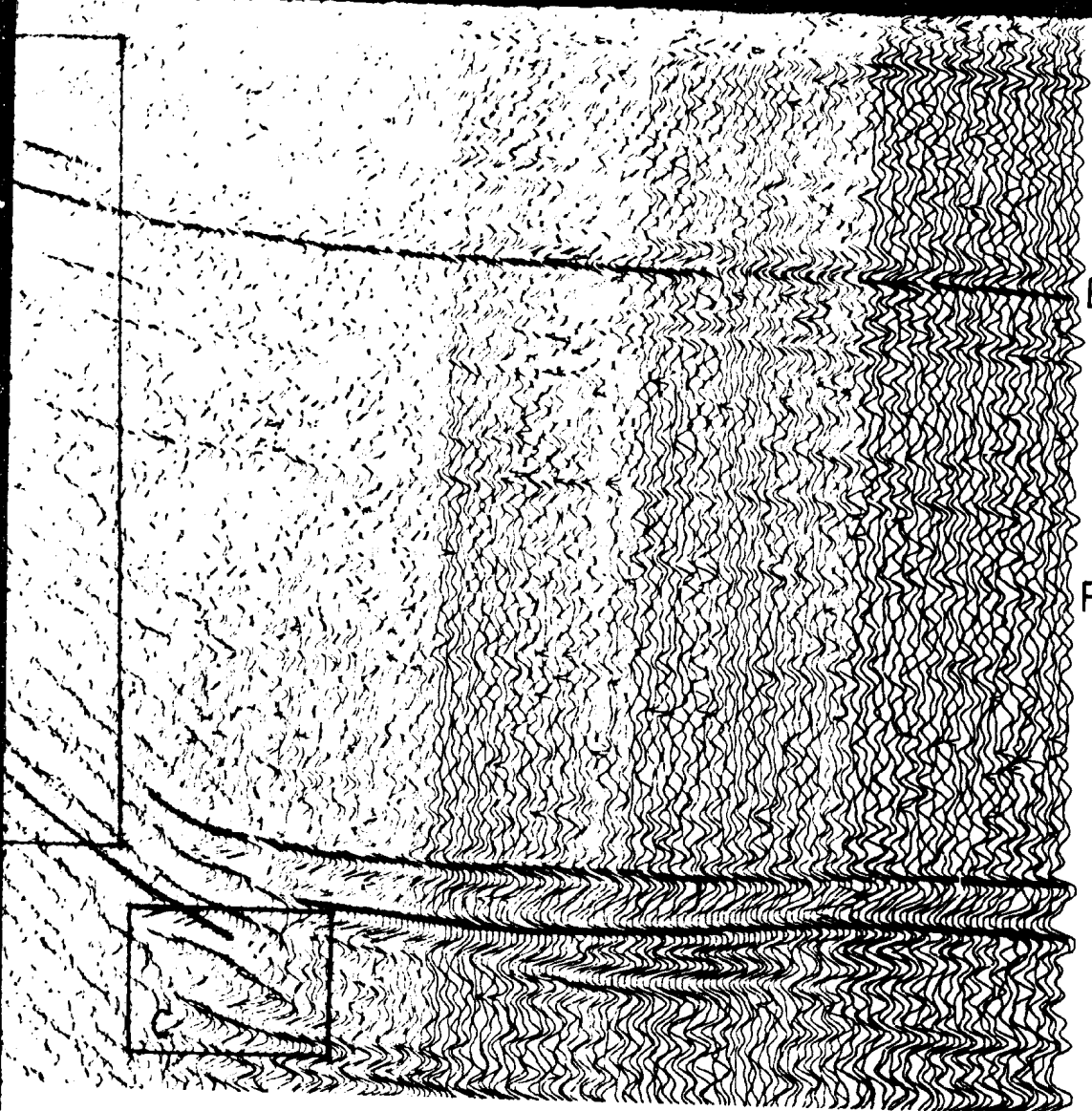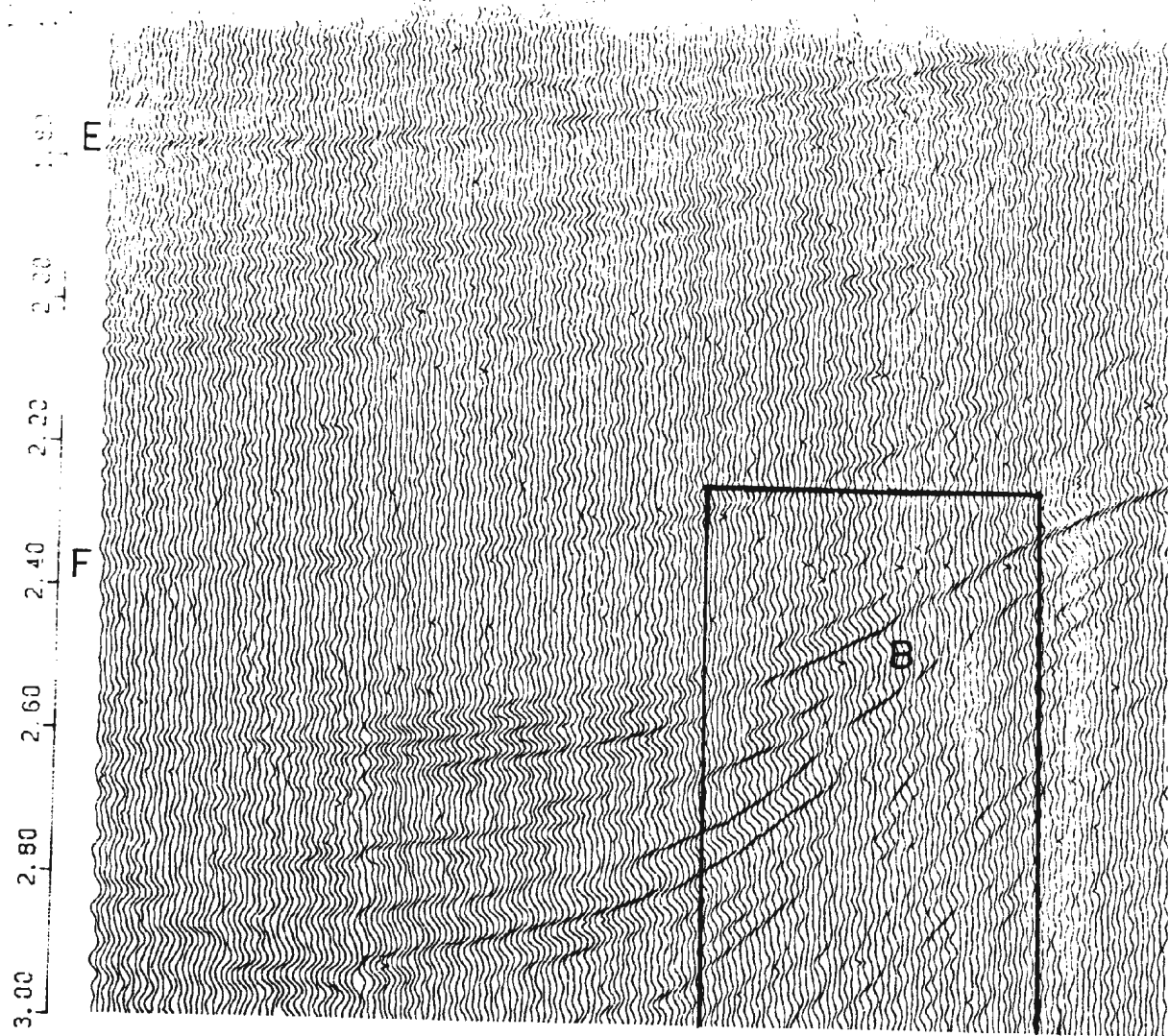
FIG. 4.4.2 SEISMIC SECTION AFTER MIGRATION
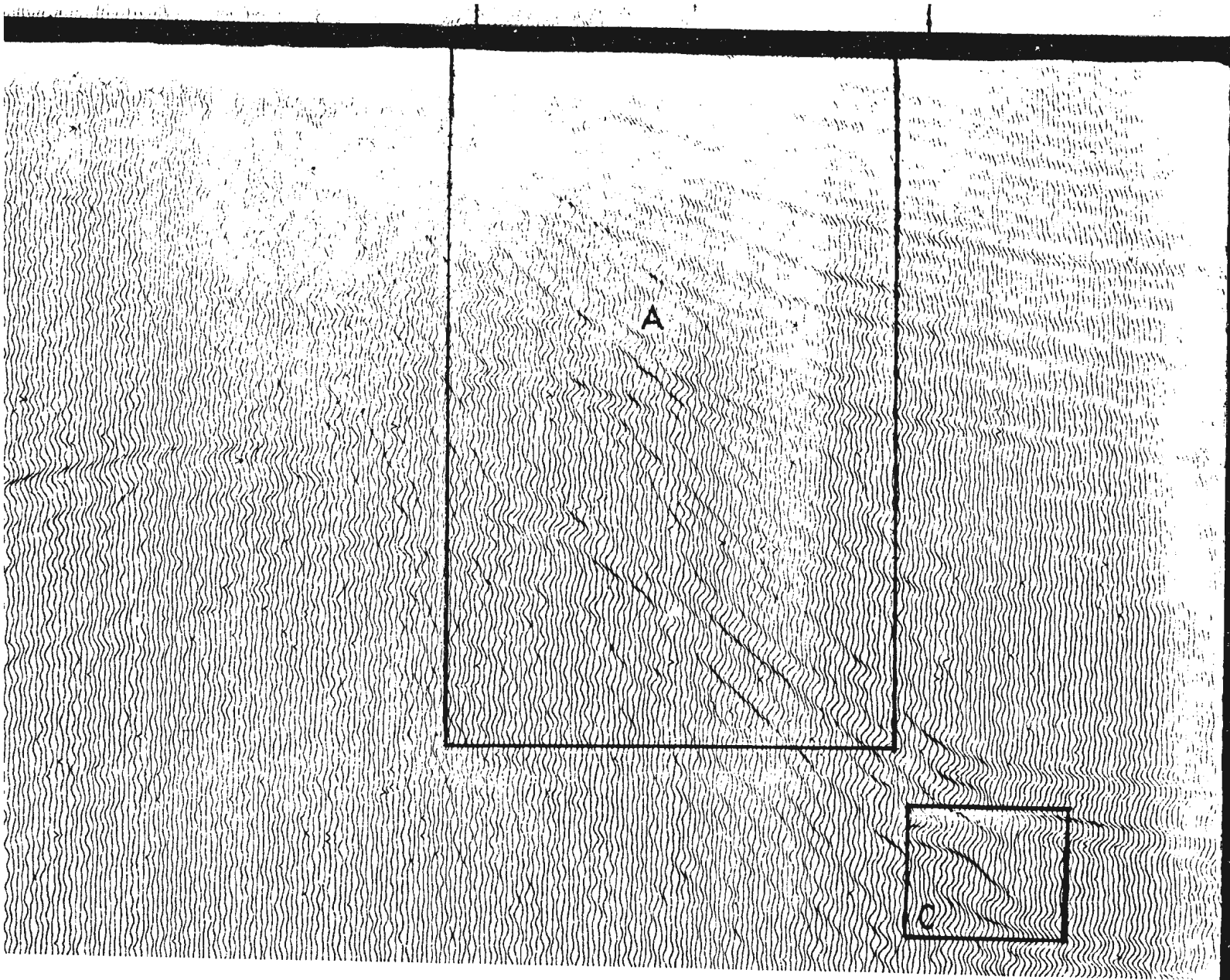
E

F
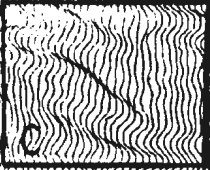
GRAND BANKS SEISMIC LINE-G583B

MIGRATION VELOCITY=3500 M/S

504

D

E
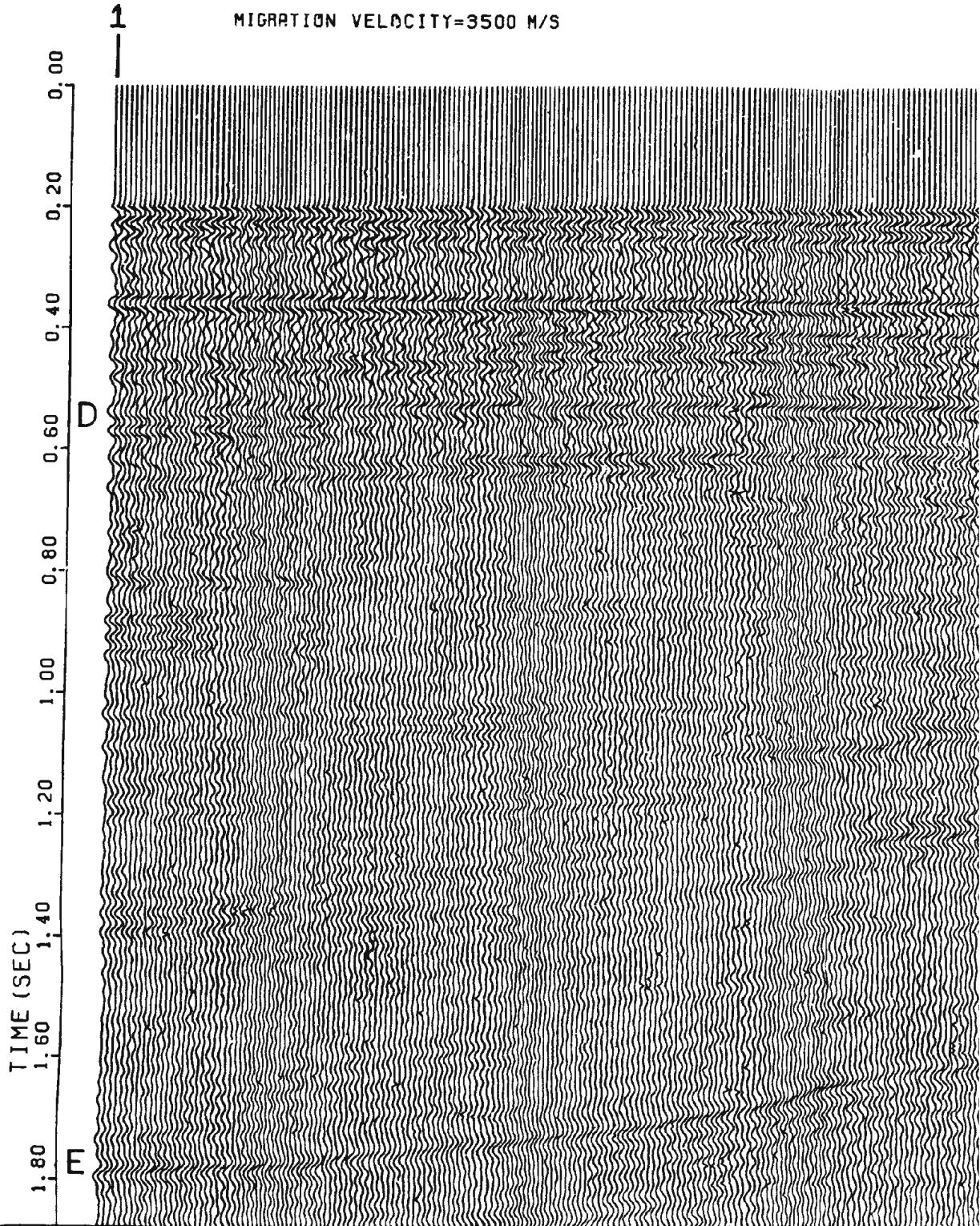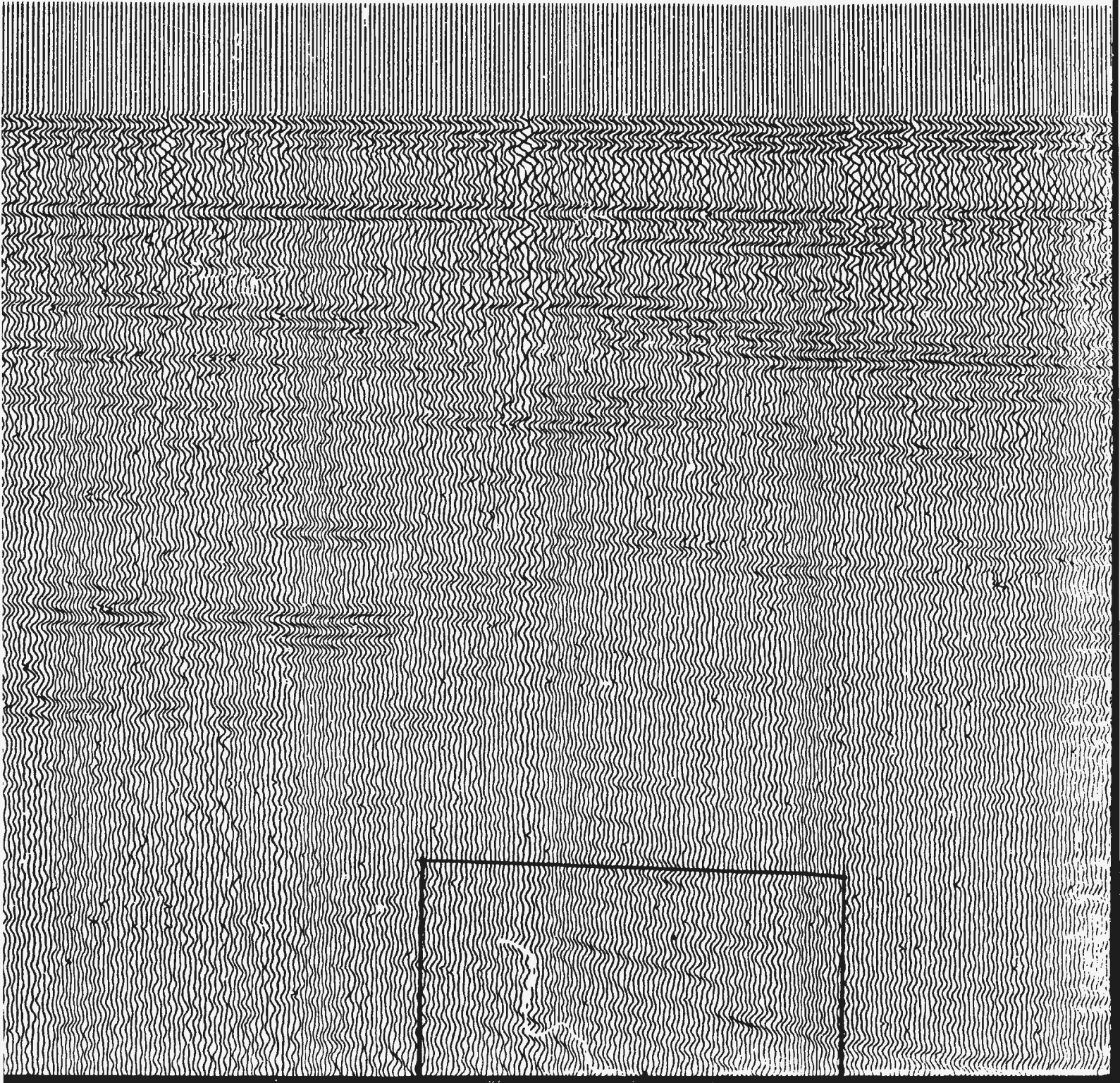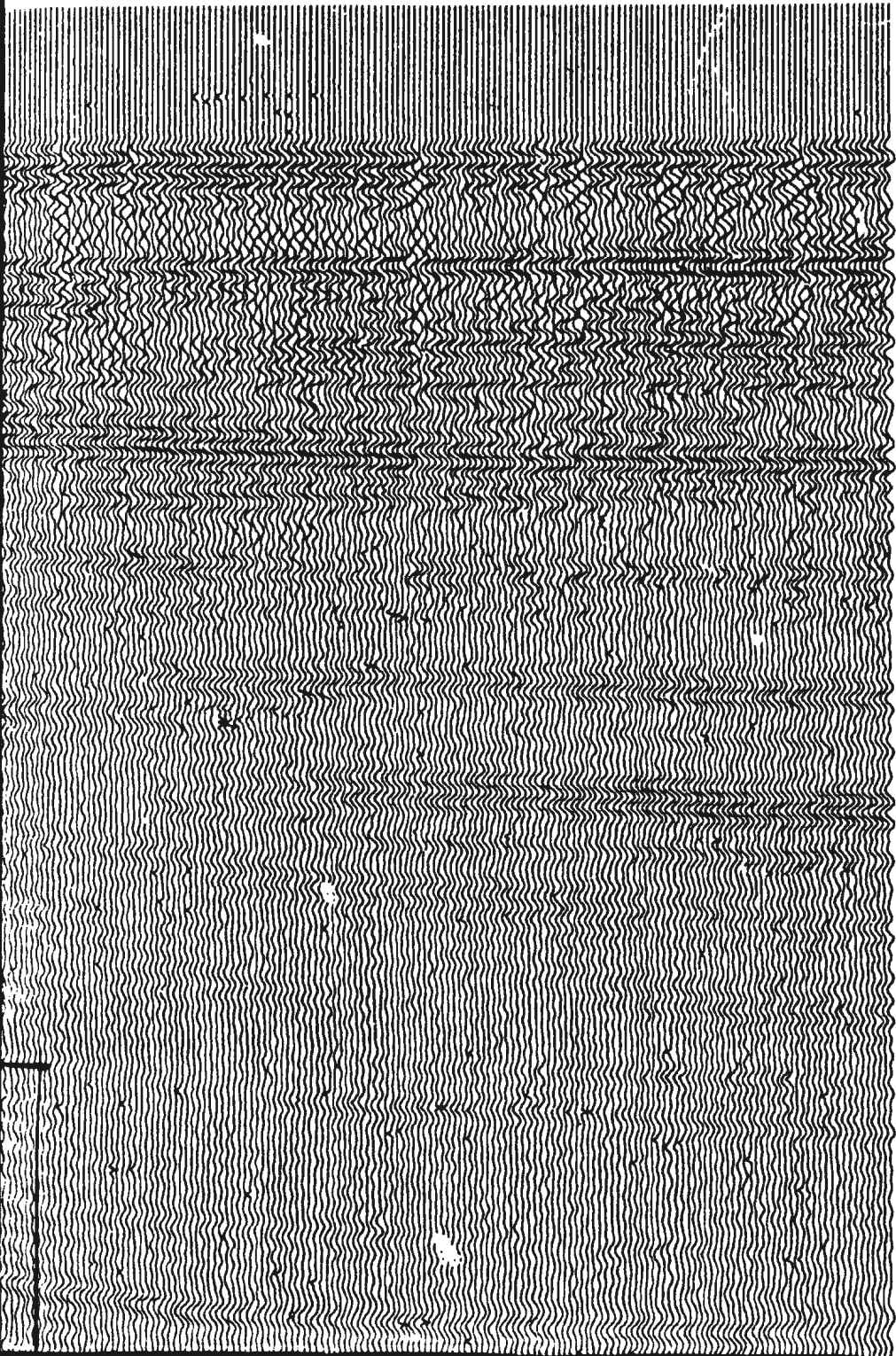
GRAND BANKS SEISMIC LINE-G583B

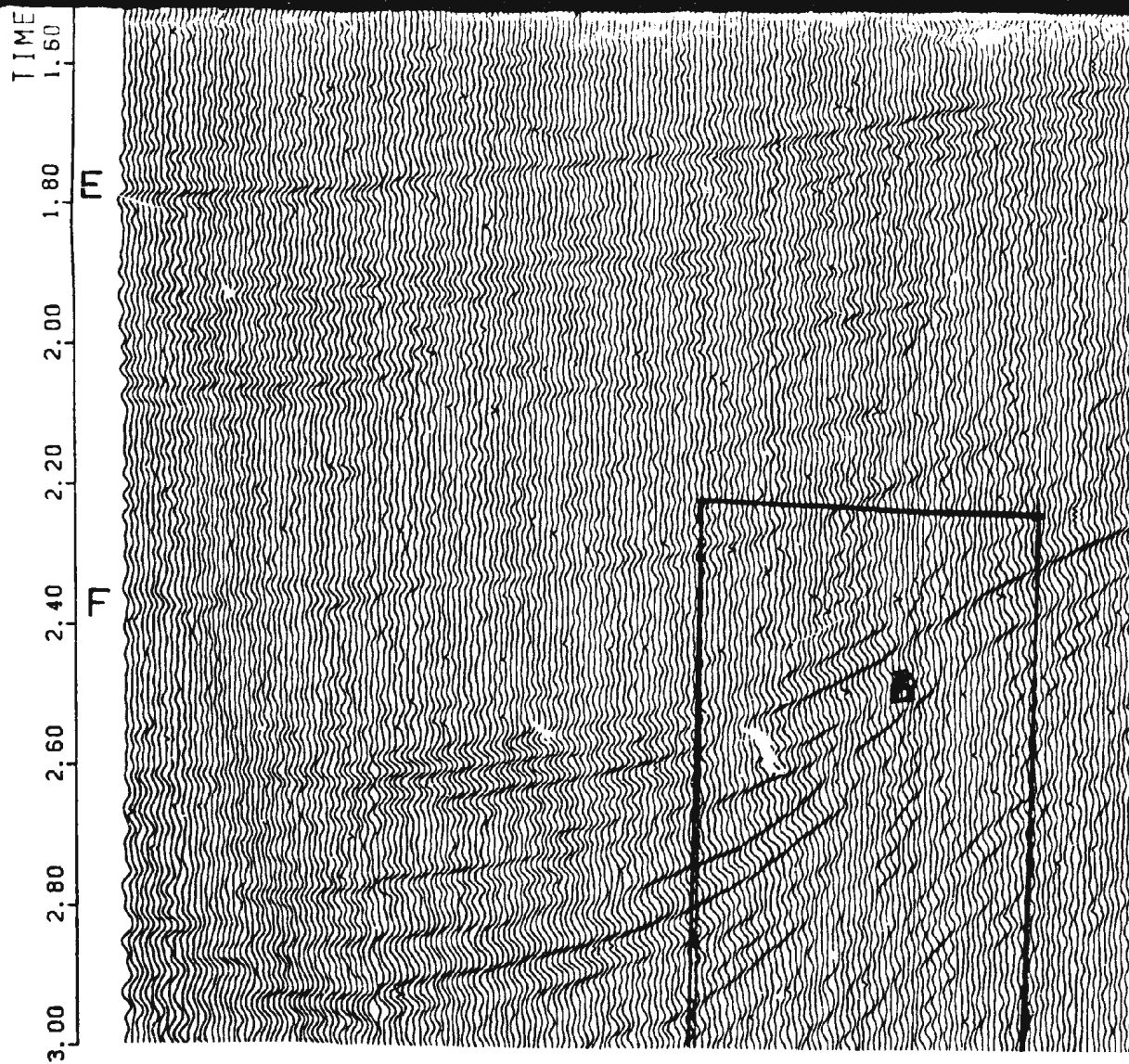MIGRATION VELOCITY=4500 M/S

504

D

E
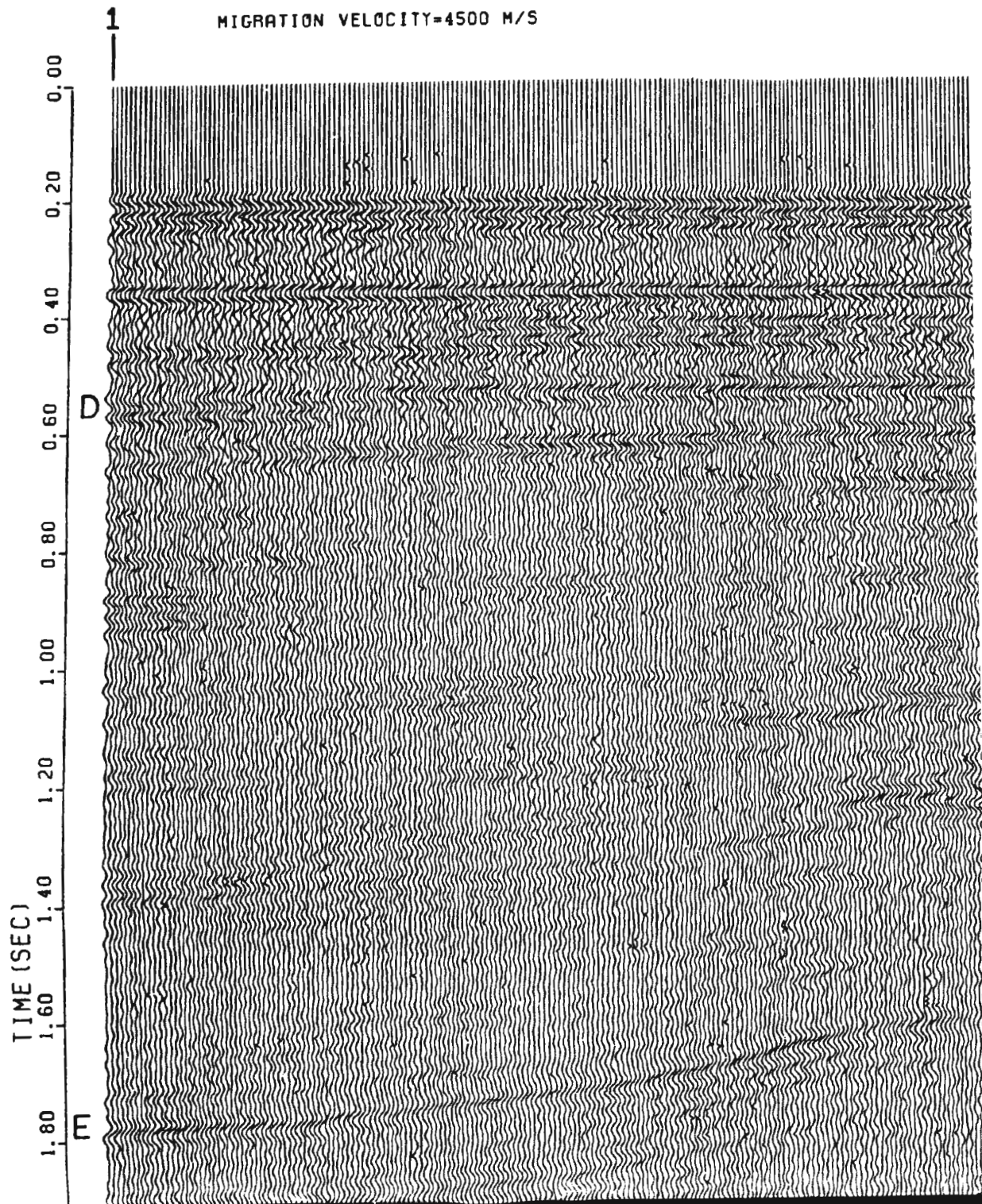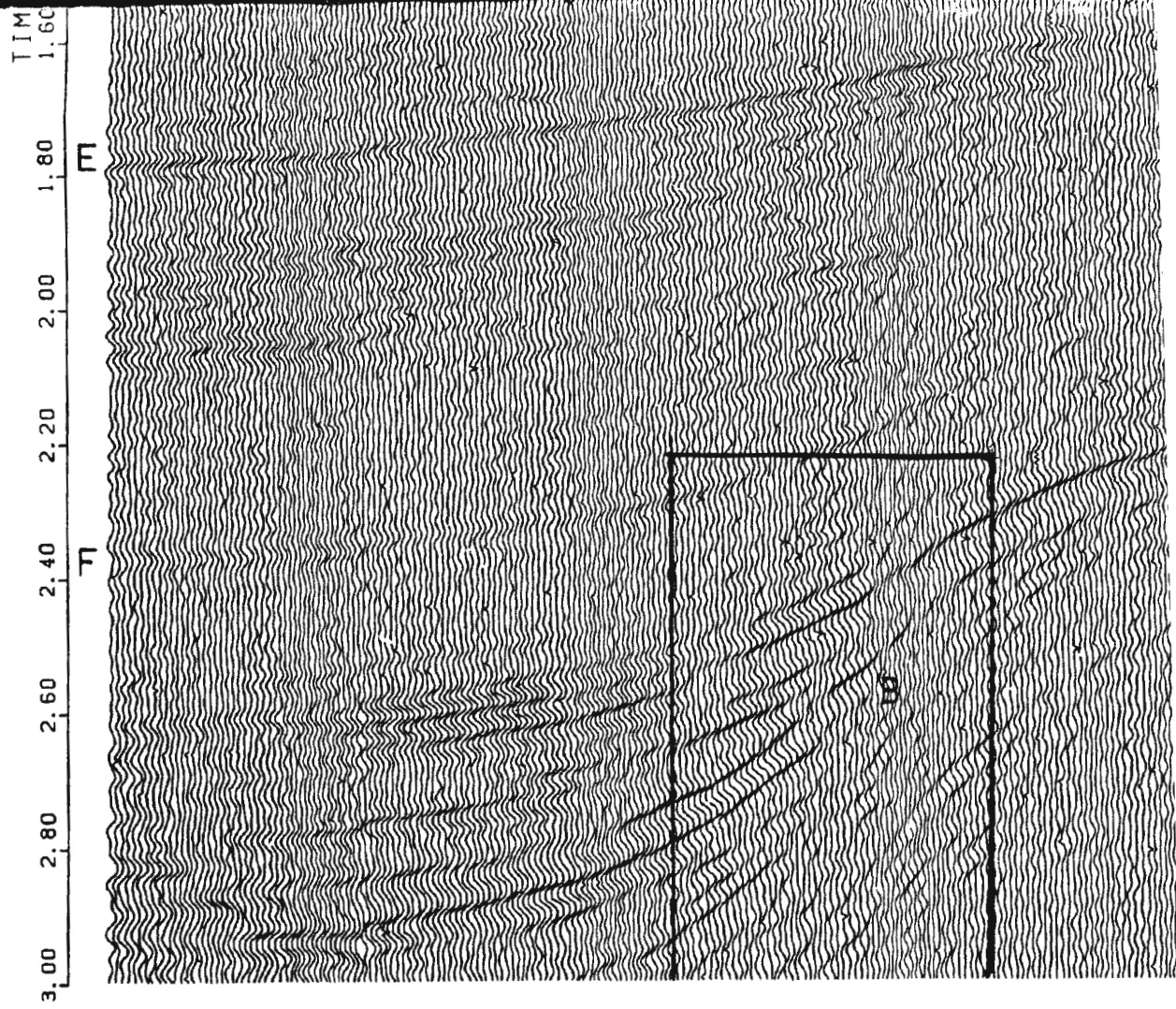
FIG. 4.45 SEISMIC SECTION AFTER MIGRATION
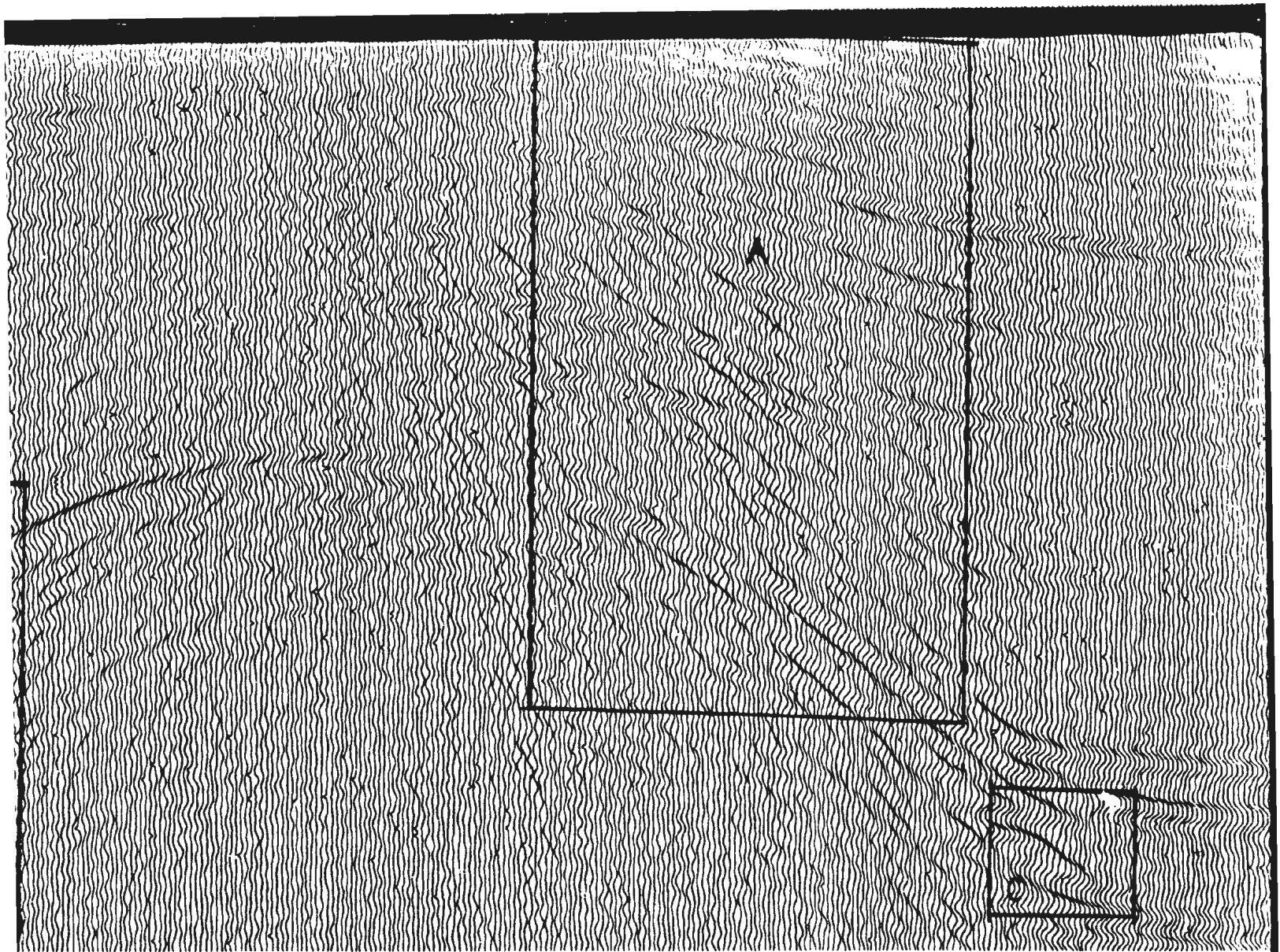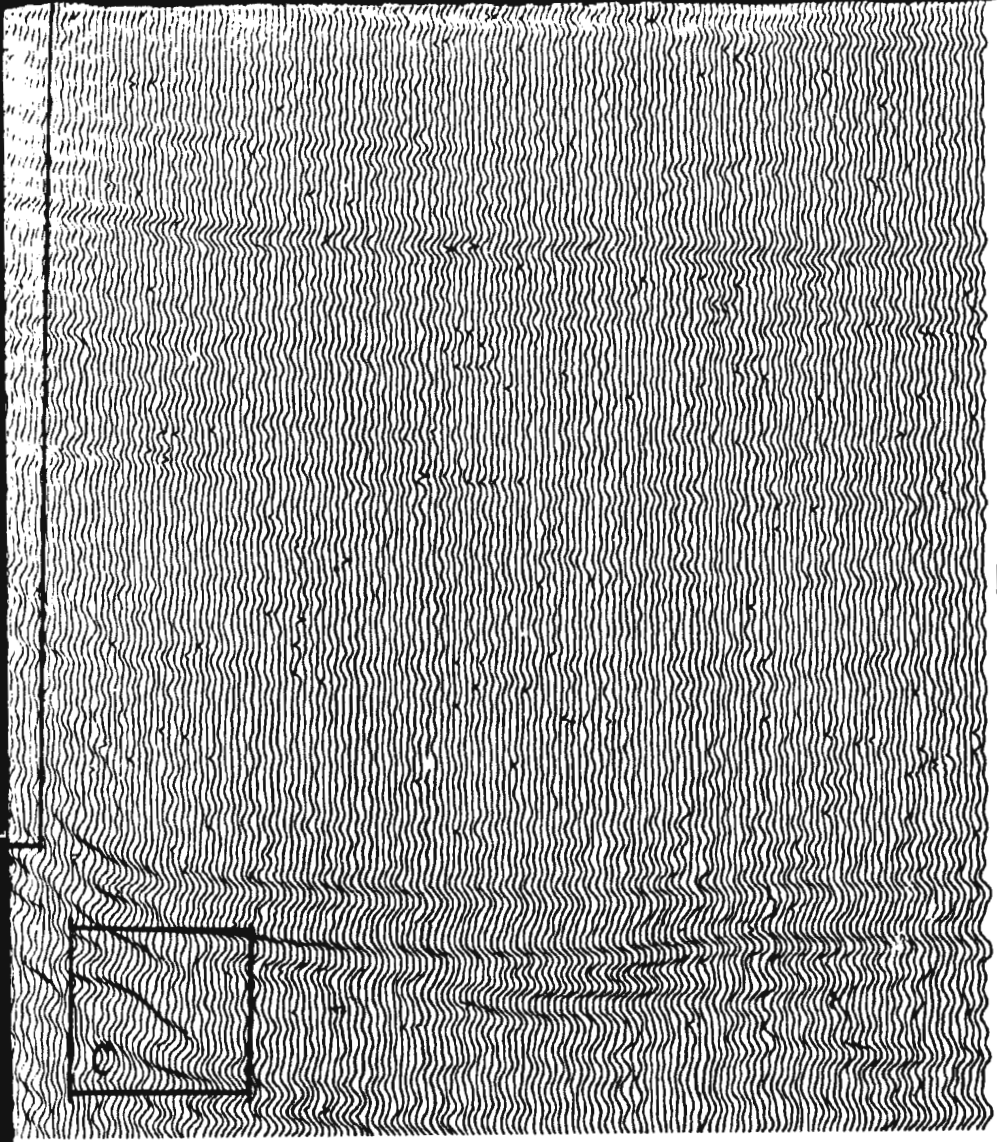
E

F

FIG. 4.4 SEISMIC SECTION AFTER MIGRATION

E

F